



Department of Mechanical and Aerospace Engineering

**Development of bottom-up heat models for buildings
identified for the Cloud ZUoS smart-grid project
in Huntly, Aberdeenshire**

Author: Anya Krawczyk

Academic Supervisor: Nick Kelly

Industry Supervisor: Jim O'Donnell

A thesis submitted in partial fulfilment for the requirement of the degree

Master of Science

Sustainable Engineering: Renewable Energy Systems and the Environment

2020

Copyright Declaration

This thesis is the result of the author's original research. It has been composed by the author and has not been previously submitted for examination which has led to the award of a degree.

The copyright of this thesis belongs to the author under the terms of the United Kingdom Copyright Acts as qualified by University of Strathclyde Regulation 3.50. Due acknowledgement must always be made of the use of any material contained in, or derived from, this thesis.

Signed: Anya Krawczyk

Date: 19/08/2020

Abstract

This project explores the best-fit method for creating bottom-up heat models for buildings identified for the Cloud ZUoS smart-grid project in Huntly, Aberdeenshire. In addition to this, the work designs a proposed modelling and evaluation approach, and creates models in an appropriate building simulation software. The more detailed white-box models will be used to validate more simplified models, requiring less data inputs. These simplified models will, therefore, be more scalable for a roll-out of the Cloud ZUoS platform.

Acknowledgements

Firstly, I wish to express my appreciation and gratitude to Dr. Nick Kelly, without whom this project would not have been possible. Nick provided great guidance and encouragement throughout the project and his insight and communication were invaluable. I would also like to thank the staff and lecturers within the Sustainable Engineering Department at Strathclyde University for the support and input throughout the MSc programme.

My grateful thanks also to everyone at Scene Connect, especially within the Cloud ZUoS team for welcoming me and guiding me during this project. This venture was part of their wider vision and I was thrilled to be a part of it. Additionally, I would like to show gratitude to the Santander University SME Internship Programme for their financial support, especially in times of such economic uncertainty.

And lastly, I would like to share a special thank you to my family and loved ones for their unconditional support throughout a bizarre academic year.

Table of Contents

Copyright Declaration	i
Abstract	ii
Acknowledgements	iii
Table of Contents	iv
Table of Figures	vii
List of Appendices	x
1 Introduction	1
1.1 Background	1
1.2 Motivation	1
1.3 What is Cloud ZUoS	2
1.4 Energy Systems Catapult (ESC) & Living Lab Data	3
1.5 Energy-as-a-Service	5
1.6 Aims & Objectives	6
1.7 Thesis Structure	7
2 Literature Review	9
2.1 Energy in Homes	9
2.2 Heat Transfer in Domestic Buildings	10
2.3 Importance of Building Energy Simulation	12
2.4 Bottom-Up or Top-Down Approach	13
2.5 White-Box Models	14
2.6 Black Box Models	15
2.7 Grey Box Models	16
2.8 Comparison of Modelling Methods	20
2.9 Thermal Comfort	22
2.10 Demand Load Shifting	22
2.11 Literature Review Summary	25
3 Simulation Tools	27
3.1 ESP-r Overview	27
3.2 Gridlab-D Overview	29
3.2.1 Building Envelope Primary Inputs	30
3.2.2 Heating within Gridlab-D Model	31
3.2.3 Pros and Cons of Gridlab-D	32
4 Archetype Design	33
4.1 Huntly Pilot Area	33
4.2 Method of Stock Model Development:	34
4.3 Choosing Appropriate Stock Models for Huntly	35
4.3.1 HDDT Office Model	35

4.3.2	GHA Cluster Model	37
4.3.3	4010 Cluster Model	37
5	ESP-r Model Development and Characteristics	39
5.1	Climate and Location Data	39
5.2	Building Geometries	40
5.2.1	HDDT ESP-r Model Geometry	41
5.2.2	GHA ESP-r Model Geometry	42
5.2.3	4010 ESP-r Model Geometry	42
5.3	Construction Materials	43
5.4	Casual and Internal Gains	44
5.5	Heating and Cooling Systems	45
5.6	Infiltration Rates	45
5.7	Verification of the ESP-r models	45
6	Gridlab-D 2R2C Model	46
7	Model Comparison	48
7.1	Average Room Temps	48
7.2	Pearson Correlation Coefficient	49
7.3	What is a ‘Good’ Correlation Coefficient Value?	50
7.4	HDDT Average Temperature Analysis	50
7.5	GHA Average Temperature Analysis	52
7.6	4010 Average Temperature Analysis	54
7.7	Conclusions	57
8	Tuning Gridlab-D Model	58
8.1	Thermal Mass	58
8.2	Weather Data	60
8.3	Occupancy Data	60
8.4	Framework	61
8.5	Temperature Setpoint	61
9	Results: Data Analysis of the Errors Between Models	62
9.1	Root Mean Square Error	62
9.2	Box and Whisker Plots	63
9.2.1	HDDT Box and Whisker Plots	63
9.2.2	GHA Box and Whisker Plots	64
9.2.3	4010 Box and Whisker Plots	65
9.3	Temperature Comparisons for Each Model	66
9.3.1	HDDT Comparison	66
9.3.2	GHA Comparison	67
9.3.3	4010 Comparison	68
10	Discussion	70
10.1	What is causing the errors?	70

10.2	Seasonal Variation	70
10.3	Hourly Variation after Switch off	71
10.4	Limitations of Study	71
10.5	Key Findings	71
11	Conclusions	73
11.1	Future Work	74
11.2	Integration with Cloud ZUoS Platform	75
	References	77

Table of Figures

Figure 1 Cloud ZUoS model	2
Figure 2 Heat model within the Cloud ZUoS project	3
Figure 3 Difference between the current and future power market (Deloitte, 2020)	5
Figure 4 Digitalisations impact on achieving Net Zero (National Grid ESO, 2020)	9
Figure 5 Heat Transfer in Domestic Buildings	11
Figure 6 Data flow in an ESP-r type white box model	15
Figure 7 3R2C Lumped capacitance model (Laret, 1980)	18
Figure 8 Star Style 3R2C lumped parameter model (Braun & Chartuvedi, 2002)	19
Figure 9 Three methods of modelling dynamic systems (Kalmykov, 2015)	21
Figure 10 Flow diagram of decision making process (Dimitriou et al, 2016)	21
Figure 11 Example of demand load shifting (Lee & Braun, 2008)	24
Figure 12 Schematic of ZUoS platform shifting demand from peak to off-peak	25
Figure 13 Schematic of Gridlab-D 2R2C lumped capacitance model	29
Figure 14 Map of Huntly, Aberdeenshire (edited from Bing Maps, 2020)	33
Figure 15 Map of Huntly with the interested clusters(edited from Google Maps)	34
Figure 16 HDDT Office Building	36
Figure 17 HDDT Floor Plan	36
Figure 18 GHA Chosen Dwelling	37
Figure 19 4010 Chosen Dwelling	38
Figure 20 Annual solar radiation, Aberdeen Dyce, 1994	39
Figure 21 Annual dry bulb temperatures, Aberdeen Dyce, 1994	40
Figure 22 ESP-r Model of HDDT Office	41

Figure 23 ESP-r model of GHA bungalow	42
Figure 24 ESP-r model of 4010 semidetached house	43
Figure 25 Total weekly gains in the ESP-r models	44
Figure 26 Thermal flow in Gridlab-D model (Zhou et al., 2019)	47
Figure 27 HDDT Average dry bulb temperature correlation matrix	51
Figure 28 HDDT Temperature histogram	52
Figure 29 GHA Average dry bulb temperature correlation matrix	53
Figure 30 GHA Temperature histogram	54
Figure 31 4010 Average dry bulb temperature correlation matrix	55
Figure 32 4010 Temperature histogram	56
Figure 33 Effect of Thermal mass on internal temperatures (De Saulles, 2009)	59
Figure 34 Total internal gains exported from ESP-r for HDDT Gridlab-D tuning	61
Figure 35 HDDT Daily RMSE profile across the four seasons	64
Figure 36 GHA Daily RMSE profile across the four seasons	65
Figure 37 4010 Daily RMSE profile across the four seasons	66
Figure 38 HDDT Worst fit temperature comparison between two models	67
Figure 39 HDDT Best fit temperature comparison between two models	67
Figure 40 GHA Worst fit temperature comparison between two models	68
Figure 41 GHA Best fit temperature comparison between two models	68
Figure 42 4010 Worst fit temperature comparison between two models	69
Figure 43 4010 Best fit temperature comparison between two models	69

List of Tables

Table 1 Thermal Analogy of Electric Circuit (edited from Dimitriou et al, 2016)	16
Table 2 The fundamental differences between modelling types (edited from Fouquier et al, 2013 and Dimitriou, 2016)	20
Table 3 Parameter definition for Gridlab-D ETP model	30
Table 4 Primary inputs for Gridlab-D model	31
Table 5 Pros and Cons of Gridlab-D model	32
Table 6 Building characteristics identified in the DCLG 2013 survey (Allison et al, 2018)	35
Table 7 Parameters taken from ESP-r for Gridlab-D modelling	46
Table 8 Choice of measured average temperature for further comparison	57
Table 9 Thermal mass of un-tuned and tuned Gridlab-D models	59

List of Appendices

Appendix A – HDDT ESP-r Parameters	82
Appendix B – GHA ESP-r Parameters	85
Appendix C – 4010 ESP-r Parameters	89
Appendix D – Python Covariance Matrix Script	94
Appendix E – HDDT Monthly RMSE Boxplots	95
Appendix F – HDDT Switch off RMSE Boxplots	97
Appendix G – GHA Monthly RMSE Boxplots	99
Appendix H – GHA Switch off RMSE Boxplots	101
Appendix I – 4010 Monthly RMSE Boxplots	103
Appendix J – 4010 Switch off RMSE Boxplots	105

1 Introduction

1.1 Background

This project explores the best-fit method for creating bottom-up heat models for buildings identified for the Cloud ZUoS smart-grid project in Huntly, Aberdeenshire. In addition to this, the work designs a modelling and evaluation approach, and creates models in an appropriate building simulation software. The detailed models, with large amounts of input data, will be used to validate simplified models, requiring fewer data inputs. These simplified models will, therefore, be more scalable for a roll-out of the ZUoS platform.

1.2 Motivation:

The motivation for this thesis is to develop bottom-up energy models of the Huntly housing stock and investigate their applicability in their simplest form. The need for these sub-models is to allow for further integration into a wider model for a more flexible domestic energy system with Cloud ZUoS. Systems such as Cloud ZUoS will be necessary for the future of decarbonisation in the housing sector as they will make way for a more synergistic relationship between supplier and consumer, with reduced emissions and costs. Within this study, this thesis will address the extent to which a sophisticated model can be simplified for use in a larger system. The work will also address issues such as thermal comfort, climate change, and economics.

Overall, the work towards developing bottom-up energy models of homes seeks to reduce the necessity for building surveys, develop a greater understanding of retrofitting design, influence occupancy behaviours and facilitate demand load shifting. This alongside promoting the use of real-time consumer data to promote smart meters as an enabler of energy efficiency.

1.3 What is Cloud ZUoS

This thesis is part of a smaller venture within the larger Cloud ZUoS project at Scene Connect Ltd. Scene Connect Ltd in partnership with Locogen, Mentone Energy, and Enbala. Cloud ZUoS (Zonal Use of System) aim to facilitate favourable grid and electricity costs within a local energy market (LEM) environment. This facilitation will be achieved by the integration of supply control, storage systems, and demand side response technologies. The initial pilot located in Huntly, Aberdeenshire, combining domestic and commercial users, and local energy generators.



Figure 1 Cloud ZUoS model

ZUoS is an Energy Services Platform for optimising energy use at the building, the neighbourhood and at a local network level, through real-time monitoring, communication and control of Distributed Energy Resources (DERs). There are three levels to which the ZUoS platform is aiming to service: the individual building, local distribution level, and the wider distribution level. This cross-level service will allow suppliers to automate energy services, and increase efficiency. This added flexibility in the network will enable a more flexible system whilst lowering emissions and reducing consumers' bills as they "pay for the grid you use". The ZUoS platform is being

developed to defer network investment and support the electrification of the heat and transport. The overall ZUoS solution will enable the smart control of EVs (Electric Vehicles), heat pumps and batteries in accordance with local generation and network generation (Figure 1).

For integration with the ZUoS platform (Figure 2) it is required to understand how heating within a home can be scheduled, and how the electrical load is placed on the network under BAU (Business as Usual) scenario. This project begins that aspect of the research in developing detailed heat models and assessing heat scheduling within them.

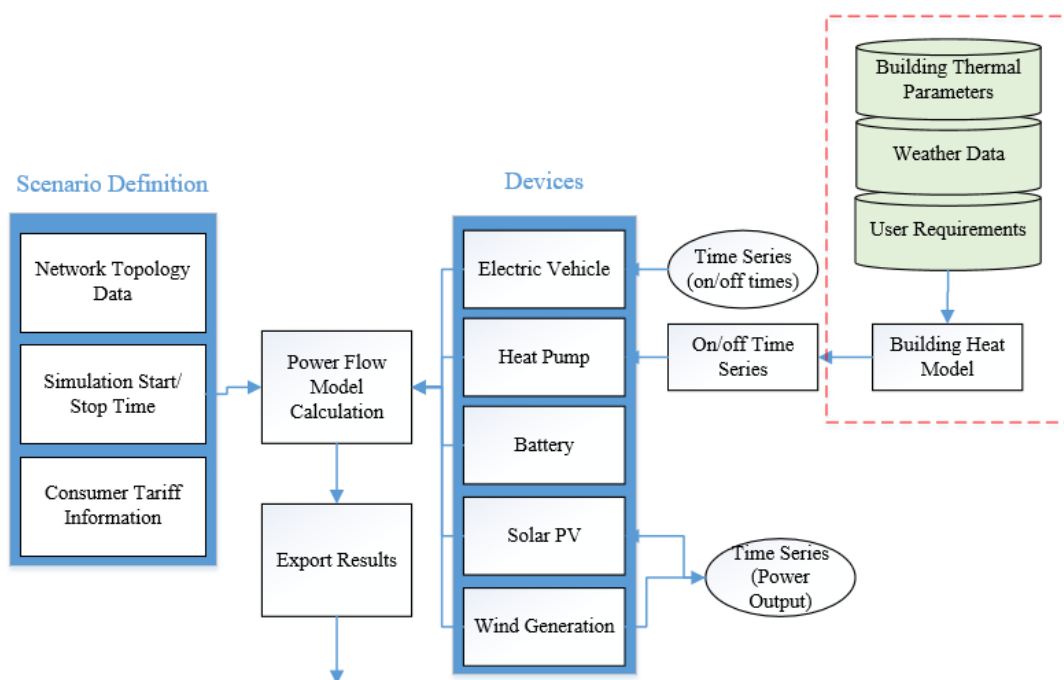


Figure 2 Heat model within the Cloud ZUoS project

The heat modelling is supported by wider industry stakeholders, including the Energy Systems Catapult.

1.4 Energy Systems Catapult (ESC) & Living Lab Data

ESC was developed to transform the UK energy system to promote clean energy options for businesses and consumers. It is a not-for-profit centre that connects government, industry, academia, and researchers. They implore a whole-systems

approach to the energy sector to highlight market needs and barriers, to reduce carbon emissions in the most economical way.

Their objectives are to increase the demand for new innovations by removing policy barriers and opening niches in the energy market. Their organisation allows and promotes innovators in the UK within the initial stages of commercial development to test their products and services. Additionally, a plethora of international contacts has been created for innovators to increase the rate of decarbonisation within the UK's energy sector. ESC's main objective is to raise awareness of the risks and opportunities that are often associated with low carbon evolution.

ESC has employed a 'Whole System Modelling and Analysis' approach to allow for greater insight into the energy systems within homes. This greater insight will lead to a greater result in the goal of decarbonisation of heat. ESC has created a resource to analyse the synergy between the control, HVAC system, building materials, occupants' comfort, and climate data. Their toolkit allows a detailed analysis of the impacts and benefits of different methods for decarbonising homes. Their platform also connects the energy sector together more as it allows for a synergistic relationship between businesses, policymakers, regulators, and investors.

ESC introduced the Living Lab in 2016, which has connected 100 homes across Wales, Newcastle, Manchester, and the West Midlands. The Living Lab allows for the real-time analysis and design of decarbonisation tools where businesses can market test and research at once whilst validating existing tools and software. This real-time and real-world analysis is also financially beneficial as it is attractive to investors.

The Living Lab installed smart controls and individual room sensors in each household to allow new SMEs (Small and Medium-sized Enterprises) to test their energy system products. The Living Lab covers a large range of dwelling types and occupancy numbers, and each user's controls are connected to a cloud system to allow for a greater understanding of energy use and preferences. This is extremely beneficial for market research as you receive automatic customer feedback.

1.5 Energy-as-a-Service

With digital markets changing how people do everything from ordering a taxi to ordering their groceries and booking holidays it has become increasingly clear that the energy sector will undergo a similar transformation. Simultaneously, anthropogenic effects on our climate are motivating the energy sector to develop a cleaner, cheaper and more connected energy supply. This niche in the market has created the ‘Energy-as-a-Service’ (EaaS) business model. This model allows consumers to pay for their energy consumption through a subscription and pay for *how* they use energy rather than *how much* they use (Dowling, 2018). Consumers’ payments will be based on their desired energy needs; rather than the passive consumption pattern we currently use (Figure 3 below).

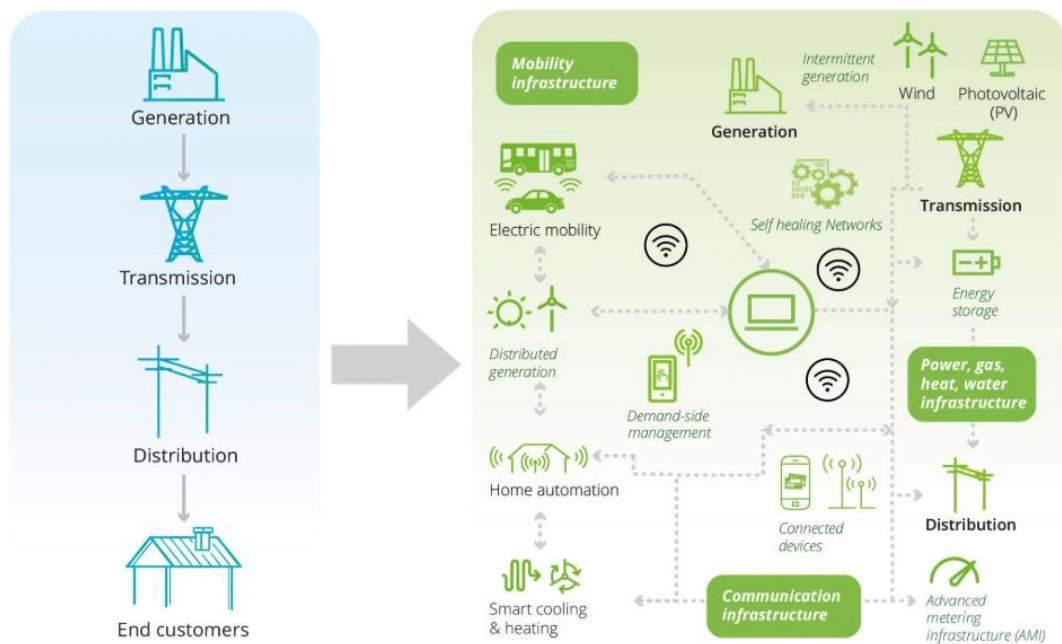


Figure 3 Difference between the current and future power market (Deloitte, 2020)

The EaaS model delivers omnipresent management of consumers’ energy assets and services via wireless Internet of Thing (IoT) sensors and advanced analytics. Within districts, customer’s resources are combined into a ‘smart energy community’, allowing energy demand profiles to be forecast and reducing the demand on the grid. EaaS has

recently promoted the use of advancing technologies, and growing the implementation of modern low carbon technologies (Deloitte, 2020). Most energy service providers are developing their EaaS business models to capitalise on the predicted growth in the market. Companies at the forefront of this advancement will be developing their artificial intelligence, data analytics and cloud systems. This intricate development across technologies will create more flexible energy solutions. However, the growth of the EaaS business model is highly dependent on policy, regulations, technological advancements, economic growth and environmental projections (Alptekin, 2019; Deloitte, 2020).

The importance of EaaS in the wider ZUoS project is that it no longer matters how much energy you use, but rather when you use it. ZUoS hopes to be able to provide consistent warm temperatures and high levels of thermal comfort for customers for the same cost, but with maximum renewable supply. Additionally, this will help decrease network costs by scheduling in a ‘smart’ way.

1.6 Aims & Objectives

Aim: This project aims to create bottom-up heat models for buildings identified for the Cloud ZUoS smart-grid project in Huntly, Aberdeenshire. These are used to validate simplified models used by the Cloud ZUoS platform. This simulation and validation project will aid the transition to lowering the energy demand of buildings, with the end goal of integrating the simplified models with a predictive tool and smart meters to shift load profiles.

Initially, the project goal was based on receiving data profiles from up to 100 homes in the UK. This data included heating set points of homes, building parameters, energy consumption and internal temperatures. The ideal project would have developed these buildings in ESP-r to compare with real data and to help validate the more simplistic models built in Gridlab-D. However, due to time constraints and the lack of data the project was based on archetypes within Huntly and stock models created within ESP-r. Ultimately, this research will be continued with Scene Connect later this year to utilise the ESC dataset and provide greater insight into thermal predictions and behaviour of

buildings, reducing demand and thus reducing carbon emissions. This tool will be extremely useful in mapping energy consumption in residential and urban areas.

Objectives:

- Search and research relevant academic papers.
- Review the data and information that Scene have on the project so far.
- Investigate and define the different methods of building energy modelling.
- Choose the most appropriate lumped capacitance model for comparative analysis with ESP-r models.
- Create and design archetypes of an office building and two homes based on the pilot information from Huntly, Aberdeen.
- Build these archetypes as separate models within ESP-r for data extrapolation to aid the development of more simplistic lumped capacitance models.
- Analyse and justify the use of average house temperatures for the comparison with lumped capacitance models.
- Help Scene with the development and tuning of the lumped capacitance model to deliver similar outputs to the ESP-r models.
- Choose a suitable method of comparison between the two modelling methods.
- Establish an outline for future work to utilise the ESC Living Lab Data and provided survey data.

This project hopes to inspire further work in the development of thermal modelling and predicting thermal response of buildings to be used in a wider IoT (Internet of Things) model.

1.7 Thesis Structure

As described previously, this body of work aims to develop a number of archetypes in ESP-r and to export the necessary parameters for use in creating a more simplistic building modelling tool. This work will explain the full research, design, methodology, and results in the following structure:

Chapter 1 (current chapter) introduces the background of the project and the aims and objectives of the proposed work.

Chapter 2 presents the findings of the literature review, from energy in homes, climate change to modelling techniques.

Chapter 3 gives an overview of the simulation software that have been chosen for the modelling section of this work. It also gives a brief overview of the input parameters require for the simplified Gridlab-D model.

Chapter 4 is a description of the chosen archetypes to be modelled, based on clusters of homes in Huntly, and the design process that entailed.

Chapter 5 provides a detailed description of how the three models were developed in ESP-r.

Following this, in **Chapter 6** the tuning and development of the simplified model in Gridlab-D is described.

Chapter 7 inspects the average temperatures taken from ESP-r for appropriate comparison with the Gridlab-D model.

Chapter 8 presents the results of the comparative study between ESP-r results and Gridlab-D results in a number of ways.

Chapter 9 discusses the implications of the results and places them in a wider context of the overall project.

Finally, in **Chapter 10**, conclusions and recommendations for future work, specifically how these findings and the simple Gridlab-D model will be utilised in the rest of the Cloud ZUoS project.

2 Literature Review

This research review will be categorised into sub-sections to methodically present the literature that was analysed preceding any modelling and simulation work. This review will assess the basics of domestic heat transfer systems, the variety of energy modelling software, the chosen software ESP-r and simpler methods of energy modelling.

2.1 Energy in Homes

It is becoming increasingly apparent that data-driven performance-based energy models will be pivotal in the journey to decarbonisation as they give insight into the operating systems and retrofit savings (Figure 4). 14% of the UK's greenhouse gas emissions are currently emitted from energy use in homes for their use of space heating and domestic hot water (CCC, 2019), and 80% of this heat being supplied by natural gas (Palmer and Cooper, 2013). With two-thirds of UK homes below current energy efficiency targets according to the CCC (Committee on Climate Change) and national data. Currently, the UK's attempt at reducing carbon emissions from homes is lagging behind the increasing risks of climate change. It is becoming increasingly important to improve the quality and design of the housing market with new technologies to combat our anthropogenic influences. Our efforts will aid in improving occupants' thermal comfort, health, and wellbeing and reduce greenhouse gas emissions (Ramallo-González et al., 2013).



Figure 4 Digitalisations impact on achieving Net Zero (National Grid ESO, 2020)

Methods of adaptation are not proceeding at the necessary pace to reach 2050 net-zero targets. Goal number 7 of the United Nations Sustainable Development Goals (SDGs) was defined to ensure global access to affordable, reliable, sustainable, and modern energy (Clarke & Hence, 2015). This goal includes the improvement in energy efficiency and increasing the share of renewable energy. This aims to balance the energy trilemma, to find the balanced relationship between energy security, energy equity, and environmental sustainability (Villavicencio Calzadilla and Mayger, 2018; Rosenow et al., 2018).

Historically, and currently, the UK's grid is powered by a centralised system partially powered by coal, oil, and gas. As CO₂ emissions rise as with the demand for renewable supply, more stochastic sources are being used (e.g. hydro, solar, wind). This centralised grid is no longer convenient as patterns of supply and demand are no longer predictable. The UK energy system needs to be remodelled to ensure that it meets these goals in the future, requiring a comprehensive whole system approach to service policy and financial investments. The future of the UK's system will be decarbonised, decentralised, democratised and digitalised (ESC publications). Currently, we are undergoing the shift from controllable generation (fossil fuels) and uncontrollable demand, towards uncontrollable generation (renewable supply) and controllable demand. To comply with this transformation and the increasing dependence on periodic resources, coupled with the electrification of transport and heat a localised approach will be necessary to increase efficiency, decrease fuel poverty, and curtail greenhouse gas emissions.

2.2 Heat Transfer in Domestic Buildings

Heat transfer in buildings is the mechanism of heat exchange between different environments. In its' most simplistic form, heat transfers from a warm environment to a cold environment. The basic knowledge of heat transfer is necessary for building energy models to reduce energy consumption and increase the thermal comfort of occupants (Wang et al., 2013).

There are three basic descriptions of heat transfer: those being conduction, convection, and radiation.

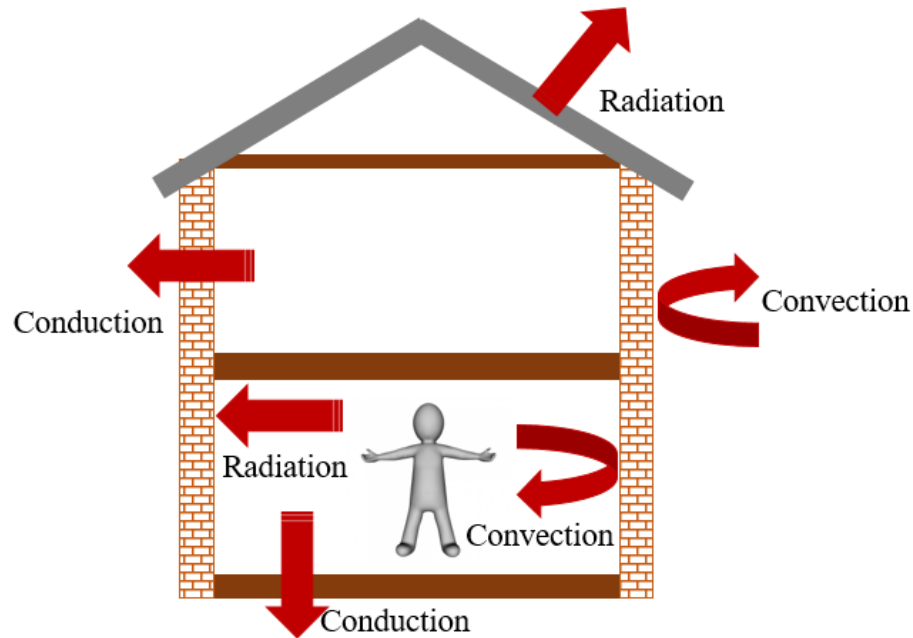


Figure 5 Heat Transfer in Domestic Buildings

The figure above demonstrates these basic thermal transfer mechanisms in homes. The boundary conditions of a building (solar irradiance, weather patterns, building fabric and external temperature) are the main contributing factors to its heat transfer process (Cengel, 2007).

Firstly, thermal conduction in buildings is caused by the difference in external and internal temperatures. Conduction is apparent through the ventilation of air through windows and doors and the infiltration through cracks and drafts. It is also evident by the heat losses and gains of the buildings' material properties. Radiative heat transfer in homes is generated by solar gains passing through windows. The home may gain or lose heat in the form of electromagnetic radiation as it is absorbed by the building fabric. Lastly, convection is the system of heat transfer through the movement of fluids, such as gas or liquid. Convection is caused by a thermal difference that drives a circulation, causing warm fluids to rise and colder fluids to sink. This circular motion, with a temperature gradient, aids the heat transfer process (Rajput, 2005).

The heating and cooling loads of a building can be expressed as the amount of energy required to heat or cool a zone. In a house, the thermal loads are affected by transmission losses, internal gains from equipment and occupants, and solar radiation gains. Greater temperature losses and gains are expressed when there is a larger temperature difference between the inside and outside environments (Cengel, 2007; Rajput, 2005).

Many properties of homes are important, however, the most valuable in basic energy models are thermal resistance and capacitance. The thermal resistance, R , of building material is defined as the ratio of the temperature difference across the material to the rate of heat flow per area (K/W). In other words, resistance is a material's ability to resist heat flow. Inversely, thermal capacitance is related to the dwelling's ability to store energy (thermal mass) and is defined as the heat flow required to change the temperature of a zone by one unit in one second (J/K) (Dimitriou, 2016; BPI, 2016).

2.3 Importance of Building Energy Simulation

Domestic buildings are one of the key areas for targeting emission reductions and energy modelling is one of the fundamental tools which can be used to study the thermal and energy performance of housing stock. The information gathered from energy modelling can be used for future building design and retrofitting purposes to reduce the overall carbon footprint of the domestic energy sector (Ramallo-González et al., 2013). The energy simulation and digitalisation sector is predicted to be worth £45 billion by 2025, and an investment of £20 million will be necessary to upgrade electricity networks by 2035 to meet the evolving structure (ESC publications).

Recent trends in carbon-reducing policies coupled with the rise in greenhouse gas emissions have led to the urgency for complex modelling in aid of predicting building performance (Clarke, 2006). Combined energy modelling is the best method of energy simulation as it combines sustainability, the environment and occupants' health and wellbeing (Kavgic et al., 2010). Building simulations also allow for design improvement, sizing of HVAC equipment, utility cost predictions and thermal and visual comfort optimisation. There is a huge benefit of co-simulation as it combines

the strengths of many different approaches to achieve a more desirable outcome (Clarke & Strachan, 1994). Errors can be minimised during the building simulation process with the use of operational data. The use of internal temperatures, fuel consumption, and climate parameters can lead to the development of performance based models (Child et al., 2019).

Building simulation tools are an excellent approach to analysing demand load for residential dwellings, to assess their efficiency, and to give an overview of the potential for demand-side management (Neu et al., 2014). The use of energy modelling and monitoring is and will be essential in policy making, designing future emission reduction plans, eradicating fuel poverty and informing decision making from a local level through the analysis of the UK's residential sector.

When choosing any model for simulating there is a balance to be struck between complexity, effort and available input data. There are loosely three widely accepted modelling approaches; white-box modelling; grey-box modelling and black-box modelling.

2.4 Bottom-Up or Top-Down Approach

There are two types of approaches to building energy models: bottom-up and top-down. The bottom-up approach relies on energy load profile data which then groups them with similar building stock. Bottom-up approaches are generally more appropriate for creating detailed energy demand profiles, through the gathering of individual dwelling data. The bottom-up models are often more complex and demanding but are extremely beneficial in highlighting individual energy contribution to the housing stock. Conversely, the top-down approach calculates the energy demand of individual households from derivations from larger areas or regions. Top-down models are often beneficial for suppliers as they aid in delivering demand forecast data (Neu et al., 2014). Generally, bottom-up models are more valuable in guiding policy framework and reaching governmental goals, in highlighting the areas of possible energy savings (Kavgic et al., 2010).

Smaller-scale resolution such as the modelling of individual dwellings or neighbourhood districts such as the project in Huntly is better suited to the bottom-up approach. The design of archetypes in Huntly in combination with a bottom-up approach will give detailed energy load analysis and effectively demonstrate how efficient the heating systems are. Whereas the top-down approach is better suited to large scale housing stock projects (Cerevo et al., 2015).

2.5 White-Box Models

White Box (finite difference) modelling of the thermal behaviour of buildings is a physics driven method. A white box model is transparent in its' process, inputs and outputs. The process is based on a very detailed description of the building, and detailed heat and mass transfer equations. This forward modelling technique is often performed within a simulation tool such as ESP-r, EnergyPlus, or TRNSYS (Ramallo-González et al., 2013; Dimitriou, 2016).

White Box modelling often requires an experienced user, and is very time consuming and often expensive in the data collection and start up phases (Braun & Chartuvedi, 2002). This type of modelling is often best used at the design stage of a building as it can generally estimate the input parameters, and tends to be more difficult in collecting existing building information. White box modelling of a building requires a large range of input data from boundary conditions, 3-D geometry, material properties, occupancy behaviour to HVAC systems (Foucquier et al, 2013) (Figure 6).

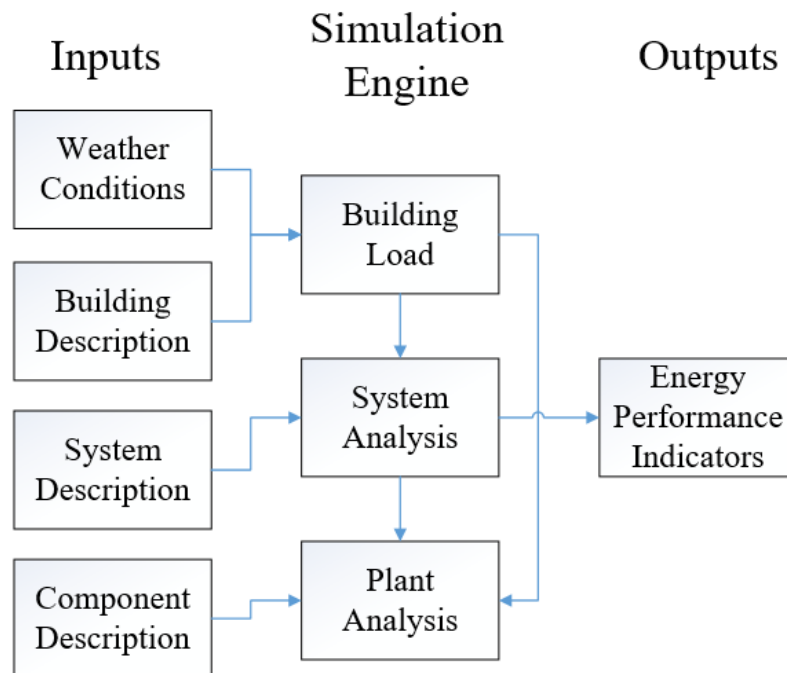


Figure 6 Data flow in an ESP-r type white box model

2.6 Black Box Models

The black box method or data-driven model is based on machine learning techniques to describe the thermal properties of a building type. Black box methods are generally more beneficial when less information is known about the building envelope. The statistical models consider the relationship between heating loads and operational data. This kind of black box model is dependent on initial ‘training data’ of on-site measurements to develop future predictions. Black box models are generally quicker to compute once set-up than white and grey box models, however, they require vast amounts of data and are constrained to the building system they were trained for so they often produce large forecasting errors when the data range is insufficient.

Black box models generally do not need the technical details of a building (i.e thermal properties and physical description). The technique is sometimes referred to as curve fitting as it attempts to fit the model to the input and output data. This can lead to difficulties in interpreting the data as it is not often in a user friendly format.

Black box empirical models' computational speed tends to be fast enough to combine with model predictive control. However, these models require large datasets and often take their inputs from detailed white box models. Additionally, there are often difficulties in people understanding the outputs of black box models in physical terms.

2.7 Grey Box Models

Definition: “The lumped thermal capacity model is the simplest transient heat conduction approach. In this model, the temperature of the solid body is a function of time only, which means that the temperature is assumed to be spatially independent” (Wojtkowiak, 2014).

In other words, the lumped capacitance method of thermal modelling is categorised in the ‘grey box’ approach. Unlike white box models such as ESP-r, grey box modelling requires the analysis of performance based data, which can be gained through the use of smart meters and sensors within people’s homes. As these technologies become more accessible and more economically viable, so too does the ability to use the grey box modelling approach.

Lumped capacitance models are calculated on the theory that the thermal mass of a building is amalgamated into a diverse number of thermal capacitances. The lumped capacitance model is also often known as the xRyC model (x being the number of thermal resistances, and y being the number of thermal capacitances) the theory of which is based on a comparable electric circuit. The table below displays the connection between the electrical and thermal circuits.

Table 1 Thermal analogy of electric circuit (edited from Dimitriou et al, 2016)

Electrical Circuit	Thermal Circuit
Electric Charge	Temperature
Voltage	Temperature Difference
Electric Current	Heat
Resistor	Thermal Resistance
Capacitor	Heat Capacitance

These approaches depend on defined time-dependent parameters such as: wall characteristics, zone approximation and heat transfer mechanisms (Vivian et al., 2017). Underwood (2014) demonstrated that thermal resistance and capacitance of materials in buildings can be readily calculated through the use of the CIBSE Guide A on material properties.

The lumped capacitance method is the least cumbersome, achieved through the use of an optimisation algorithm and similar outcomes can also be achieved through a linear parametric model of a neural network (black box approach). The lumped capacitance method relies on certain boundary conditions of the building geometry, the outside temperature, and the internal heat gains within the building. These time-dependent values based on climate data and internal gains can be calculated in ESP-r based on inhabitants and their desired set points obtained by ESC data (Ramallo-González et al., 2013).

With this kind of model comes the reduced need for detailed surveys of the housing stock, thus reducing the time and costs associated with existing building assessments. The use of dwellings' energy performance certificates (EPCs) are often a good initial method of informing the necessary inputs. Therefore, in line with this project, further work in data collection through domestic sensors will be imperative in informing modelling processes. This non-intrusive approach allows for more detailed and less intensive building energy models, whilst reducing the need for constant communication with the occupants. Further benefits of this approach include the scaling up of a domestic building to a whole neighbourhood or district (Dimitriou et al., 2020) It was also highlighted that this less intensive method could reduce the cost of human input by 30% (Underwood, 2014).

In modelling a typical UK domestic building in Loughborough, Dimitriou et al., (2015) outline the building materials, and occupancy of the household. The performance based data gathered in this research were of internal air temperature, gas consumption, external air temperature, and solar irradiance. Dimitriou et al., stated that this method with the resistance and capacitance values derived from the CIBSE guide is often more accurate in newer dwellings. The simple model below (Figure 7) shows the dynamic

behaviour between the internal temperature of the building and the outside temperature. This model is coupled with the differential heat equation used to calculate heat transfer at the internal node:

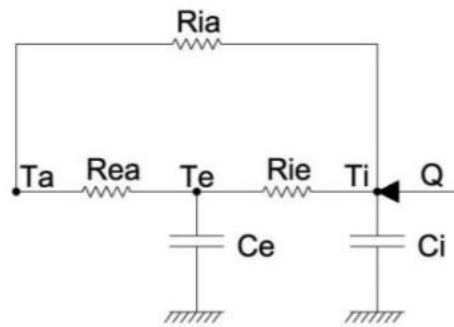


Figure 7 3R2C Lumped capacitance model (Laret, 1980)

Dimitriou et al., (2015) also use the Ordinary Least Squares (OLS) method on their calculated building parameters to obtain a better fit with the performance data. Dewson et al., (1993) also proved the OLS method was sufficient to determine parameter estimates.

Extensive research has been undertaken within the field of Lumped Capacitance in the search of the best approach. Ramallo-González et al., (2013) highlighted the dominant layer methodology. This method appointed a material layer with the greatest capacitance value and excluded all other layers. This simplification delivered a more exact depiction of the building. Many have agreed that a 3R2C (3 Resistance 2 Capacitance) approach is most accurate such as the one below designed by Braun & Chaturvedi (2002). Their model incorporates four elements; internal partitions, ceiling, ground and outside wall connected to an internal air node (Figure 8).

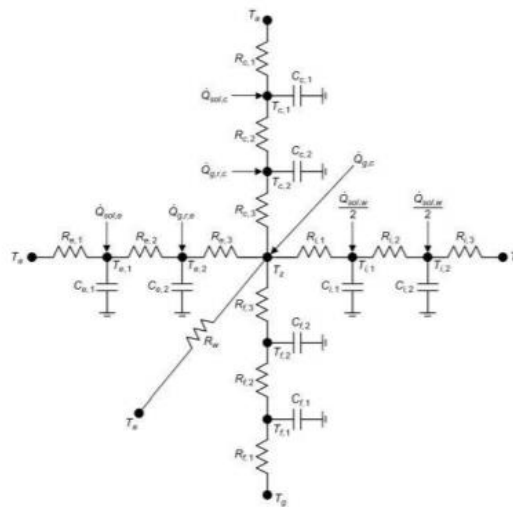


Figure 8 Star Style 3R2C lumped parameter model (Braun & Chartuvedi, 2002)

Fouquier et al., (2013) comprehensively explained the often used grey box technique as it couples the physical building model with algorithm identification of best-fit parameters. The known parameters of a model are calculated on a combination of algorithm use and then tested on the physical thermal building envelope. This allows the errors of the output to be evaluated, with the best-fit outputs having the smallest fitness values.

Van Leeuwen (2017) suggests that a 2R2C model is sufficient for the purpose of this study. The measured error between their 2R2C lumped capacitance model and their white box model created in TRNSYS was very low. The mean average percentage error (MAPE) indice was recorded below 0.55% throughout the full 10-day simulation. It is known that a less complex model is often more accurate in terms of its' predictive abilities, whereas a more complex model is often more necessary quantifying thermophysical relationships for design and retrofitting purposes (Hagerty & Srinivasan, 1991).

In conclusion, lumped capacitance, 'grey box' models in combination with a greater roll out of smart meters and stricter policy measures will be a great option for large scale thermal modelling and performance indicators. The readily available performance data delivered from real-time homes will be invaluable for energy modelling in the

future. Additionally, when white box modelling is done well, it can be more accurate, hence why it is used as our benchmark for comparison. However, the time consuming nature of the white-box method means it is not as scalable as grey box modelling for a commercial product.

2.8 Comparison of modelling methods

In conclusion, the grey box method such as Lumped Capacitance uses the best aspects of physical and statistical methods. The final outcome does not require a meticulous physical description nor an in depth analysis of the heat transfer mechanisms of a building (explained in Table 2).

Table 2 The fundamental differences between modelling types (edited from Fouquier et al, 2013 and Dimitriou, 2016)

Method	Building Parameters	Training of Model	Interpretation
White Box	Very detailed physical building parameter is needed	The model does not need any training	The results can be readily interpreted in 'physical' terms
Black Box	No physical building parameter information is needed	The model needs in depth complex training data	The results require detailed analysis and technical interpretation to be translated into 'physical' terms
Grey Box	Limited physical building parameter information is needed	The model needs reduced amount of training data	The results can be readily interpreted in 'physical' terms

In addition to this, figure 9 below adequately visualises the level of mechanistic understanding of each model that has been described.

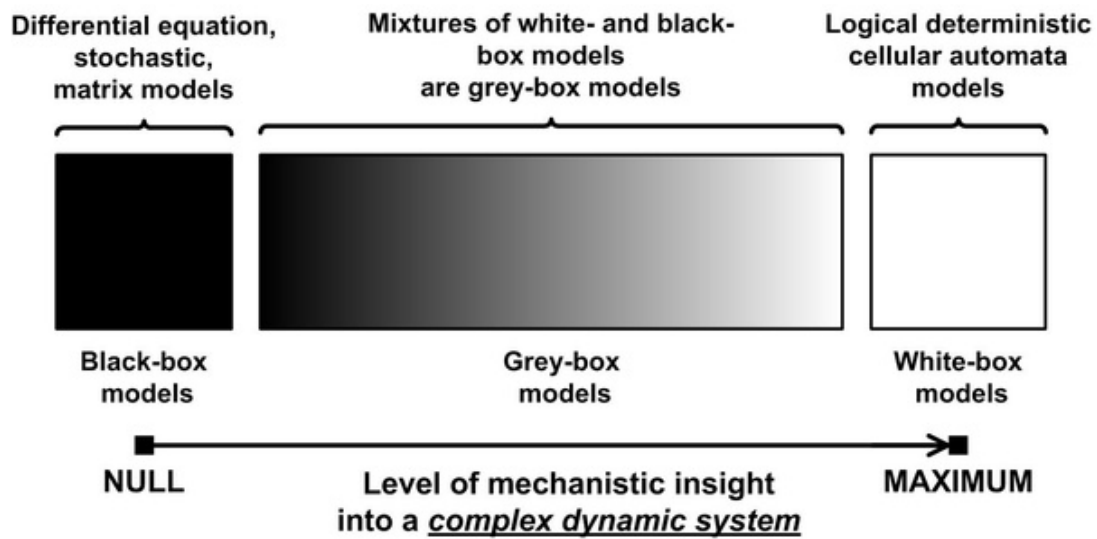


Figure 9 Three methods of modelling dynamic systems (Kalmykov, 2015)

In conclusion, due to the vast technical requirements of white box models, and the infeasibility of readily interpreting black box, a combination of the two, a grey box model is preferred (Figure 10). The grey box method will deal with limited physical building characteristics and limited measured data. The results from our grey box models will be easily interpreted in comparison to the other two modelling types.

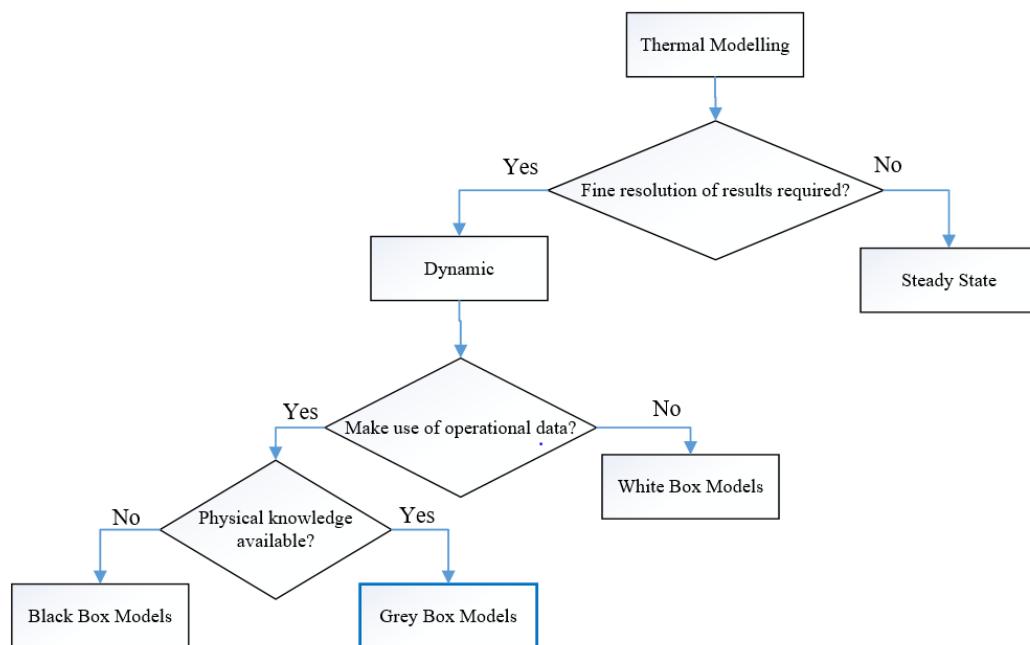


Figure 10 Flow diagram of decision making process (Dimitriou et al, 2016)

2.9 Thermal Comfort

“Thermal comfort can be described as the satisfaction of the mind in an environment” (Ekici, 2013). This so-called ‘satisfied environment’ allows for greater mental and physical productivity. In recent years, we have strived to create more comfortable conditions for living and working through the use of HVAC systems. Through this endeavour, Fanger developed the ‘comfort equation’, based on a variety of environmental and individual parameters (Fanger, 1973).

Thermal comfort is dependent on a number of factors, including: activity and clothing levels, air temperature, mean radiant temperature, air velocity, and humidity values (Sung & Hsiao, 2020). With these values and the thermal comfort equation, two outcomes can be calculated: The Predicted Mean Vote (PMV) and the Predicted Percentage of Dissatisfied (PPD).

According to ASHRAE (The American Society of Heating, Refrigerating and Air-Conditioning Engineers) between 80% and 90% of people’s lives are spent indoors. This behaviour has led to an imperative need for more developed understanding about thermal comfort and occupants’ relationship with their indoor environments. Additionally, due to the current pursuit of decarbonisation and sustainable building regulations, there has been a slight omittance into the research of thermal comfort of inhabitants (Arif et al., 2016; Olesen & Brager 2004). Braun and Altan (2014) expressed that with the increase in climate change, thermal comfort of occupants in dwellings will become more of an issue. ESP-r is a great tool for modelling occupancy behaviour within buildings, however, it does not take into account adaptive thermal comfort (Neto & Fiorelli, 2008).

2.10 Demand Load Shifting

Demand load shifting is a crucial and profitable tool used by local energy providers. Extensive energy reductions can be created using this form of DSM (Demand Side Management) system, in the form of peak reductions and off-peak filling. This method

of DSM incentivises the reduction in dependency on fossil fuels, as energy during the peak hours is generally more carbon intensive and more expensive.

In addition, to the aforementioned DSM benefits, demand load shifting is significantly important when implementing more stochastic renewable supply. A flexible load profile will allow reduction in whole-system costs of renewable energy, and create greater energy security. It will hopefully allow fossil fuels to be a peripheral contributor with the crux of our energy system supplied by renewables (Wimmler et al., 2017).

Demand load shifting is incredibly useful in terms of the thermal behaviour of buildings, and in particular homes. The approach uses the built in thermal mass of a building to reduce energy consumption at peak times. The method is appropriately demonstrated in Figure 11 below by Lee & Braun (2008).

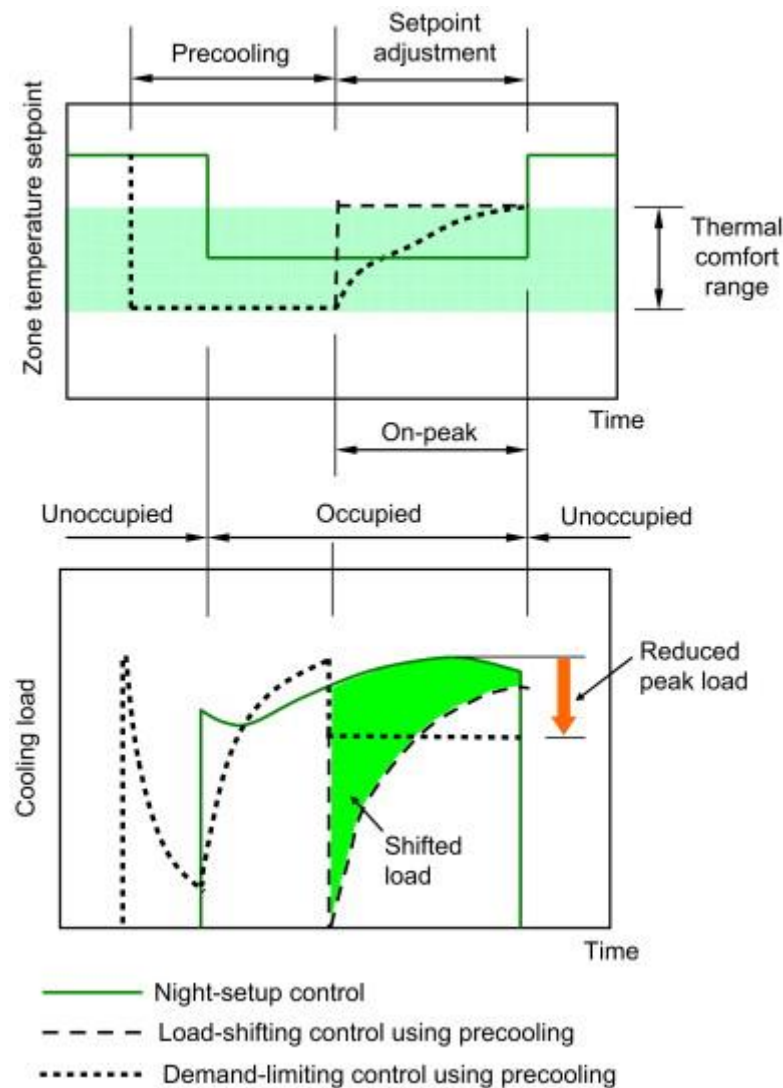


Figure 11 Example of demand load shifting (Lee & Braun, 2008)

Their example explains the method with cooling set points, however, the same method could be used to heat buildings in colder climates. The zones within the building are pre-cooled to specific set points at the lower end of occupants' thermal comfort, before a period of reduced demand. Then the inside temperatures are adjusted to follow an upwards path to control the load under a stated set point. Their efforts resulted in nearly 30% reduction in cooling loads in relation to their other method of night control as highlighted above.

This method of reducing demand has is hoped to be implemented in the ZUoS project. At ZUoS a consumer would permit their provider to control energy intense appliances

like dishwashers and washing machines to only work during off-peak hours. The outcome of this being cheaper for consumers and more environmentally friendly.

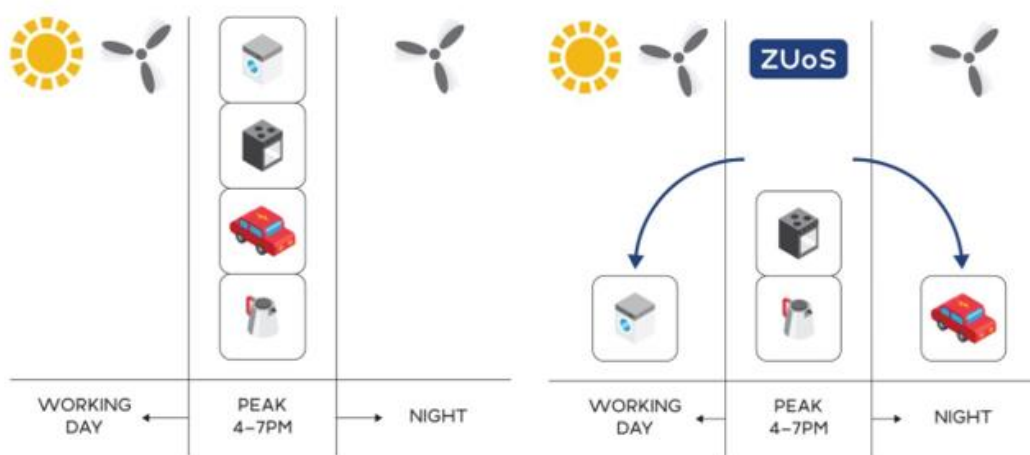


Figure 12 Schematic of ZUoS platform shifting demand from peak to off-peak

It is hoped that the ZUoS platform coupled with the heat model will be able to reduce stress on the grid whilst facilitating the development of renewable energies. During off-peak hours, the grid becomes overwhelmed and has to curtail renewable supply. Additionally, when demand is high during peak hours, non-renewable sources like oil and gas need to fill the energy void. In the future ZUoS will support excess renewable generation, and decrease the need to switch local generators off. Costs will also be reduced as the need for investments will decrease as upgrades to current infrastructure will not be needed.

2.11 Literature Review Summary

In summation, this literature review has covered the main background research that was needed for this project. The subjects covered so far are; energy in homes and climate change; heat transfer in domestic buildings; the importance of thermal simulations; an overview of the types of modelling techniques and a brief description of demand load shifting. The first section of the literature review covered the huge amounts of energy that is needed to heat people's homes in the UK and the effect this is having on our climate. Next, the main processes of heat transfer in homes, that being radiation,

convection & conduction were identified. The subsequent content explained the three categories of thermal modelling methods; the physics driven ‘white box’ method, the data-driven ‘black box’ method and the combination ‘grey box’ method. After identifying the three modelling techniques, they were compared in relation to their applicability, required inputs and user-friendliness to choose the best method for this project. The white box method is the initial tool that will be used, as it requires detailed inputs about the building envelope and end use. It was concluded that the typical black box method required too much training, and the outputs were often too difficult to interpret. Therefore, the grey box method, and in this case, the lumped capacitance tool was chosen as a best fit for our comparative model. In addition to this, a small section on demand load shifting and its applicability within the wider ZUoS project was explained.

The use of white box and grey box models and the chosen software will be further discussed in the following chapters.

3 Simulation Tools

For this research, two simulation tools were chosen, ESP-r and Gridlab-D. The first simulation tool that was chosen was ESP-r due to its' white box set-up and its' affiliation with Strathclyde University. The ability of ESP-r to enter a wide variety of building data was why it was initially chosen to hopefully represent the data acquired from ESC. Although the data was not acquired for the first stage of this project, ESP-r was still beneficial in the initial stages for its' future use in the rest of the project, and for its inbuilt default models.

The comparative simulation tool chosen for this project had to be a self-trained lumped capacitance model or one that could be implemented within a pre-made programme. Gridlab-D was investigated and noted that the 2R2C lumped capacitance model could be created and the code could be easily altered within the software. Gridlab-D was chosen for its ability to be integrated with the rest of the ZUoS project at a later stage. The power flow solver within Gridlab-D is open source and command line based, meaning it can be readily implemented within a cloud platform.

3.1 ESP-r Overview

ESP-r (Environmental Systems Performance Research) is an integrated energy modelling program developed to simulate building performance. The modelling tool facilitates the analysis of heat, air flows, humidity, and power flow within buildings at user-specified spatial and temporal resolution. The software was initially designed for Linux, however, it can also be used in Windows 10. ESP-r was licensed in 1974 by the University of Strathclyde and it has continuously supported development since (Clarke, 2001). The extensive validation of ESP-r has included empirical validation, and interprogram and analytical comparison (Strachan et al., 2008). Other similar simulation programmes are available such as TRNSYS, Energy Plus and DOE-2.1. ESP-r was chosen for this thesis due to the vast amount of knowledge and expertise at Strathclyde University. Detailed simulation programmes like ESP-r are necessary for a more explicit understanding when forecasting more complex energy loads, and thermal behaviour of buildings over shorter time scales.

ESP-r employs the Crank Nicolson method to model the thermal domain, which depends on discrete zones within a building's envelope. These zones such as air, material constructions, and interfaces are coupled with an energy balance, then placed into a matrix to solve synchronously. The Crank-Nicolson method relies on the heat equation and other related differential equations (Wills et al., 2012). Therefore, ESP-r is categorised as a white box method of energy modelling. Integrated energy modelling requires a certain level of preservation of the building parameters and plant systems. This preservation allows the building to remain systemic, dynamic, non-linear and complex (Clarke & Hensen, 2015).

ESP-r has been used in a variety of ways from modelling responsive demand, comparing archetypes with real-time data, designing retro-fit possibilities, creating bottom-up models, integrating the human thermoregulatory processes and installing renewable supply (Allison et al., 2018; Lomas, 1996; Kavgic et al., 2010; Rida & Kelly, 2017; Clarke & Kelly, 2001).

There are some noted constraints that arise from using typical white box models such as ESP-r. The major limitations being that it's dependent on complex and often difficult to obtain building information, its time-consuming nature, and dependence on users' abilities. The use of systems such as ESP-r generally increases with the implementation of new policies and initiatives. Therefore, it is hoped that in the future users will be able to simulate a model without the base knowledge of thermodynamics and building processes (Clarke & Strachan, 1994).

It is critical whilst using ESP-r that the user realises their limits, as with added complexity of a model this increases the risk of fatigue and error. For the comparison with future predictions and other models, often a very detailed model in terms of volume, description, and controls is necessary. Thus, highlighting the need for a more simplistic model to be used for load forecasting on a larger scale.

3.2 Gridlab-D Overview

Gridlab-D was used as an open source simulation tool for our comparative lumped capacitance model. The software combines power flow calculations with distribution network models, energy and appliance demand of buildings and market models. Gridlab-D bases its thermal modelling of buildings on a simplified electrical circuit (Figure 13). This allows the complex ESP-r model to be reduced to an equivalent electric analogy or equivalent thermal parameter model (ETP). This reduction takes similar heat flow paths from the white box model and lumps them into thermal mass elements for implementation in the ETP. The benefit of this obviously being the loss of complexity and minimal input data necessary, whilst decreasing the simulation process.

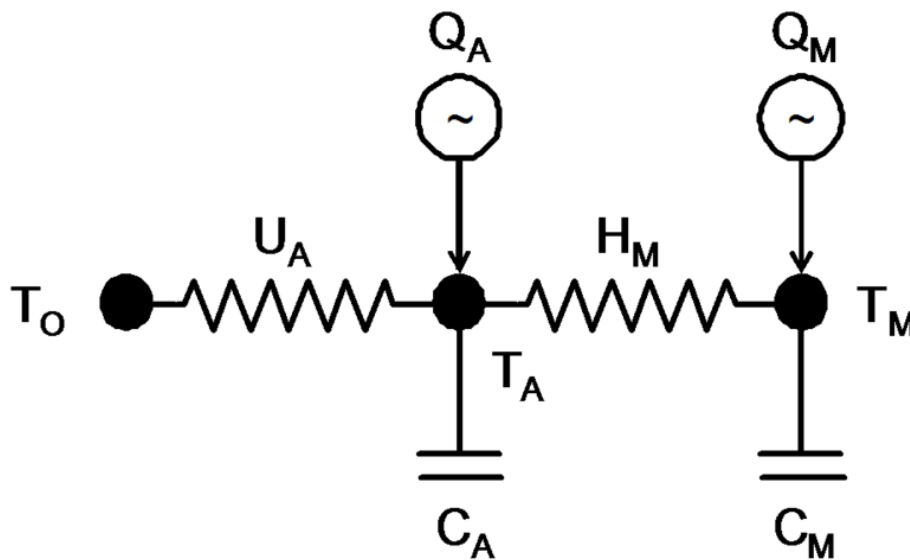


Figure 13 Schematic of Gridlab-D 2R2C lumped capacitance model

The equivalent circuit model is a great tool for capturing the thermal behaviour of buildings, in terms of heat loss and thermal mass dependent on different boundary conditions such as weather and occupancy patterns.

The parameters needed for the Gridlab-D model are listed in Table 3. The modelled building has a conductance, U_A , through which heat flows from the inside temperature

T_A , to the external temperature, T_O . The conductance of the thermal envelope, U_A , is the combination of heat flow through all building components (walls, air infiltration, roofs, windows, ceilings and floors). The conductance is more significant than the masses of each component and the mass is therefore lumped as one, C_M . The interior mass is described as the mass of the air, C_A , this reduces the effect of heat transferred to the air, Q_A . Without the C_A node the internal temperatures would react instantaneously to a change in heating or cooling set point. Outside factors such as solar gains and occupancy behaviour also add to the internal heat gains, Q_A . The Gridlab-D model accounts for the building fabric to absorb a set fraction of the overall heat, Q_M .

Table 3 Parameter definition for Gridlab-D ETP model

Parameter	Definition
U_A	Heat Loss Coefficient
T_A	Indoor Air Temperature
T_O	Outdoor Air Temperature
T_M	Temperature of Building Mass
C_M	Total Thermal Mass
C_A	Total Air Mass
Q_A	Heat Gains to the Air
Q_M	Heat Gains to Thermal Mass
H_M	Interior Mass Surface Conductance

Gridlab-D also permits the input of heating and cooling set points over an occupant defined time series. This is based upon modelling of the HVAC system, the energy demand, capacity and its' efficiency under the set boundary conditions.

3.2.1 Building Envelope Primary Inputs

For Gridlab-D to calculate the inputs for the thermal circuit, there are a number of primary inputs needed. These primary inputs are based on the building envelope and can be seen below:

Table 4 Primary inputs for Gridlab-D model

Primary Input Parameter	Symbol
Floor Area	A
Floor Aspect Ratio	R
No. Stories	n
Ceiling height	h
Exterior ceiling, fraction of total	ECR
Exterior floor, fraction of total	EFR
Exterior wall, fraction of total	EWR
Window/exterior wall area ratio	WWR
Doors	nd
Area of 1 door	A_{1d}
Glazing layers	GL
Glazing material	GM
Window frame	WF
Glazing treatment	GT
Window, exterior transmission coefficient	WET
R-value, walls	R_w
R-value, ceilings	R_c
R-value, floors	R_f
R-value, doors	R_d
Infiltration volumetric air exchange rate	l
Interior/exterior wall surface ratio	IWR
Interior surface heat transfer coefficient	h_s
Solar gain fraction to mass	f_s
Internal gain fraction to mass	f_i
HVAC delivered fraction to mass	f_m

3.2.2 Heating within Gridlab-D Model

When modelling the chosen building in Gridlab-D, there is a variety of different heating systems to choose from. The building can be modelled with:

- No heating system.
- A resistance heating system, where heat is delivered through a resistive heating coil. The heating coil is given a set point and therefore cycles on and off to sustain the chosen air temperature. The coil is given a COP of 1 and therefore is not affected by outside conditions.
- A gas system, where heat is delivered by a boiler or furnace and also works cyclically to maintain an internal temperature.
- A heat pump, dependent on the reversed vapour compression cycle, using the external to internal temperature difference. This system is also cycled on and off to sustain the desired internal air temperature set point.

3.2.3 Pros and Cons of Gridlab-D

Table 5 Pros and Cons of Gridlab-D model

Pros	Cons
Models exist to connect end uses to the grid	House model has not been validated
Models can also be run as stand alone	
Easily connected to local distribution network	

In the table above it is clear that the pros of Gridlab-D outweigh the cons, and that our work moves towards the validation of their heat model. Additionally, there is a significant cost benefit to the use of Gridlab-D as it will require considerably less effort and will benefit the end-use of integration with the wider ZUoS project.

4 Archetype Design

4.1 Huntly Pilot Area

Huntly, located in the north-east of Scotland (Figure 14) was chosen as the pilot town. Huntly was chosen due to its' integration of local domestic and commercial consumers, prosumers and local generators. This pilot was developed and coordinated with Huntly District and Development Trust (HDDT) to create the platform.



Figure 14 Map of Huntly, Aberdeenshire (edited from Bing Maps, 2020)

The trial is an attempt to engage local homes and businesses with renewable technologies, and with people who are keen to install new low carbon technologies and smart meters. One of the incentives to the local community (apart from lowering their carbon emissions) is that the installation process was to be partially funded.

The initial response to the Cloud ZUoS survey was very encouraging and outlined specific zones of interest within the town. From the feedback, small pools of interested dwellings were highlighted, which would form the clusters from which the study would

be based. The need for clusters of homes and not singular dwellings is due to the requirement to study energy flows at a local level.



Figure 15 Map of Huntly with the interested clusters(edited from Google Maps)

4.2 Method of Stock Model Development:

A bank of building stock models has previously been created by Allison et al. (2018) at the University of Strathclyde. A varied bank of housing models was developed using information from an English housing survey (DCLG, 2013). The most common dwellings in the UK were determined and detailed models were created to represent the British housing stock. The use of English information for UK wide projections was validated by the statistic that around 80% of the UK dwellings are located in England. Allison et al., (2018) developed 380 individual archetypes based on an array of different building parameters (Table 6 below).

Table 6 Building characteristics in the DCLG 2013 survey (Allison et al, 2018)

House Type	Floor Area (m ²)	Wall Construction	Roof Insulation	Glazing Type
Variants: 6	Variants: 9	Variants: 7	Variants: 11	Variants: 6
Semi-Detached	20-40	Filled Cavity	0	Single Glazing – wood frame
Mid Terrace	40-60	Cavity	0-25	Single Glazing – metal frame
Detached	60-80	Solid Brick	25-50	Single Glazing – UPVC frame
End Terrace	80-100	System	50-75	Double Glazing – UPVC frame
Flat- purpose built	100-120	Solid Brick – external insulation	75-100	Double Glazing –metal frame
	120-140	Timber Frame	100-125	Double Glazing – wood frame
	140-160	System – external insulation	125-150	
	160-180		150-175	
	180-200		175-200	
			200-250	
			250-300	

These archetypes were modelled in ESP-r. Each model takes into account the 3-D building profile, construction materials, and general internal heat gains and set points.

4.3 Choosing Appropriate Stock Models for Huntly

For this research, an office building and two residential dwellings were to be modelled. A visual approach was taken to identify the best-fit housing stock model for Huntly archetypes. This approach was taken via Google Maps and the street view function to compare the available stock models with the dwelling types in Huntly, Aberdeen. For the HDDT office building, the basic building parameters were available and the building was visible on google maps for further assumptions.

4.3.1 HDDT Office Model

The Huntly District and Development Trust office is situated in a former RBS Bank building (Figure 16). The building parameters were available, although subject to change as the HDDT office had not been developed yet.



Figure 16 HDDT Office Building

The future plans (Figure 17) for this office space was to create an open-plan work place with a heat pump system for heating within the building.

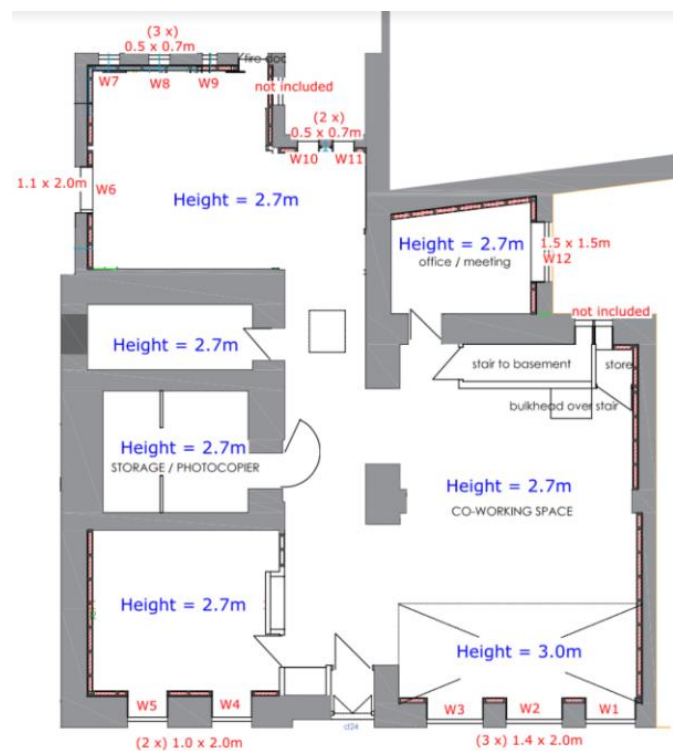


Figure 17 HDDT Floor Plan

4.3.2 GHA Cluster Model

For GHA and 4010 two homes within the identified clusters were chosen based on their similarity to the stock models available within ESP-r. The stock models available were; bungalow, detached, flat conversion, flat purpose built, mid terrace and a semidetached home.

The chosen dwelling within the GHA Cluster was aptly named GHA, and was located on Rowan Avenue (Figure 18). Section 5 displays the ESP-r bungalow model that was most similar to this chosen home on Rowan Avenue.



Figure 18 GHA Chosen Dwelling

4.3.3 4010 Cluster Model

Lastly, the chosen home within the 4010 Cluster was named 4010 and represents a traditional semi-detached home (Figure 19). This home on Richmond Road was also chosen for its similarities to its' representative stock model within ESP-r.



Figure 19 4010 Chosen Dwelling

Again, due to the inaccessible data from ESC, the best approach was to choose the best suited dwellings in the highlighted pilot areas. The nature of these dwellings being best-suited was based on a visual approach of the homes in the areas and the available stock models within ESP-r.

5 ESP-r Model Development and Characteristics

The development of the ESP-r model required significant amounts of data. The location and climate data, the 3-D building geometry, construction materials, casual and internal gains, infiltration rates, and heating and cooling systems.

5.1 Climate and Location Data

It is important to consider the geographic location of the model before any assumptions are made. Huntly, Aberdeen is a town in the north-east of Scotland, that sits at 57.4 degrees north, identified by its North Atlantic climate. This corresponds with the Koppen-Geiger Classification as Cfb (C being mid-latitude and temperate, f being wet and b being with a hot summer). This classification means that the coldest month averages above 0 °C, and all months' average temperature is below 22 °C, with at least a quarter of the year above 10 °C. Additionally, there is no convincing rainfall difference among seasons (Praznikar, 2017). It should be noted that in a climate such as Huntly, with a heating-dominated energy demand, climate change with its' predicted warmer temperatures will also reduce energy demand in dwellings. Figures 20 and 21 below display the annual solar radiation and annual temperatures taken from ESP-r.

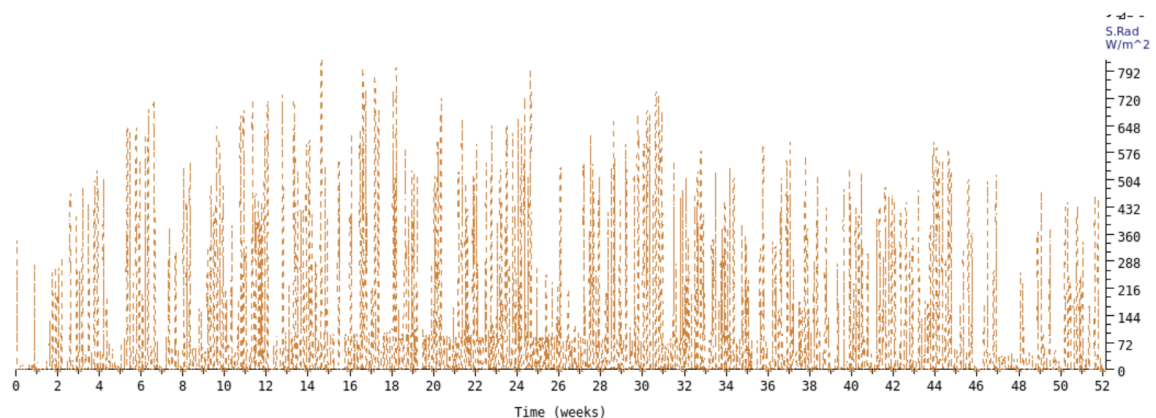


Figure 20 Annual solar radiation, Aberdeen Dyce, 1994

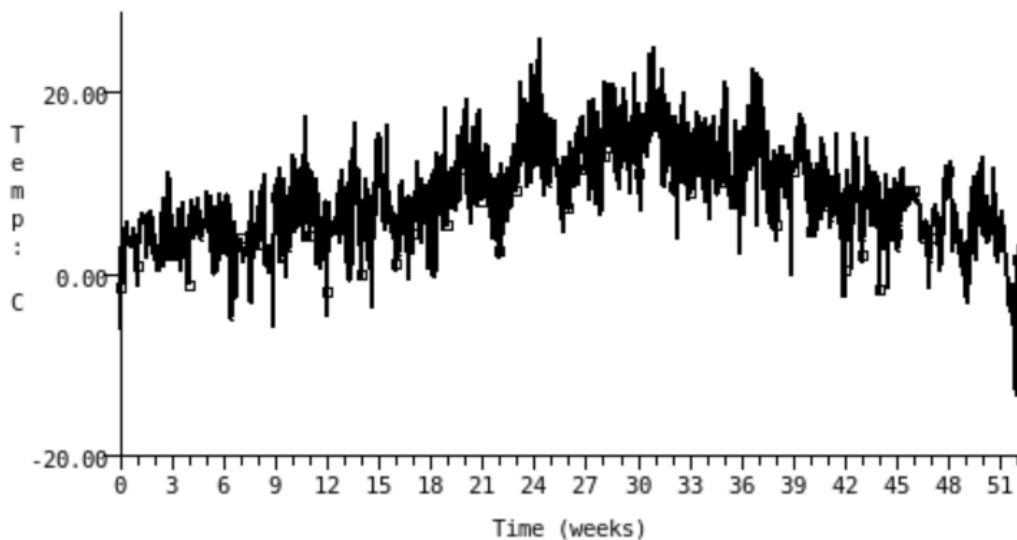


Figure 21 Annual dry bulb temperatures, Aberdeen Dyce, 1994

The majority of ESP-r weather files are derived from EPW (Energy Plus Weather) files as EPW is the most widely used configuration. EPW are a specific format of climate file that cover more than 2100 global regions. These climate files present hourly time resolution weather data including: dry bulb temperatures, relative humidity, atmospheric pressure, wind direction, wind speed, direct normal and global horizontal solar radiation. However, ESP-r does not account for cloud type, cloud cover, dew point, precipitation or ground temperatures.

The climate year used, was 1994 as it was held within the ESP-r climate database and easily utilised. For analysis 4 weeks across the year were used, the first week in January, April, July and October. This even seasonal spread across the year was thought to be sufficient for model development and validation. The covered spread, even in the North of Scotland would allow for an adequate representation of time when space heating was necessary and not necessary.

5.2 Building Geometries

For each archetype the building geometry was needed to be defined. For HDDT, a simplified model was created to represent acquired building data on the future projections of the HDDT office. For GHA and 4010, Google Maps was used to identify two representative buildings within the clusters that closely represented the building

stock models in ESP-r. The building materials are extremely important in regards to the overall thermal behaviour of the building. Often, it is difficult to create a model based on a pre-made building, due to lack of data, such as, occupancy details, floor plans and construction materials. The most important parameter whilst developing energy models of buildings is the U-Value (thermal transmittance) of the building. This value allows calculations on heat losses within a building to be made (CIBSE, Guide A, 2006).

5.2.1 HDDT ESP-r Model Geometry

As aforementioned, the HDDT ESP-r model (Figure 22) was based on a simplified version of development plans for a new open plan office type building within a former bank.

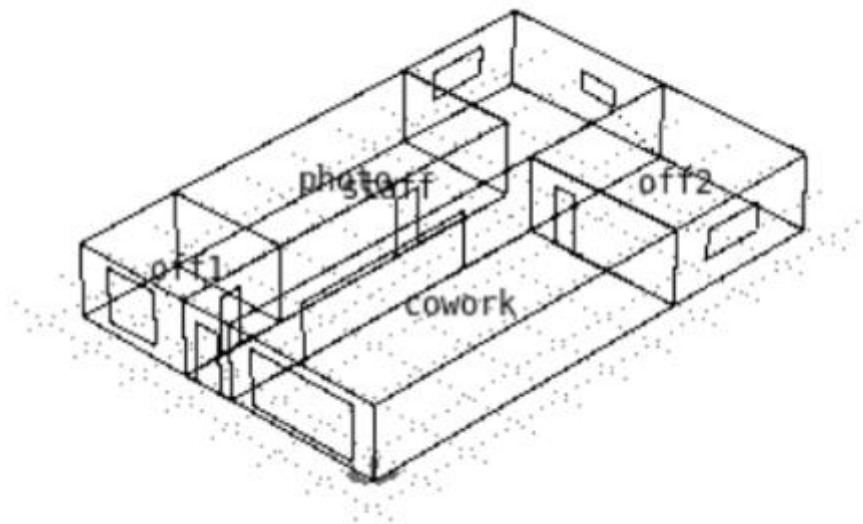


Figure 22 ESP-r Model of HDDT Office

The HDDT model comprised of 5 separate zones: co-work space, staffroom & hallway, photocopy room, office 1 and office 2. To avoid complexities in the modelling process, the multiple windows along the front of the building were modelled as two individual elements rather than five.

5.2.2 GHA ESP-r Model Geometry

For **GHA**, the bungalow stock model (Figure 23) was chosen to represent a bungalow observed on Rowan Avenue.

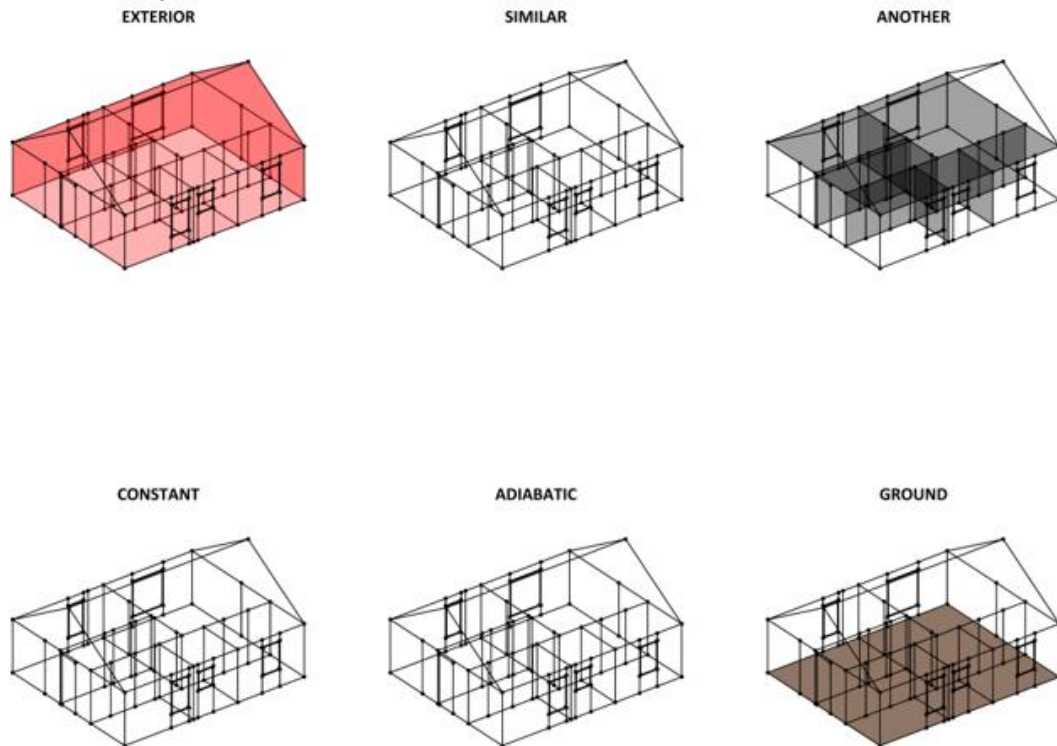


Figure 23 ESP-r model of GHA bungalow

The bungalow stock model consisted of 7 zones: bedroom 1, bedroom 2, bathroom, hallway, living room, kitchen and roof.

5.2.3 4010 ESP-r Model Geometry

Lastly, for the 4010 archetype a semidetached stock model (Figure 24) was chosen to represent a semidetached home on Richmond Road.

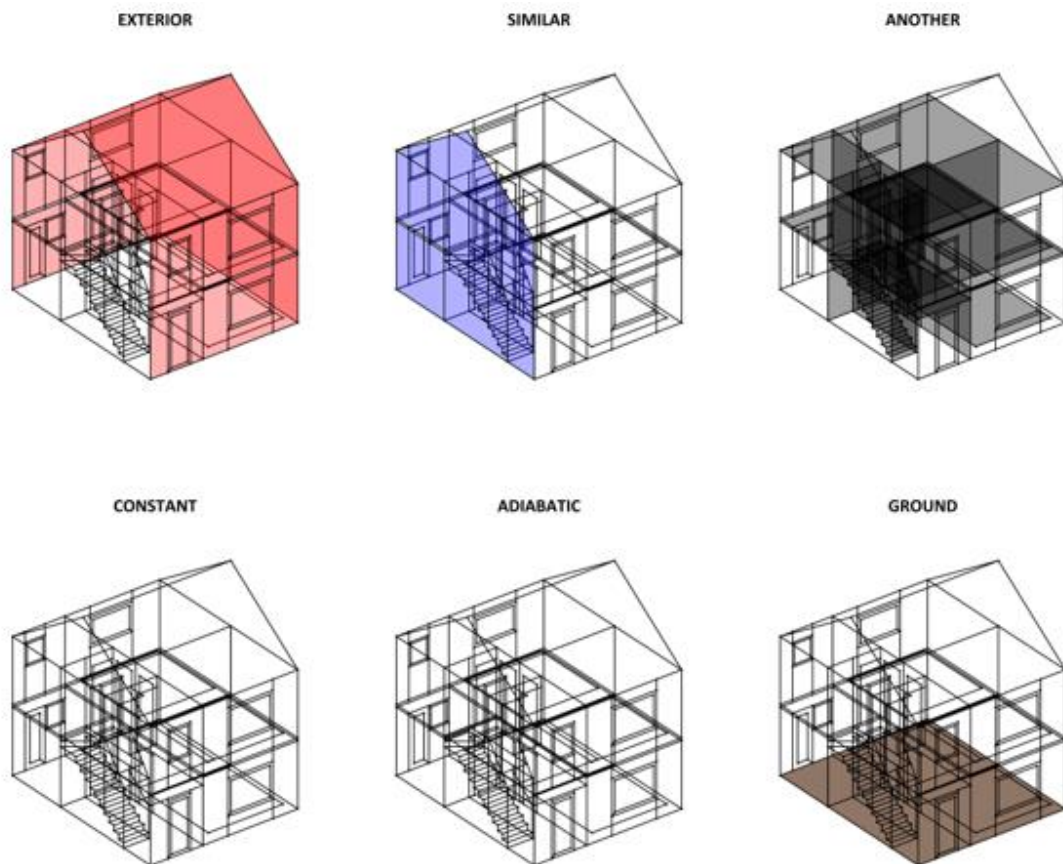


Figure 24 ESP-r model of 4010 semidetached house

The semidetached stock model in ESP-r consists of 9 individual zones: bedroom 1, bedroom 2, bathroom, cupboard, hallway, upper hallway, living room and roof space.

5.3 Construction Materials

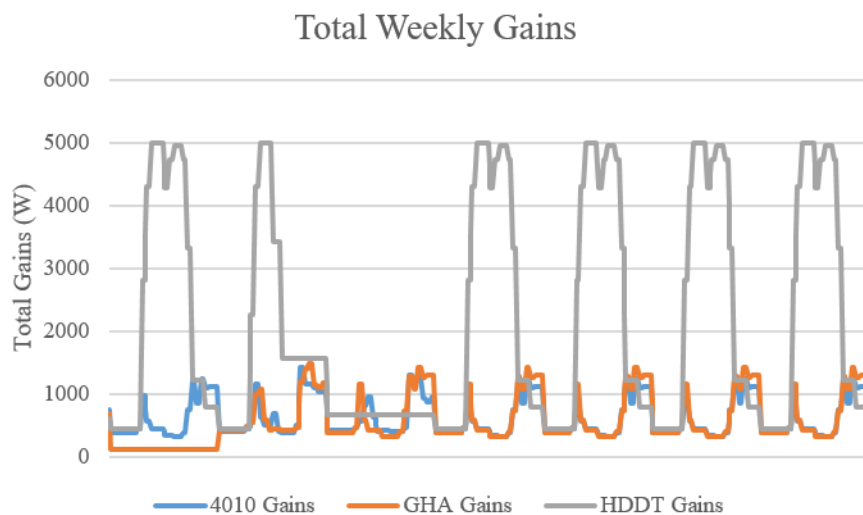
Due to the heuristic approach taken when developing these models, recreating them in Gridlab-D and for later analysis, the materials of the models were less important. Thus, the materials could be readily changed in both model types when real-life data is obtained in the future. Generic building materials were therefore used in all three models to help with identifying issues in both models with less complexity (Table 7). The full list of construction materials can be found in Appendix A, B and C.

Table 7 U-Values of construction materials in each model.

Material	HDDT U- Value	GHA U-Value	4010 U-Value
External Walls	0.291	0.295	0.433
Internal Walls	1.072	1.166	0.723
External Doors	1.322	1.074	1.322
Windows	2.243	2.243	2.243

5.4 Casual and Internal Gains

As each model was different, they all were modelled with different casual and internal gains. The casual and internal gains arise from occupancy gains, and small equipment electrical gains. They were modelled based on average number of people working in an office for HDDT, and average number of people living in a semidetached home and a bungalow. For HDDT, the gain profile followed a different profile of that of the dwellings due to the times that people spend in the work place is often the opposite of the time people spend at home. This is displayed in figure 25, with the much higher gains in the office building due to the office appliances on during the day such as printers, computers, photocopiers and lighting. The dwellings have two peaks during a day which highlights the time preparing for work in the morning and after work when people tend to use a lot of energy to prepare dinner and watch TV.

**Figure 25 Total weekly gains in the ESP-r models**

5.5 Heating and Cooling Systems

For all models a simple HVAC system from ESP-r was installed. For the comparisons it was decided to create three temperature scenarios. For the purpose of this research a basic control with 12 hours of heating and 12 hours with no heating at 5°C, 15°C and 25°C was implemented. No cooling system was modelled, as is standard in Scotland. Additionally, the task at hand was to assess how the models differ in their reaction after heating is switched off, so an additional cooling system was unnecessary.

5.6 Infiltration Rates

The infiltration rate assigned to a building, has a strong influence on the energy performance of a home or office building. It is the rate of air exchange between the outside environment with the internal building. For the purposes of this modelling and comparison experiment, the infiltration of air flow was included in the model design. Due to the complex behaviour of air flows in buildings due to temperature differences, wind speed and direction and occupancy behaviour and thermal comfort, a standardised value was used in the model. The standard value in ESP-r is 0.5 ac/h (air changes per hour), thus this standardised value was used throughout all zones in all three models for consistency (CIBSE Guide A, 2006).

5.7 Verification of the ESP-r models

After the initial development process of each model and once the building parameters were defined, the model had to be validated. The validation process is important to determine the applicability of the models. As ESP-r has been extensively validated by Strachan et al., (2008), and described at length by Clarke (2001) this verification process was very basic to account for large scale errors that may have gone unseen in the development process.

A logistical approach was taken when developing the model. For each model a normal heating period was defined and results were checked against a typical winter and a typical summer period to assess if the models represented real life situations.

6 Gridlab-D 2R2C Model

As previously described, the Gridlab-D 2R2C model needed certain input parameters to calculate the internal equations within the model. The parameters needed and gathered from ESP-r are listed in Table 8 below:

Table 8 Parameters taken from ESP-r for Gridlab-D modelling*

Primary Input Parameter	4010 Values	GHA Values	HDDT Values	Unit
Floor Area	106.8	106.9	237.5	m ²
Gross Wall Area	95.3	77.9	100.9	m ²
Ceiling Height	7.5	4.4	2.7	m
Aspect Ratio	1.2	1.2	1.5	none
Window Wall Ratio	0.1	0.07	0.12	none
Wall area	95.3	73.1	114.1	m ²
Window area	8.5	4.8	13.9	m ²
Number of Doors	7	6	4	none
Exterior Wall Fraction	0.9	100	42.8	%
Interior Exterior Wall Ratio	1.1	0.9	1.5	none
Exterior Ceiling Fraction	100	100	-	%
Exterior Floor Fraction	40.1	50	100	%
Number of Stories	3	2	1	none
R roof	2.3	2.3		m ² K/W
R wall	2.3	2.7	3.1	m ² K/W
R floor	1.5	1.4	3.6	m ² K/W
R windows	0.4	0.4	0.4	m ² K/W
R internal doors	0.4	0.4	0.4	m ² K/W
R external doors	0.8	0.8	0.8	m ² K/W
Window Shading	0.7	0.7	0.7	none
Window Exterior Transmission Coefficient	60	60	60	%
Glazing Layers	2	2	2	none

***Figures are rounded to nearest decimal place**

More extensive building information can be seen in Appendix A, B, & C.

A select few of the necessary parameters were not found in the ESP-r model, thus the Gridlab-D default numbers were used, such as 60% for the transmission coefficient.

Following on from the Gridlab-D overview in Section 3, the below configuration (Figure 26) was calculated within the software to give the results seen in section 8.

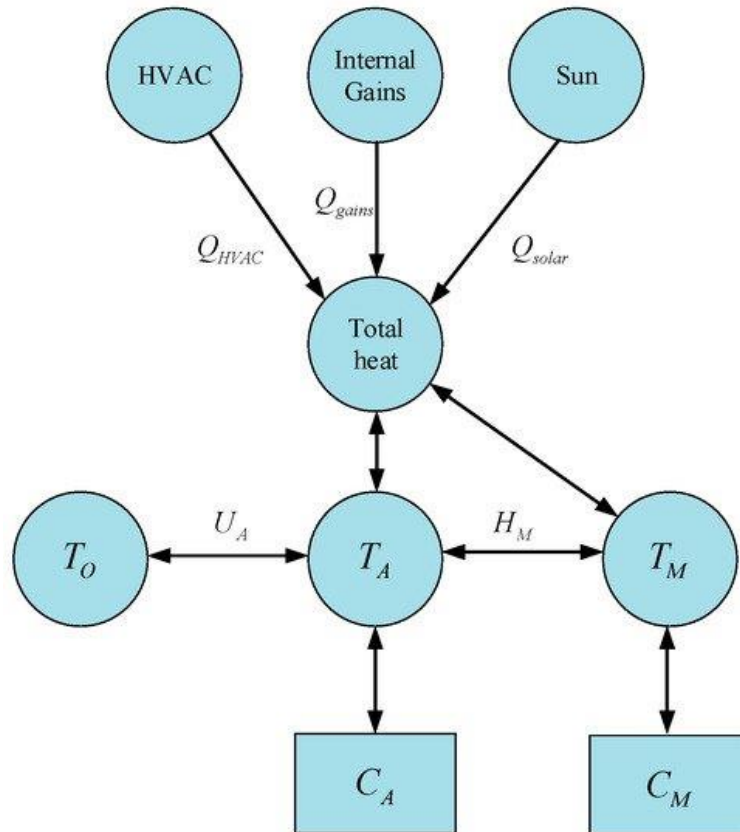


Figure 26 Thermal flow in Gridlab-D model (Zhou et al., 2019)

The air temperature and wall temperature node can be derived from the equations below:

$$Q_A - U_A(T_A - T_O) - H_M(T_A - T_M) - C_A \frac{dT_A}{dt} = 0$$

&

$$Q_M - H_M(T_M - T_A) - C_M \frac{dT_M}{dt} = 0$$

The first equation is used to calculate T_M , and is then used within $C_M \frac{dT_M}{dt}$, t being time (Zhou et al., 2019). A heuristic approach was used to alter the Gridlab-D inputs until the two models outputs were more comparable.

7 Model Comparison

7.1 Average Room Temps

The largest difference between the results from ESP-r and those from Gridlab-D is the internal temperature outputs. As Gridlab-D is a lumped capacitance model it ‘lumps’ the internal temperature as one, whereas ESP-r gives temperature results for each modelled zone within the building.

When comparing the two models it was necessary to use a validated internal air temperature within the ESP-r model for a more accurate comparison. There were a few methods of obtaining the best-fit average internal air temperature, a weighted average or a non-weighted average temperature. The weighted temperature would account for the volume of each room to calculate the total average temperature. Therefore, for larger rooms it would have a greater influence on the overall average than a smaller room would, and would not account for other factors such as occupancy or solar gains. Dimitriou et al., (2016) analysed and studied the effects of using a weighted or non-weighted average and came to the conclusion that the non-weighted average was a better fit, with an average r value of 0.93 in their Pearson’s Correlation calculations. They compared the two averages over an 8-week period and the non-weighted average delivered a smaller difference of 0.2°C compared to 0.4°C of difference with the weighted average. The use of the non-weighted average is beneficial when comparing the large datasets required for this thesis.

For this research, the collinearity between the internal air temperature of zones and the average temperature was analysed to identify any discrepancies between the variables. It was necessary to calculate whether Dimitriou’s (2016) analysis worked similarly on the models created in ESP-r of the archetypes in Huntly before further comparison.

7.2 Pearson Correlation Coefficient

The Pearson Correlation Coefficient is one of a few ways to calculate the relationship between two variables, given the Greek symbol ρ , (rho). It is calculated by dividing the covariance of the two values by the standard deviation, as in the equation below:

$$\rho(X, Y) = \frac{COV(X, Y)}{\sigma_X \sigma_Y}$$

The above equation uses the formula for covariance, $COV(X, Y)$. It is denoted as the expected value of the sum of the variance of X and Y from their corresponding means, which is further explained below:

$$COV(X, Y) = E[(X - \mu_X)(Y - \mu_Y)]$$

Thus, making the overall Pearson's Correlation equation clearer:

$$\rho(X, Y) = \frac{E[(X - \mu_X)(Y - \mu_Y)]}{\sigma_X \sigma_Y}$$

The relationship between two variables can be expressed as their collinearity. The more the two variables relate to one another the greater the collinearity. This method is often undertaken to identify the affinity between independent variables (Ebrahim, 2020).

The correlation coefficient between the average temperature and the air temperature of each individual room was calculated for all three archetypes in Python (Appendix D). One week in October was chosen for each matrix to allow for suitable comparison. The temperature set point in this week was set to 25°C, and switched off at 6am to show how the rooms behaved during the day after the heating was switched off. The below correlation matrices display the correlation coefficients between each variable, this allows for further analysis.

7.3 What is a ‘Good’ Correlation Coefficient Value?

The above Pearson Correlation equation can give results between -1 and +1. The positive values closer to +1 imply a high positive correlation between the two variables. On the other hand, values closer to -1 indicate a high negative correlation. If the result is around 0 then there is a lack of linear relationship between the values (Benesty et al., 2009).

Although there is a scale of results that the Pearson Correlation can deliver, there is no ‘good’ or ‘bad’ value. Generally speaking, a small correlation has values $0.1 > 0.3$, a moderate correlation is $0.3 > 0.5$, a large correlation $0.5 > 0.9$, and a certain correlation over 0.9. It should be noted that there is no causality between the compared variables (Benesty et al., 2009).

7.4 HDDT Average Temperature Analysis

As discussed previously, the HDDT model was developed specifically based on measurements available. A simplified version of their proposed development was created in ESP-r. The covariance matrix below (Figure 27) aptly displays the strong relationship between four out of the five rooms and the average dry bulb temperature, with values of 0.8 and above. The anomaly here was the staffroom, as identified before, the staffroom was an open plan room connected to the main hallway of the office building. As the main door of the office was part of the staffroom this could account for the lower correlation of approximately 0.45.

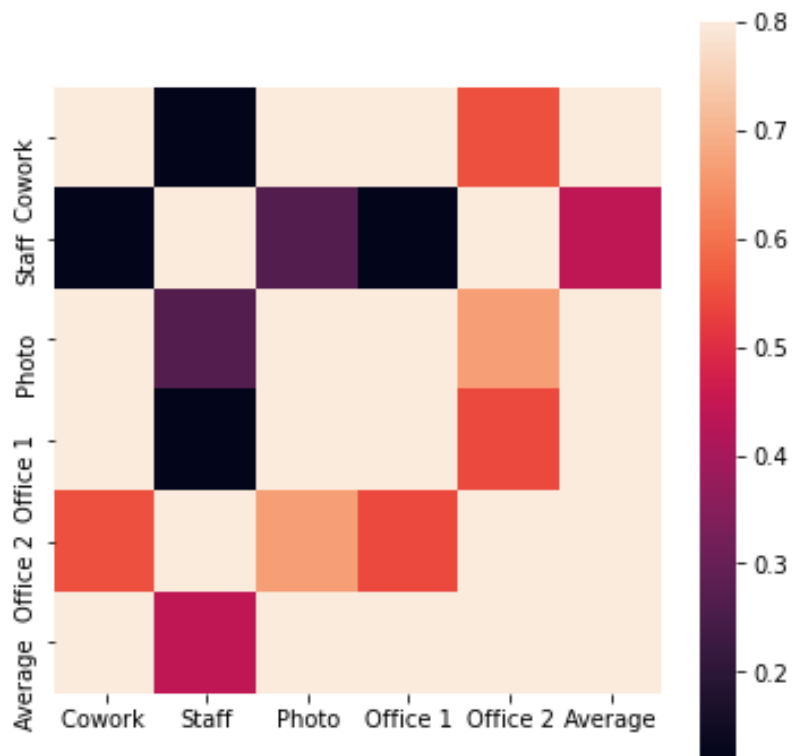


Figure 27 HDDT average dry bulb temperature correlation matrix

This theory is further explored when the histogram of internal temperatures was plotted in figure 28 below:

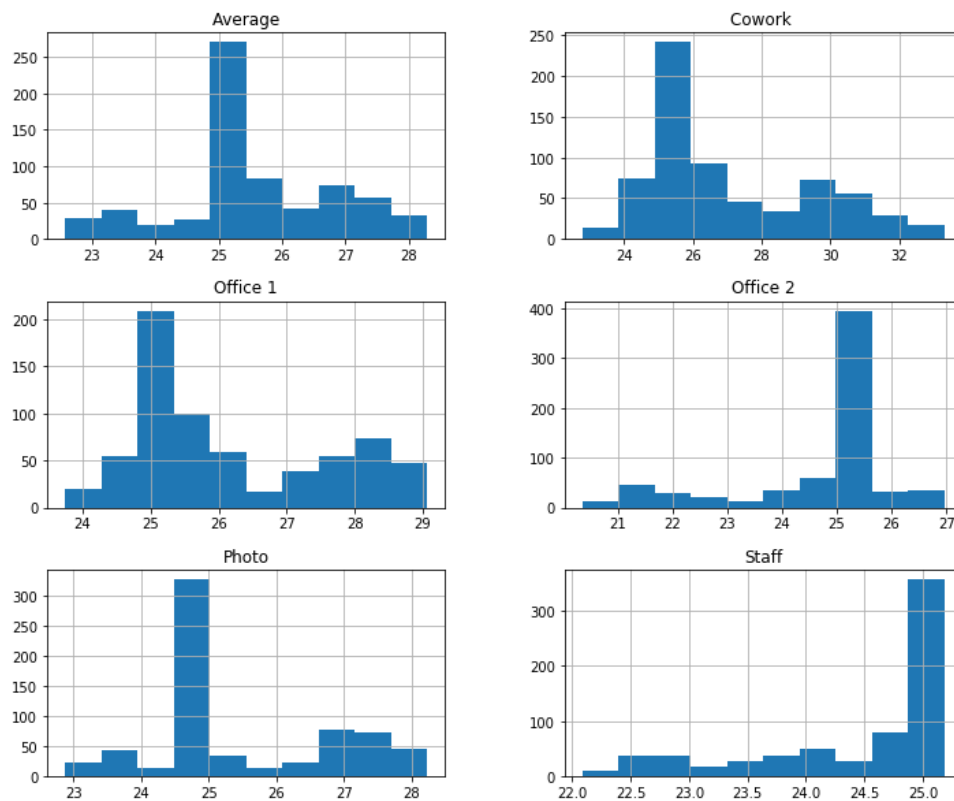


Figure 28 HDDT temperature histogram

The histogram of the temperature range in the rooms in clearly shows that the thermal behaviour of the staffroom differed greatly from the other rooms. The highest temperature in the staffroom was that of the set point, and thus external factors such as occupancy behaviour, equipment and solar gains had little effect on this room compared with the others. As aforementioned, the operational main door probably had a large impact on the lower temperatures within this zone.

7.5 GHA Average Temperature Analysis

The results from GHA were slightly different from HDDT. The covariance matrix for GHA (Figure 29) demonstrates that four of the seven zones in the bungalow have a strong relation with the average temperature, two zones (the kitchen and bedroom 1) show a slightly weaker correlation and the roof is very unrelated at 0.2.

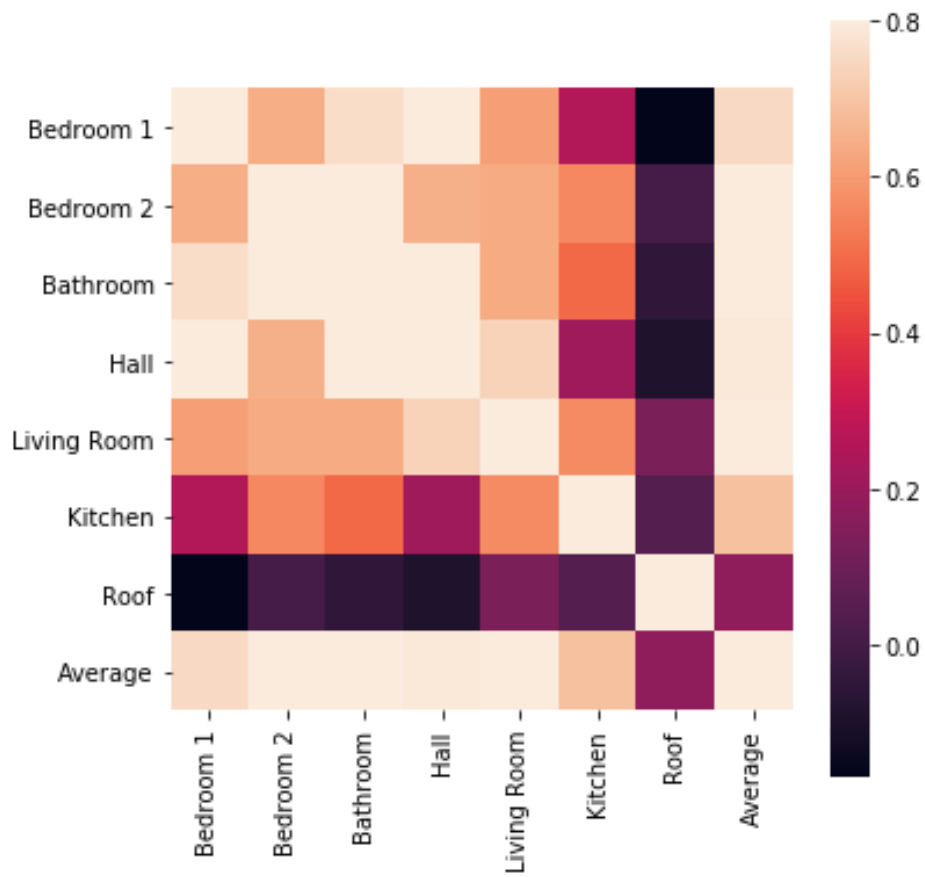


Figure 29 GHA average dry bulb temperature correlation matrix

The histogram (Figure 30) was used for further analysis to help identify the cause or root of the anomalies with bedroom 1, kitchen and the roof. The roof anomaly was due to the heating not being allocated to the roof space due to normal occupancy behaviour.

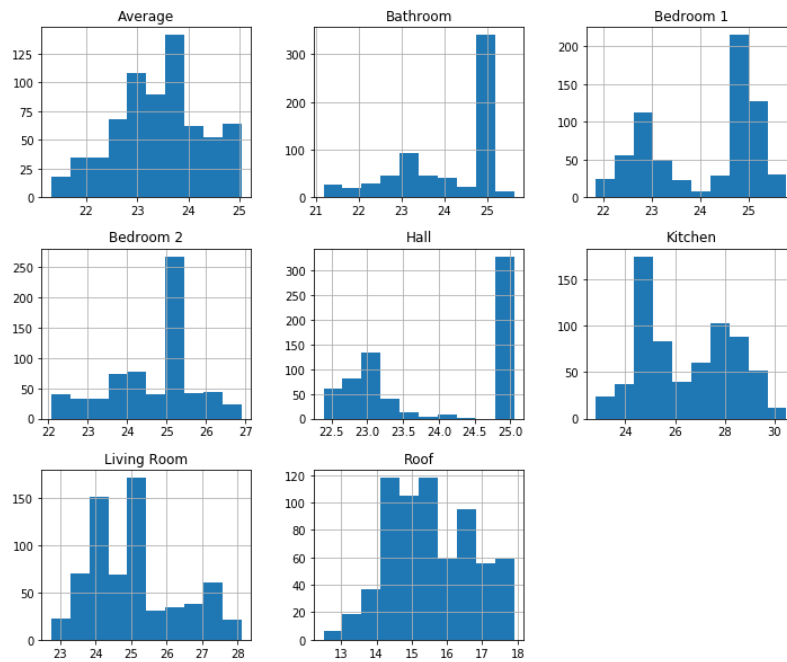


Figure 30 GHA temperature histogram

Additionally, the colder temperatures in the roof are due to the heat being lost through the roof to the outdoors. The kitchen as is warmer due to the small size, and greater internal gains from occupants and cooking equipment. Lastly, bedroom 1 is slightly warmer than the other rooms due to two occupants sleeping there and the solar gains it receives.

7.6 4010 Average Temperature Analysis

As expected, the 4010 correlation matrix (Figure 31) was similar to the output from GHA. Just as GHA, the roof and the kitchen were the main zones of disarray, with results of 0.2 and 0.4, respectively.

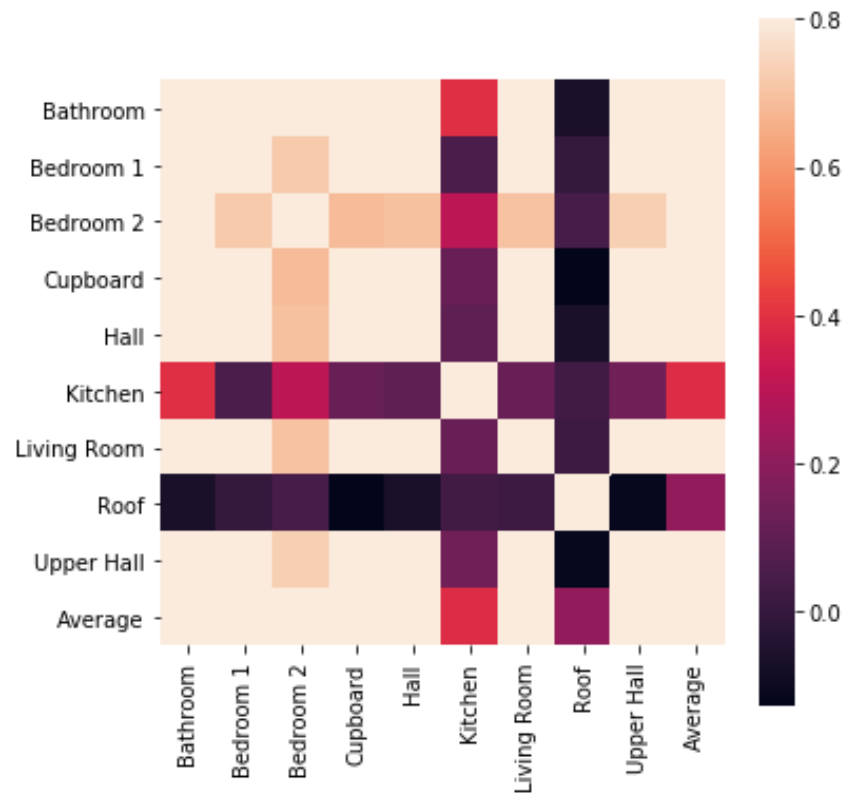


Figure 31 4010 Average dry bulb temperature correlation matrix

The histograms of internal dry bulb temperatures in Figure 32 are also similar to those of GHA. The kitchen in 4010 occasionally reaches temperatures 4°C higher than the rest of the rooms in the house. This can be accredited to the increased occupancy and equipment gains within this zone. In addition, to the kitchen, the roof is also an anomaly. As mentioned before, this is due to the temperatures being lost through the roof to the outside due to the temperature difference and due to the lack of heating within that zone.

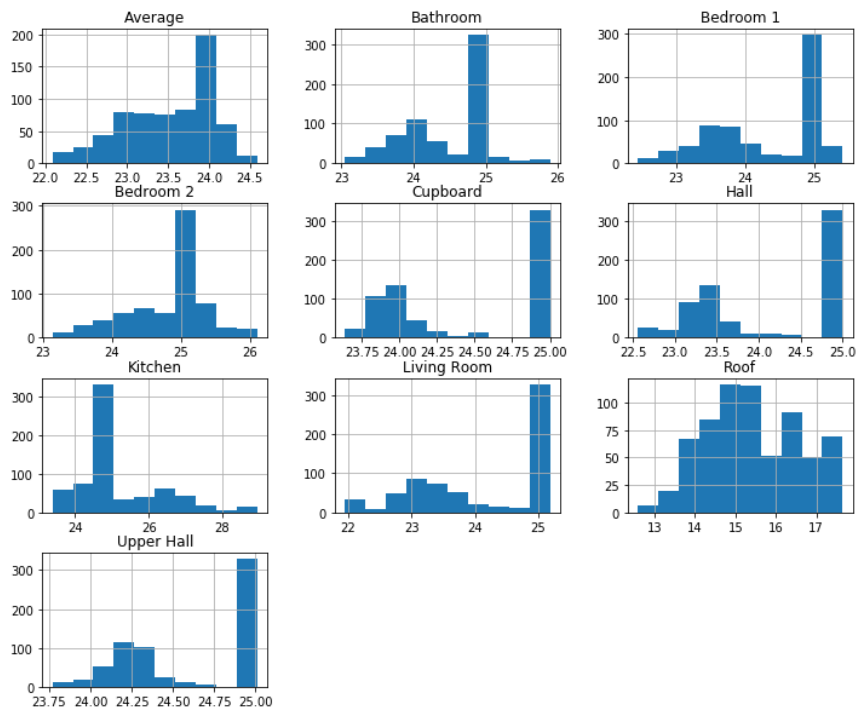


Figure 32 4010 Temperature histogram

7.7 Conclusions

In conclusion, the average dry bulb temperature for each archetype shows expected correlations throughout the majority of each model. However, due to air flows, unheated zones, and internal gains some zones do not show a strong correlation with the average temperatures. As values over 0.5, still determine a ‘large correlation’, it could be said that the average dry bulb temperature for HDDT could be used for further analysis. For GHA and 4010, removing the roof temperature from the average calculation would create a stronger relationship between the average and the individual zones. Therefore, for further analysis the average temperature was used for HDDT and for GHA and 4010 the average temperature (excluding the roof) was used.

Table 9 Choice of measured average temperature for further comparison

Model	Choice of Measured Average Temperature for Comparison
HDDT	Average Dry Bulb Temperature
GHA	Average Dry Bulb Temperature (excluding roof)
4010	Average Dry Bulb Temperature (excluding roof)

8 Tuning Gridlab-D Model

From the initial stages of our research and simulations it was clear that the inputs given to Gridlab-D from ESP-r did not manage to achieve similar outputs. Our initial hope was that editing the basic physical properties in Gridlab-D could give a representative model. However, this was not the case, as the Gridlab-D model of a house is based on a typical wood frame residential home.

A number of modifications were made to the Gridlab-D model to train it to produce similar outputs as the ESP-r models. The process of ‘tuning’ is to calibrate the model to maximise its function, without overfitting to the original data points. This process was done by visualisation of the outputs, comparisons, deliberations and the selection of ‘hyper-parameters’ to tune the model to.

The overall house model created in Gridlab-D is built to represent a single family home, to create anything different from this, simple commands can be implemented. These small alterations generate a standardised house with default parameters described later in this section. This standard house can be readily modified in terms of floor area, window to wall ratios etc. Below is a detailed review of the basic house model created in Gridlab-D and an explanation of how it was modified.

8.1 Thermal Mass

Thermal mass of a building determines how well it stores and retains thermal energy. As highlighted in figure 33, a high thermal mass can prevent a building from overheating, or cooling too quickly after the heating has been turned off. This increases the ‘thermal lag’ in buildings to slow down the heat loss. The Gridlab-D parameters for total thermal mass per m^2 floor area was $0.35 \text{ KJ/m}^2\text{K}$. However, in reality Scottish buildings tend to have a much higher thermal mass (De Saulles, 2009).

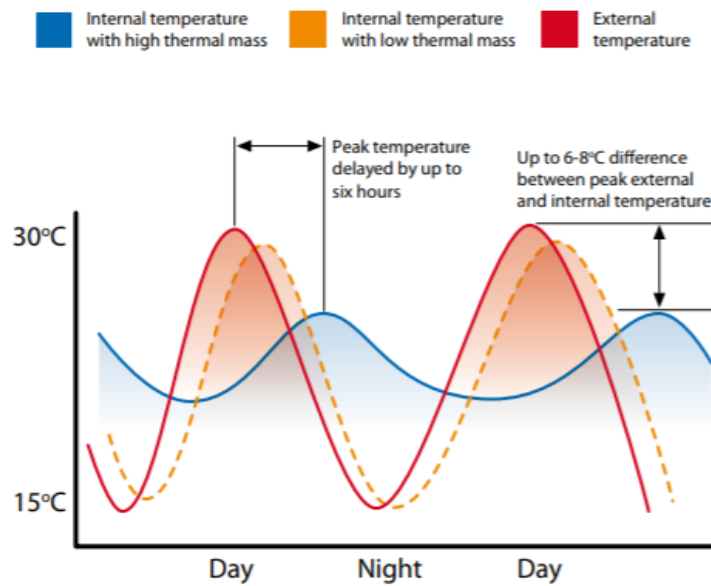


Figure 33 Effect of Thermal mass on internal temperatures (De Saulles, 2009)

The thermal mass parameter is calculated by dividing the sum of construction elements by the total floor area (Greenspec, 2020), see equation below:

$$TMP = \frac{Cm}{TFA}$$

Cm = sum of (area x heat capacity) construction elements

TFA = Total Floor Area

The values in the table below were used in the Gridlab-D simulations:

Table 10 Thermal mass of un-tuned and tuned Gridlab-D models

Model	Thermal Mass – Untuned Models (KJ/ °Cm ²)	Thermal Mass – Tuned Models (KJ/ °Cm ²)
HDDT	270	0.7
GHA	270	500
4010	270	400

Above, you can see that the default thermal mass was changed in Gridlab-D to represent a standard Scottish house with a thermal mass of 270 KJ/ °Cm². However, when tuning

the model, it was found that we needed more thermal mass for the house archetypes, and less thermal mass for HDDT. The extremely low value of HDDT in comparison with the other two models was definitely a cause for concern. This could be to do with the floor area for HDDT being larger, and also that the building type is quite different as it is open plan vs the multi roomed residential buildings. Additionally, there could be added uncertainties with the HDDT model as it was created from scratch. Thus, the attempt to tune this aspect of HDDT was not representative of its ‘real’ thermal mass.

8.2 Weather Data

The same weather data used in ESP-r was used for the Gridlab-D simulations for consistency. However, solar gains in Gridlab-D were adjusted by altering the window shading parameter (the amount of solar irradiance that enters the modelled building). The default in Gridlab-D was set to 0.67, however it was reduced to allow less solar into the house similar to ESP-r.

8.3 Occupancy Data

The occupancy data in Gridlab-D was exported from ESP-r as total internal gains. This time-series data from ESP-r was then extrapolated for use directly in Gridlab-D. Figure 34 below is an example of weekly total gains of each room in the HDDT office.

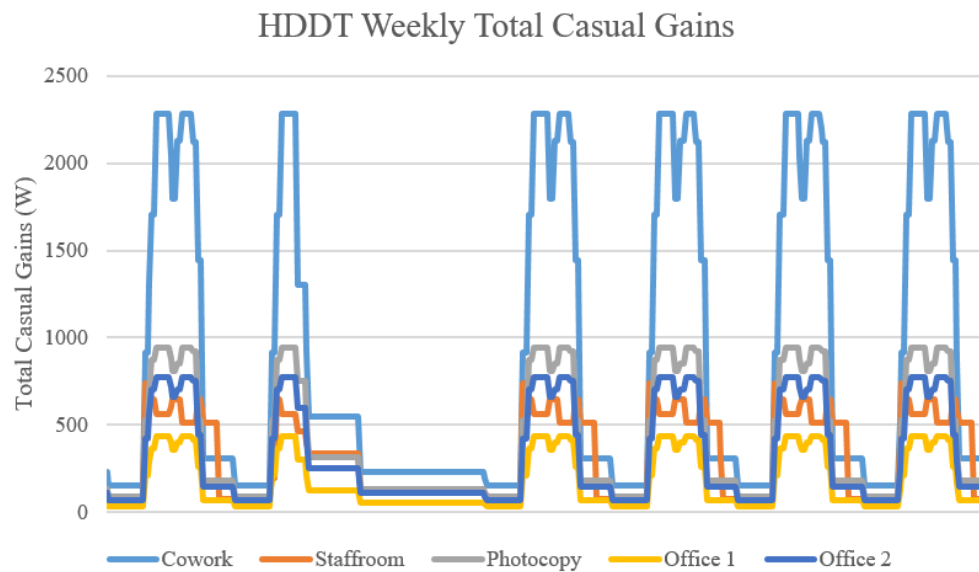


Figure 34 Total internal gains exported from ESP-r for HDDT Gridlab-D tuning

8.4 Framework

The initial framework has been developed for future simulations and comparisons, primarily in Python and Gridlab-D. This will allow for the real pilot data to be readily implemented when it is received from both Huntly and from ESC. When the live trial data has been made available, the houses will be modelled directly and the errors between our predictions and the live data will provide vital analysis.

8.5 Temperature Setpoint

After our initial overview of the thermal behaviour of the two models, it was obvious that the Gridlab-D model was not reacting in the same way as the ESP-r model. This was due to the Gridlab-D model not responding to the outside boundary conditions. Thus, the models had to have a set point initiated from which they would normalise from. The Gridlab-D models compared in the next section have an internal set point of 25°C from which they start, which allows them to behave more similarly to the ESP-r models, in that they use the boundary conditions to regulate their thermal behaviour.

9 Results: Data Analysis of the Errors Between Models

Once, the models were developed in ESP-r and Gridlab and ‘tuned’ to be of use, they were further compared to visualise at which points throughout the year and throughout the day they were most similar or most dissimilar. This was achieved by running 48 simulations for each model, 144 in total.

Simulations were run for a week over four months (January, April, July and October) to analyse the seasonal behaviours of the models. In addition to this, simulations were set at 3 different set points (5°C, 15°C and 25°C) to see how the models reacted to different temperature settings in different seasons. Finally, the heating was switched off at different times in the day (6am, noon, 5pm, and 8pm) to see how boundary conditions such as occupancy, and solar gains affected the models. Each was run for 12 hours at a constant temperature then switched off for the following 12 hours. To visualise the accuracy of how the models reacted thermally, RMSE values were also noted 0.5, 1, 2, 4, 6 and 12 hours after the heating was switched off. Additionally, the models were run through Python to create a consistent temperature comparison for each simulation.

For this research, the errors between each model were calculated with the Root Mean Square Error (RMSE) method. Following this, the errors were displayed in box and whisker plots (Appendix E – J and Section 9.2) to further explore the position of the inaccuracies between the two models.

9.1 Root Mean Square Error

The Root Mean Square Error (RMSE) method measures the standard deviation between known results and unknown results (the residuals). Therefore, RMSE measures the accuracy of fit between predicted (f) and observed values (o).

$$RMSE = \sqrt{(f - o)^2}$$

In other words, the RMSE is a way of measuring the spread of data from the regression line or line of best fit. It is a standard way of verifying results in data analysis.

9.2 Box and Whisker Plots

To get an initial overview of the data, the overall RMSE values for each model were plotted as Box and Whisker plots.

9.2.1 HDDT Box and Whisker Plots

The overall range of RMSE values from HDDT across the full year and at every temperature switch off point was between 0 and 11, which shows there is a large range of errors (Figure 35). However, the median of this data was approximately 3, which is significantly lower than the highest RMSE value of nearly 11. Additionally, when the monthly profiles are studied (Appendix E), there is a large difference in the median value and overall range. January has a median range between 2 and 3, April between 3 and 5, July between 6 and 8 and October between 0 and 2. Finally, the errors after the heating was switched off were analysed to see what time of the day was more accurate at predicting the internal temperature (Appendix F). The lowest median range was with a 6am switch off or 8pm switch off. However, the overall RMSE range for these was 7 and 10, respectively. The lowest range of errors after switch off was within 0.5 hours and the full 12 hour profile, with highest errors around 4-6 hours after switch off.

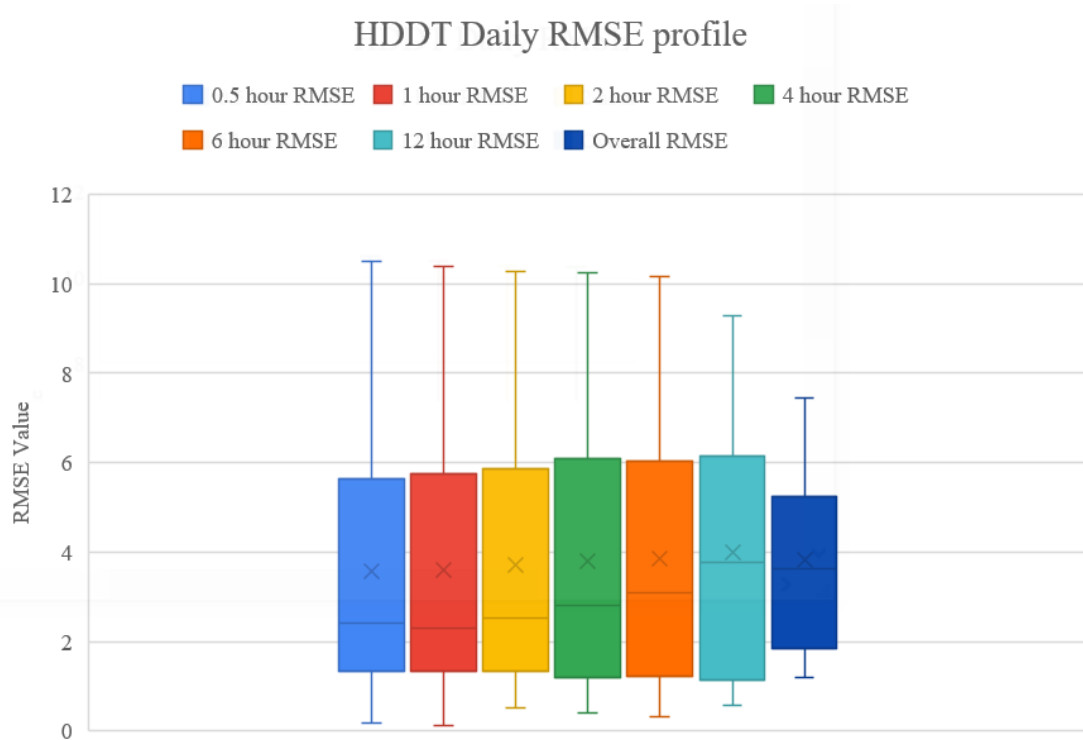


Figure 35 HDDT Daily RMSE profile across the four seasons

9.2.2 GHA Box and Whisker Plots

For GHA, the overall RMSE values for the year are plotted in Figure 36. The overall range of values was between 0 and 7, still highlighting a high range, but less than that of HDDT. Additionally, the median was lower than HDDT between 2 and 3.

The monthly profiles were also evaluated (Appendix G), highlighting January with a median range between 4 and 5, April around 2, July between 3 and 4, and October between 1 and 2. Then again, the after switch-off errors were analysed (Appendix H) and the range was consistently below 6 across each switch-off time. Also, the median range for each switch-off plot was consistently between 2 and 3, with the exception of 8pm switch off between 2 and 4. In this case, the largest error after switch-off tended around the 2 hour mark.

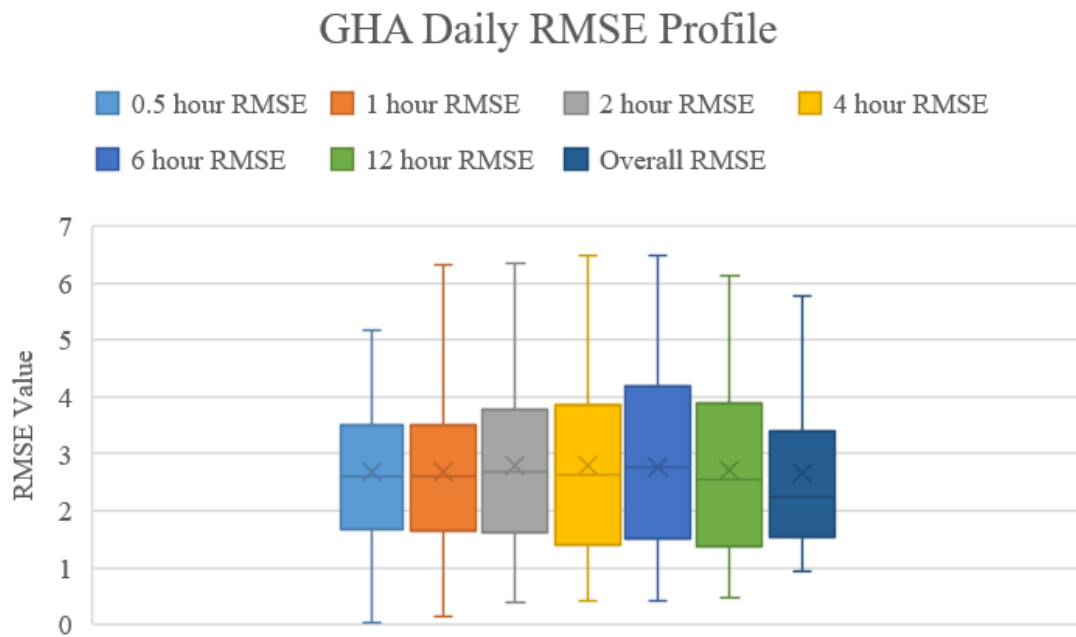


Figure 36 GHA Daily RMSE profile across the four seasons

9.2.3 4010 Box and Whisker Plots

Finally, for 4010 the overall range of RMSE across the year was up to 8 with a median between 3 and 4 (Figure 37), slightly higher than the bungalow model. Further studying of the monthly profiles (Appendix I) shows January with a median range between 3 and 4, April between 2 and 3, July between 3 and 5 and October less than 1. Lastly, the after switch-off errors for 4010 (Appendix J) are shown. After each switch off the range is up to 8 with a median between 2 and 4, except for after noon switch off where the range is up to 4 and median values between 2 and 3. For the 12 noon switch off, the lowest ranges of errors was after 4 and 6 hours. Whereas the other switch off times show smallest errors within half an hour.

These results are further discussed in Section 10.

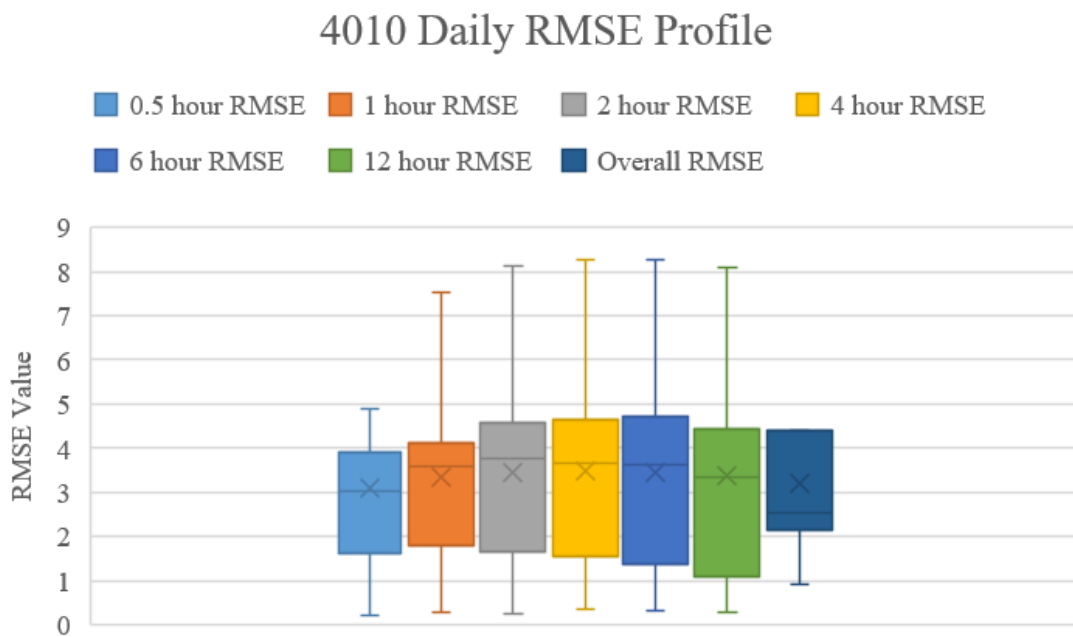


Figure 37 4010 Daily RMSE profile across the four seasons

9.3 Temperature Comparisons for Each Model

In Appendix K, you can see the best and worst RMSE values across all 48 simulations for each model highlighted as green and red. Below is a comparison of each models best and worst fit simulation across the year. The average dbT (dry bulb temperature) is compared against the GL_T:indoor temp (Gridlab-D tuned indoor temperature):

9.3.1 HDDT Comparison

For HDDT the worst fit simulation was with the 5°C set point, and the 8pm turn off during July (Figure 38). It is clear that both models react similarly to daily fluctuations, however the Gridlab-D model seems to retain heat more than the ESP-r model.

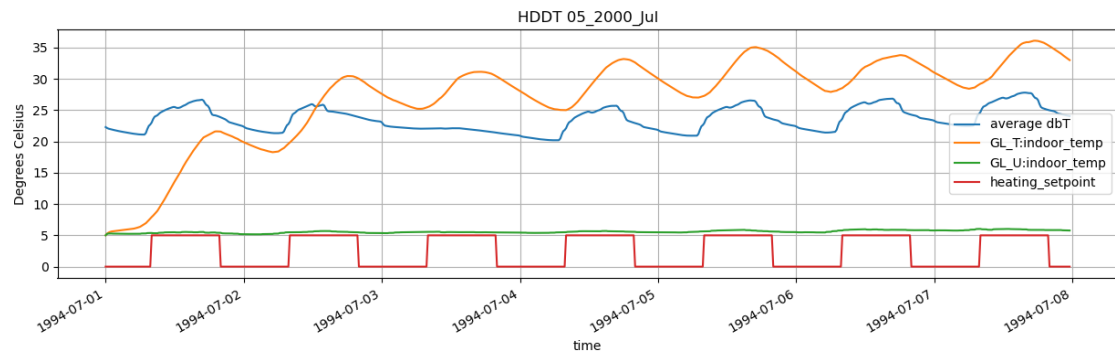


Figure 38 HDDT Worst fit temperature comparison between two models

However, the best-fit simulation was the 25°C, after the 8pm switch off during the month of October (Figure 39). This demonstrates much clearer how the models are acting similarly in a cooler climate, with a higher temperature set point. Due to the heating not being necessary during the warmer summer months, these results are not too problematic.

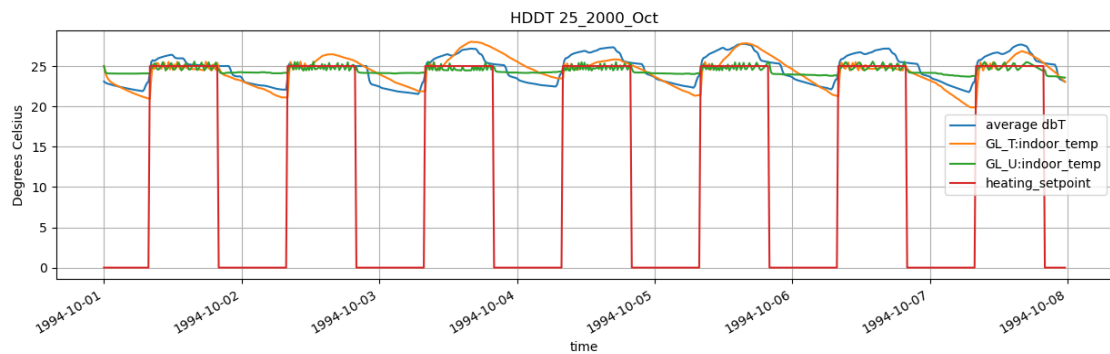


Figure 39 HDDT Best fit temperature comparison between two models

9.3.2 GHA Comparison

The same thing was done with the GHA model to visualise the fit between the ESP-r and Gridlab-D models. For GHA, the worst-fit simulation was that at 5°C set point, and the 12 noon switch off during January (Figure 40). The Gridlab-D model ‘flat-lines’ rather than responding to daily changes such as solar gains and occupancy gains, this could be due to the cold month of January, and the high thermal mass of the building.

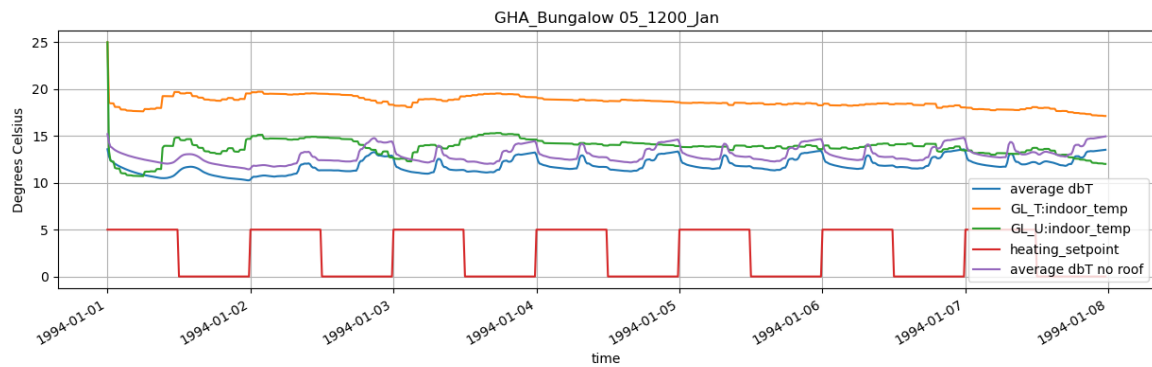


Figure 40 GHA Worst fit temperature comparison between two models

Similarly to HDDT, the best-fit simulation for GHA was during October. However, the temperature set point was 5°C and the turnoff time was 12 noon (Figure 41). The tuned Gridlab-D model doesn't seem to respond to daily fluctuations in the same way as the un tuned model. However, the temperature values are much more closely related to that of the ESP-r model.

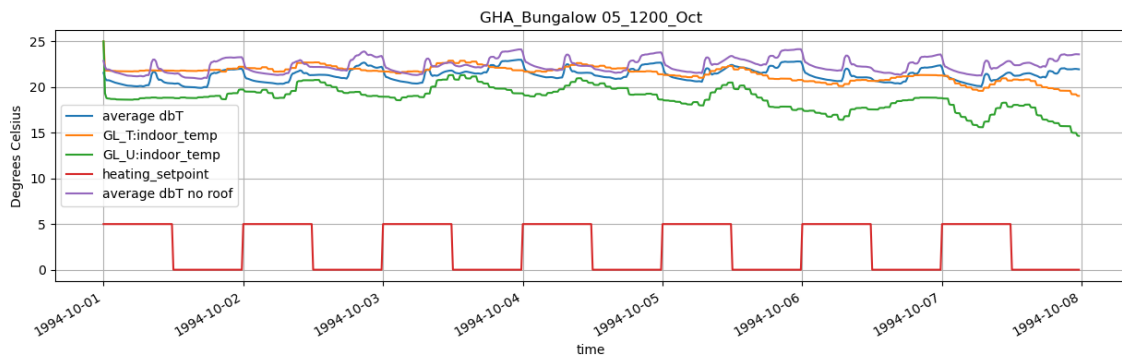


Figure 41 GHA Best fit temperature comparison between two models

9.3.3 4010 Comparison

Finally, for the 4010 semi-detached house model the worst fit simulation was that of 5°C set point, at noon switch off during January (Figure 42). The Gridlab-D models are significantly warmer than the ESP-r models, due to the high thermal mass parameter. Similarly to the other two models, the daily fluctuations are not visible, possibly due to the colder weather and darker days.

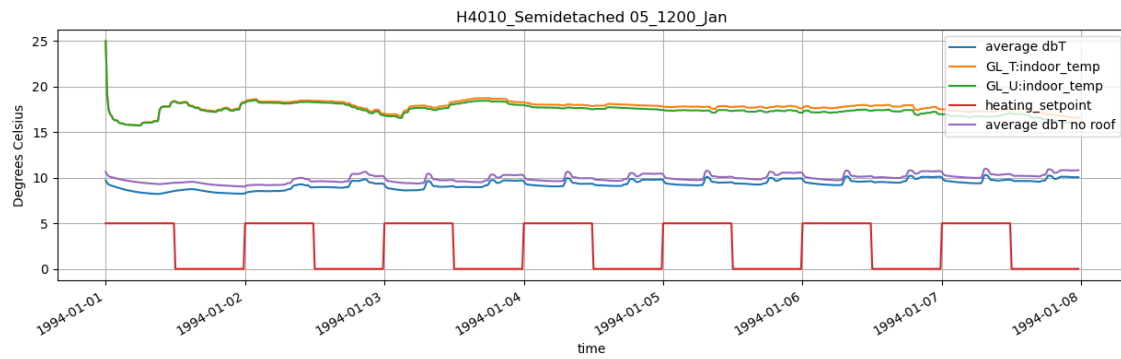


Figure 42 4010 Worst fit temperature comparison between two models

Similarly to the other models, for 4010 the best-fit simulation (Figure 43) was during October, at the 15°C set point, after the 8pm heating switch off time.

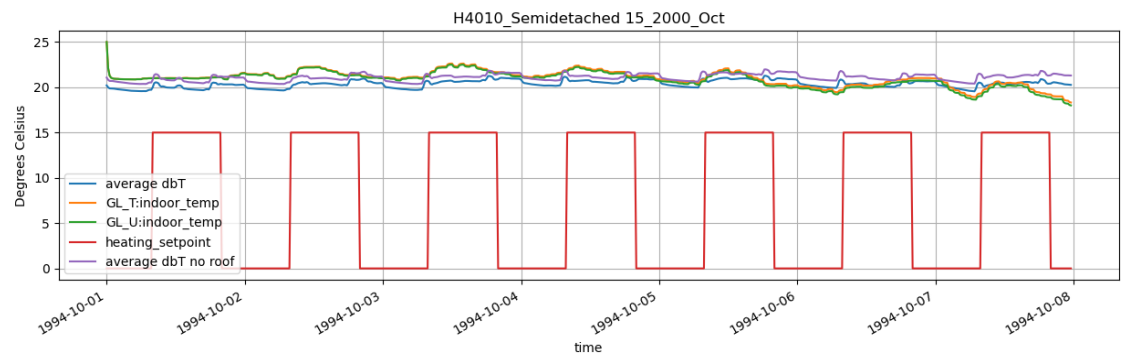


Figure 43 4010 Best fit temperature comparison between two models

Furthermore, the October month shows best fit between the two models. In this example the daily fluctuations are visible in the tuned Gridlab-D model and the ESP-r model, with similar profiles after the heating is switched off.

10 Discussion

For this body of work, our initial hope was that editing the basic physical properties could give a representative model in Gridlab-D. However, this was not the case, as the Gridlab-D model of a house is based on a typical wood frame residential house. This work composed of of running simulations and comparisons and re-running with ‘tuning’ until the level of discrepancies decreased. In hindsight, a few more weeks of tuning and understanding the Gridlab-D model would have been extremely beneficial in our development.

10.1 What is causing the errors?

After the errors in Section 9 were highlighted it was crucial that an evaluation of the potential causes was undertaken. One error may be from the flatter temperature profile from the Gridlab-D models. As previously discussed, this is due to the forced background temperature within the model. Thus, in future development of the 2R2C model within the Cloud ZUoS project this will have to be investigated further. In addition, the weekly profiles may be too short a time period for suitable comparison. To account for this, yearly outputs from ESP-r could be generated. This yearly profile would enable a greater visualisation of when the models correlate best. Lastly, the high thermal mass values of the residential dwellings and the low value for HDDT could be leading to the ‘flat-lining’ of temperature profiles. This problem will also be further addressed with the use of existing building data.

10.2 Seasonal Variation

The comparison has shown that through tuning and calibration that the correlation between the two models is determined by seasonal changes. The results show that all three ESP-r models and their Gridlab-D counterparts are most similar during the month of October and most dissimilar during April and July. The accuracy for the warmer

months is less important than that of October of January due to the smaller need for heating during these months.

10.3 Hourly Variation after Switch off

For future use, the comparability between the two models after the heating was switched off was assessed to determine how useful the Gridlab-D model would be for predicting internal air temperatures. The two residential dwellings were generally more comparable in their reaction to the heating being switched off. The three models median range of variation across the year was between 2 and 4. This means that on average they vary between 2°C and 4°C of one another. Although this number doesn't seem large, it could be the difference between 16°C (uncomfortable) and 20°C (comfortable) within your home. All three models were consistently well tuned in the first half an hour after heating was turned off, especially in the colder months. However, analysis of HDDT showed that overall it wasn't as similar. This dissimilar behaviour could be related to the downstairs of the office being modelled without the influence or knowledge of the floor above.

10.4 Limitations of Study

The greatest limitation of this study was the that the work was developed on archetypes with no real data for validation. One of the other major limitations to using Gridlab-D model for comparison was its inability to normalise its thermal behaviour in response to boundary conditions without forcing a temperature set point on it.

10.5 Key Findings

The key findings of this research is that it is possible to create a simplified lumped capacitance model based on a white box models outputs. A heuristic approach to tuning a simplified 2R2C model is possible when guided with the results from a more detailed white box model developed in ESP-r. Both models were designed to determine whether

they react similarly once a heating system has been turned off. The main finding has been that with the colder months of January and October, and higher heating set points of 15°C and 25°C the errors were lower. Conversely, the warmer months show greater errors. Therefore, larger errors with no heating (5°C) and the warmer months, is not too problematic as the heating would not be as likely to be running for as long or as high.

11 Conclusions

The main aim of this thesis was to develop bottom-up heat models for buildings identified for the Cloud ZUoS smart-grid project in Huntly, Aberdeenshire. With the aid of researching relevant academic papers and similar industrial platforms, an overview of bottom-up heat models was gathered and two energy modelling tools were chosen. Due to the ESC Living Lab data being unavailable, three archetypes were developed and created in ESP-r based on information gathered from the initial survey of Huntly. The Gridlab-D lumped capacitance model was chosen as a grey-box model for comparison with the ESP-r white-box model, due to its' ability to be readily integrated with the wider ZUoS platform. The simplified 2R2C model in Gridlab-D used the extrapolated building data from the ESP-r parameters. The use of average house temperatures for comparison was analysed and justified using covariance matrices and histograms. With the help of engineers at Scene, the tuning of the Gridlab-D model was undertaken to generate outputs that achieved similar results as the ESP-r models. The RMSE method of analysis was chosen to identify large areas of discrepancies between the models after certain switch off times, with different temperature set points and across four months within the year. In addition to this, the temperature comparisons were commanded through a Python script to visualise the areas of best and worst fit.

The results from this body of work concluded that:

- It is possible to create a simplified lumped capacitance model based on a white box model such as ESP-r.
- The use of average whole house temperatures for comparison is a suitable representation of the models developed in ESP-r
- The two comparative models are most similar during the winter months when heating is needed.

- The 2R2C model created in this work still needs more development to reduce errors.
- The 2R2C lumped capacitance model, once finalised will be readily implemented in the wider Cloud ZuoS platform.
- Real-time data of heating demand and building parameters will be pivotal in developing the simplified lumped capacitance model further.

11.1 Future Work

This thesis was originally designed to utilise operational data from a set of dwellings within the UK to build simple thermal building models of house in Huntly, Aberdeen. This was then hoped to explore the capability of lumped parameter models in portraying individual homes with built in heat pumps.

This research has concluded that the use of ESP-r to train more simplified models such as the lumped capacitance model in Gridlab-D is possible, with the aid of further tuning. The main area of research this paper has outlined has been the comparability of the ESP-r model to the Gridlab-D one. The residuals of both models have been substantially tested. However, an area for future work could be to plot the normal probability of the residual values to highlight any more abnormalities.

Further research could also include more detailed calibration, with the use of another covariance matrix. This covariance matrix could use all the inputs and outputs from ESP-r to find the most important ones to be used in a more simplified tool. This could allow for a stand-alone lumped capacitance model that could be more readily integrated into future simulations. This is beneficial, because ideally, the inputs for ESP-r and the lumped capacitance tool should not be different from one another. The less changes to sensitive parameters the more accurate the simplified model would be.

I suggest the following ideas for further work, to achieve a better comparison ideal for more synergistic integration with the Cloud ZUoS project:

- Use the real life data (expected from ESC in the coming months) to help train these simplified model and validate it.
- Use the acquired data for model predictive control of the homes.
- Yearly data comparison, using more machine learning methods rather than the manual comparison of 4 weeks across the year for a more exhaustive results set to visualise how the models work inter-seasonally.
- To create an extensive data base of dwelling types for more cost effective IoT modelling. This bank of building data could be deployed readily with minor manipulations and tuning.
- With the aid of the ESC Living Lab Data, thermal comfort could be further explored and validated within the ESP-r stock models.
- A study of the carbon and economic savings achieved by MPC within Huntly.
- Increase data operability and time synchronisation to enable higher accuracy of predictions so the model can react quickly to changes in temperature, occupancy, and heating set points for faster integration with IoT services.
- Integrate the simplified lumped capacitance model into the wider ZUoS platform.

11.2 Integration with Cloud ZUoS Platform

The pilot is due to start around September 2020 and run for 6 months. Before the pilot starts, we will be installing monitoring and communications equipment to assess energy flows, and new renewable technology within some of the pilot participants who are interested in investing in this technology. For each customer it is hoped that 2 EV charging points will be added, a 1MW heat pump for direct prediction and control, with 2 domestic batteries across 60 dwellings.

The overall ZUoS solution will enable the smart control of EVs, batteries and electric vehicles in accordance with local generation and network conditions. In order to understand how heating within a home can be scheduled, the electrical load it places on the network under a business as usual scenario must be understood. Then, different heating control strategies can be applied, and the consumer comfort assessed, to ensure end users are not ill affected by this control.

In the live ZUoS platform local networks will have homes represented by simplified heat models. These must have sufficient accuracy to allow for heat forecasting and scheduling, but also compute at a sufficiently high speed to allow for real time scheduling based on local network conditions. In the nearer term, this heat modelling will support the simulation work of the ZUoS project, which will test out building control strategies within homes.

References

- Allison, J., Cowie, A., Flett, G., Hand, J.W., Hawker, G. and Kelly, N.J., 2018. Modelling responsive demand from electrified domestic heating and storage under different operating strategies. *uSIM-Urban Energy Simulation*.
- Alptekin, C. 2019. *How The Energy As A Service (EaaS) Business Model Works*. Available: <https://www.iotacommunications.com/blog/energy-as-a-service-business-model/>. Last accessed 18th June 2020.
- Arif, M., Kafatygiotou, M., Mazroei, A., Kaushik, A. and Elsarrag, E., 2016. Impact of indoor environmental quality on occupant well-being and comfort: A review of the literature. *International Journal of Sustainable Built Environment*, 5(1), pp.1-11.
- Benesty, J., Chen, J., Huang, Y. and Cohen, I., 2009. Pearson correlation coefficient. In *Noise reduction in speech processing* (pp. 1-4). Springer, Berlin, Heidelberg.
- Braun, J.E. and Chaturvedi, N., 2002. An inverse gray-box model for transient building load prediction. *HVAC&R Research*, 8(1), pp.73-99.
- Braun, M.R., Altan, H. and Beck, S.B.M., 2014. Using regression analysis to predict the future energy consumption of a supermarket in the UK. *Applied Energy*, 130, pp.305-313.
- BPI. 2016. *Technically Speaking: Principles of Heat Transfer*. Available: <https://www.bpihomeowner.org/blog/technically-speaking-principles-heat-transfer>. Last accessed 5th June 2020.
- CCC, 2019. *UK Housing: Housing Fit for the Future?*
- Çengel, Y.A., 2007. Green thermodynamics. *International Journal of Energy Research*, 31(12), pp.1088-1104.
- Cerezo, C., Sokol, J., Reinhart, C. and Al-Mumin, A., 2015. Three methods for characterizing building archetypes in urban energy simulation. A case study in Kuwait City.
- Child, M., Ilonen, R., Vavilov, M., Kolehmainen, M. and Breyer, C., 2019. Scenarios for sustainable energy in Scotland. *Wind Energy*, 22(5), pp.666-684.

Clarke, J.A., 2006. Trends in building energy modelling and simulation. In *Proceedings of the World Renewable Energy Congress IX*.

Clarke, J.A. and Hensen, J.L.M., 2015. Integrated building performance simulation: Progress, prospects and requirements. *Building and Environment*, 91, pp.294-306.

Clarke, J.A. and Kelly, N.J., 2001. Integrating power flow modelling with building simulation. *Energy and Buildings*, 33(4), pp.333-340.

Clarke, J.A. and Strachan, P.A., 1994. Simulation of conventional and renewable building energy systems. *Renewable Energy*, 5(5-8), pp.1178-1189.

Deloitte, 2020. *Energy-as-a-Service The lights are on. Is anyone home?*. Available: <https://www2.deloitte.com/uk/en/pages/energy-and-resources/articles/energy-as-a-service.html>. Last accessed 18th June 2020.

Dewson, T., Day, B. and Irving, A.D., 1993. Least squares parameter estimation of a reduced order thermal model of an experimental building. *Building and Environment*, 28(2), pp.127-137.

De Saulles, T., 2009. Thermal mass explained. *Concrete Centre*.

Dimitriou, V., 2016. Lumped parameter thermal modelling for UK domestic buildings based on measured operational data (Doctoral dissertation, Loughborough University).

Dimitriou, V., Firth, S.K., Hassan, T.M., Kane, T. and Coleman, M., 2015. Data-driven simple thermal models: The importance of the parameter estimates. *Energy Procedia*, 78, pp.2614-2619.

Dimitriou, V., Firth, S.K., Hassan, T.M. and Kane, T., 2020. The applicability of Lumped Parameter modelling in houses using in-situ measurements. *Energy and Buildings*, p.110068.

Ebrahim, M. (2020). *Python Correlation Matrix Tutorial*. Available: <https://likegeeks.com/python-correlation-matrix/>. Last accessed 20th Jul 2020.

Greenspec. (2020). *Thermal Mass*. Available: <https://www.greenspec.co.uk/building-design/thermal-mass/>. Last accessed 28th Jul 2020.

Kavgic, M., Mavrogianni, A., Mumovic, D., Summerfield, A., Stevanovic, Z. and Djurovic-Petrovic, M., 2010. A review of bottom-up building stock models for energy consumption in the residential sector. *Building and environment*, 45(7), pp.1683-1697.

Dowling, R., 2018. *Energy as a Service: The next major evolution of the energy market*. Available: <https://www.current-news.co.uk/blogs/energy-as-a-service-the-next-major-evolution-of-the-energy-market>. Last accessed 18th June 2020.

Ekici, C., 2013. A review of thermal comfort and method of using Fanger's PMV equation. In *5th International symposium on measurement, analysis and modelling of human functions. Vancouver, Canada*.

Fanger, P.O., 1973. Assessment of man's thermal comfort in practice. *Occupational and Environmental Medicine*, 30(4), pp.313-324.

Fouquier, A., Robert, S., Suard, F., Stéphan, L. and Jay, A., 2013. State of the art in building modelling and energy performances prediction: A review. *Renewable and Sustainable Energy Reviews*, 23, pp.272-288.

Hagerty, M.R. and Srinivasan, V., 1991. Comparing the predictive powers of alternative multiple regression models. *Psychometrika*, 56(1), pp.77-85.

Harish, V.S.K.V. and Kumar, A., 2016. Reduced order modeling and parameter identification of a building energy system model through an optimization routine. *Applied Energy*, 162, pp.1010-1023.

Kalmykov, L.V., 2015. A white-box model of S-shaped and double S-shaped single-species population growth. *PeerJ*, 3, p.948.

Lee, K.H. and Braun, J.E., 2008. Model-based demand-limiting control of building thermal mass. *Building and Environment*, 43(10), pp.1633-1646.

Li, X. and Wen, J., 2014. Review of building energy modeling for control and operation. *Renewable and Sustainable Energy Reviews*, 37, pp.517-537.

Lomas, K.J., 1996. The UK applicability study: an evaluation of thermal simulation programs for passive solar house design. *Building and Environment*, 31(3), pp.197-206.

National Grid ESO, 2020. *Future Energy Scenarios*.

- Neto, A.H. and Fiorelli, F.A.S., 2008. Comparison between detailed model simulation and artificial neural network for forecasting building energy consumption. *Energy and buildings*, 40(12), pp.2169-2176.
- Neu, O., Sherlock, B., Oxizidis, S., Flynn, D. and Finn, D., 2014, April. Developing building archetypes for electrical load shifting assessment: Analysis of Irish residential stock. *In Chartered Institution of Building Services Engineers (CIBSE) and American Society of Heating, Refrigerating and Air Conditioning Engineers (ASHRAE) Technical Symposium: Moving to a New World of Building Systems Performance, Dublin, Ireland, 3-4 April 2014.*
- Olesen, B.W. and Brager, G.S., 2004. A better way to predict comfort: The new ASHRAE standard 55-2004.
- Palmer, J. and Cooper, I., 2013. United Kingdom housing energy fact file 2013. Department of Energy & Climate Change, Prepared under contract to DECC by Cambridge Architectural Research, Eclipse Research Consultants and Cambridge Energy. The views expressed are not necessarily DECC's, 172.
- Rajput, R.K., 2005. *Thermal engineering*. Firewall Media.
- Pražnikar, J., 2017. Particulate matter time-series and Köppen-Geiger climate classes in North America and Europe. *Atmospheric environment*, 150, pp.136-145.
- Ramallo-González, A.P., Eames, M.E. and Coley, D.A., 2013. Lumped parameter models for building thermal modelling: An analytic approach to simplifying complex multi-layered constructions. *Energy and Buildings*, 60, pp.174-184.
- Rida, M. and Kelly, N., 2017. Toward better estimation of HVAC Loads: integrating a detailed human thermal model into building simulation. *Energy Procedia*, 122, pp.1147-1152.
- Rosenow, J., Guertler, P., Sorrell, S. and Eyre, N., 2018. The remaining potential for energy savings in UK households. *Energy Policy*, 121, pp.542-552.
- Sung, W.T. and Hsiao, S.J., 2020. The application of thermal comfort control based on Smart House System of IoT. *Measurement*, 149, p.106997.
- Strachan, P.A., Kokogiannakis, G. and Macdonald, I.A., 2008. History and development of validation with the ESP-r simulation program. *Building and Environment*, 43(4), pp.601-609.

- Underwood, C.P., 2014. An improved lumped parameter method for building thermal modelling. *Energy and Buildings*, 79, pp.191-201.
- Villavicencio Calzadilla, P. and Mauger, R., 2018. The UN's new sustainable development agenda and renewable energy: the challenge to reach SDG7 while achieving energy justice. *Journal of Energy & Natural Resources Law*, 36(2), pp.233-254.
- Vivian, J., Zarrella, A., Emmi, G. and De Carli, M., 2017. An evaluation of the suitability of lumped-capacitance models in calculating energy needs and thermal behaviour of buildings. *Energy and Buildings*, 150, pp.447-465.
- Wang, W., Tian, Z. and Ding, Y., 2013. Investigation on the influencing factors of energy consumption and thermal comfort for a passive solar house with water thermal storage wall. *Energy and Buildings*, 64, pp.218-223.
- Wills, A., Cruickshank, C.A. and Beausoleil-Morrison, I., 2012. Application of the ESP-r/TRNSYS co-simulator to study solar heating with a single-house scale seasonal storage. *Energy Procedia*, 30, pp.715-722.
- Wimmler, C., Hejazi, G., de Oliveira Fernandes, E., Moreira, C. and Connors, S., 2017. Impacts of load shifting on renewable energy integration. *Energy Procedia*, 107, pp.248-252.
- Wojtkowiak J, 2014. Lumped Thermal Capacity Model. In: Hetnarski R.B. (eds) *Encyclopedia of Thermal Stresses*. Springer, Dordrecht.
- Zhou, X., Shi, J., Tang, Y., Li, Y., Li, S. and Gong, K., 2019. Aggregate Control Strategy for Thermostatically Controlled Loads with Demand Response. *Energies*, 12(4), p.683.

Appendix A – HDDT ESP-r Parameters

Multi-layer constructions used:

Details of opaque construction: Wall_Scot_no and overall thickness 0.410
In category UK_code also shown in menus as: UK code notional wall Scotland
Code compliant wall assumed for Scotland SBEM equivalent

Layer	Thick (mm)	Conduc- tivity	Density	Specif heat	IR emis	IR abs	Solar resis	Diffu m^2K/W	R m^2	Kg	Description	
Ext	20.0	0.570	1300.	1000.	0.91	0.70	19.	0.04	26.0		Render External (UK) : Render External (UK code)	
	2	102.0	0.770	1700.	1000.	0.90	0.70	12.	0.13	173.4	Brick outer leaf : Brick (UK code) (inorganic-porous)	
	3	50.0	0.000	0.	0.99	0.99	1.	0.18	0.1	0.18	0.18	0.18
	4	50.0	0.040	12.	1030.	0.90	0.70	30.	1.25	0.6	Min wool quilt 1030spht : Insulation (Min wool quilt with 1030 sp. ht.) (non-hygro	
	5	50.0	0.040	12.	1030.	0.90	0.70	30.	1.25	0.6	Min wool quilt 1030spht : Insulation (Min wool quilt with 1030 sp. ht.) (non-hygro	
	6	100.0	1.130	1800.	1008.	0.90	0.70	13.	0.09	180.0	Concrete med density (1800) : Blockwork (UK code)	
	7	25.0	0.000	0.	0.99	0.99	1.	0.18	0.0	0.18	0.18	0.18
Int	13.0	0.210	900.	1000.	0.91	0.70	11.	0.06	11.7		Plasterboard (UK code) : Plasterboard (UK code)	

ISO 6946 U values (horiz/upward/downward heat flow)= 0.299 0.301 0.295 (partition) 0.291
Weight per m² of this construction 392.39
Total area of Wall_Scot_no is 150.10

Details of opaque construction: gyp_blk_ptn and overall thickness 0.226
In category partitions also shown in menus as: plasterbd dabs 100mm concrete bl
partition - plasterboard on dabs over 100mm concret block.

Layer	Thick (mm)	Conduc- tivity	Density	Specif heat	IR emis	IR abs	Solar resis	Diffu m^2K/W	R m^2	Kg	Description	
Ext	13.0	0.190	950.	840.	0.91	0.22	11.	0.07	12.4		white gypboard : White painted Gypboard (inorganic-porous)	
	2	50.0	0.000	0.	0.99	0.99	1.	0.17	0.1	0.17	0.17	0.17
	3	100.0	0.510	1400.	1000.	0.90	0.65	10.	0.20	140.0	block inner : Block inner (3% mc)	
	4	50.0	0.000	0.	0.99	0.99	1.	0.17	0.1	0.17	0.17	0.17
Int	13.0	0.190	950.	840.	0.91	0.22	11.	0.07	12.4		white gypboard : White painted Gypboard (inorganic-porous)	

ISO 6946 U values (horiz/upward/downward heat flow)= 1.186 1.230 1.133 (partition) 1.072
Weight per m² of this construction 164.82
Total area of gyp_blk_ptn is 239.04

Details of opaque construction: door and overall thickness 0.025
In category doors also shown in menus as: solid wood door 25mm
solid wood oak door 25mm.

Layer	Thick (mm)	Conduc- tivity	Density	Specif heat	IR emis	IR abs	Solar resis	Diffu m^2K/W	R m^2	Kg	Description
	1	25.0	0.190	700.	2390.	0.90	0.65	12.	0.13	17.5	oak : Oak (radial cut)

ISO 6946 U values (horiz/upward/downward heat flow)= 3.316 3.682 2.928 (partition) 2.554
Weight per m² of this construction 17.50
Total area of door is 1.68

Details of opaque construction: door_u1.5 and overall thickness 0.061

In category doors also shown in menus as: insulated (U1.5) wood door 60mm
insulated (woodwool U1.5) wood door 60mm.

Layer	Thick	Conduc-	Density	Specif	IR	Solar	Diffu	R	Kg	Description
	(mm)	tivity	heat	emis	abs	resis	m ² K/W	m ²		
Ext	12.5	0.190	700.	2390.	0.90	0.65	12.	0.07	8.8	oak : Oak (radial cut)
	2	36.5	0.100	500.	1000.	0.90	0.50	5.	0.36	18.2 woodwool : Woodwool (organic-hygroscopic)
Int	12.5	0.190	700.	2390.	0.90	0.65	12.	0.07	8.8	oak : Oak (radial cut)

ISO 6946 U values (horiz/upward/downward heat flow)= 1.500 1.571 1.415 (partition) 1.322
Weight per m² of this construction 35.75
Total area of door_u1.5 is 2.10

Details of opaque construction: int_doors and overall thickness 0.025
In category doors also shown in menus as: internal wood door 25mm
internal solid oak door 25mm.

Layer	Thick	Conduc-	Density	Specif	IR	Solar	Diffu	R	Kg	Description
	(mm)	tivity	heat	emis	abs	resis	m ² K/W	m ²		
	1	25.0	0.190	700.	2390.	0.90	0.65	12.	0.13	17.5 oak : Oak (radial cut)

ISO 6946 U values (horiz/upward/downward heat flow)= 3.316 3.682 2.928 (partition) 2.554
Weight per m² of this construction 17.50
Total area of int_doors is 18.48

Details of transparent construction: dbl_glz with DCF7671_06nb optics and overall thickness 0.024

Layer	Thick	Conduc-	Density	Specif	IR	Solar	Diffu	R	Kg	Description
	(mm)	tivity	heat	emis	abs	resis	m ² K/W	m ²		
Ext	6.0	0.760	2710.	837.	0.83	0.05	19200.	0.01	16.3	plate glass : Plate glass with placeholder single layer optics
	2	12.0	0.000	0.	0.99	0.99	1.	0.17	0.0	air 0.17 0.17 0.17
Int	6.0	0.760	2710.	837.	0.83	0.05	19200.	0.01	16.3	plate glass : Plate glass with placeholder single layer optics

ISO 6946 U values (horiz/upward/downward heat flow)= 2.811 3.069 2.527 (partition) 2.243
Weight per m² of this construction 32.53

Clear float 76/71, 6mm, no blind: with id of: DCF7671_06nb
with 3 layers [including air gaps] and visible trn: 0.76
Direct transmission @ 0, 40, 55, 70, 80 deg
0.611 0.583 0.534 0.384 0.170

Layer	absorption @ 0, 40, 55, 70, 80 deg
1	0.157 0.172 0.185 0.201 0.202
2	0.001 0.002 0.003 0.004 0.005
3	0.117 0.124 0.127 0.112 0.077

Total area of dbl_glz is 17.90

Details of opaque construction: ceiling linked to ceiling_rev & with overall thickness 0.110
In category ceil_floor also shown in menus as: suspended acoustic ceiling acous
A mineral time with 100mm acoustic treatment. For use as a suspended ceiling. To be referenced from room. Reversed version is ceiling_rev

Layer	Thick	Conduc-	Density	Specif	IR	Solar	Diffu	R	Kg	Description
	(mm)	tivity	heat	emis	abs	resis	m ² K/W	m ²		
Ext	100.0	0.040	250.	840.	0.90	0.30	4.	2.50	25.0	glasswool : Glasswool (generic) (non-hygroscopic)
Int	10.0	0.030	290.	2000.	0.90	0.60	8.	0.33	2.9	ceiling mineral : Ceiling acoustic tile (mineral fibre based)

ISO 6946 U values (horiz/upward/downward heat flow)= 0.333 0.336 0.329 (partition) 0.323

Weight per m² of this construction 27.90
 Total area of ceiling is 237.50

Details of opaque construction: v3_1_floor_n and overall thickness 1.075
 In category UK_code also shown in menus as: UK abstract notional ground flr
 Taken from SBEM for use as a notional slab-on-grade floor in code compliance work.

Layer	Thick (mm)	Conduc- tivity	Density heat	Specif emis abs	IR resis m ² K/W	Solar m ²	Diffu W	R m ²	Kg	Description
Ext	150.0	1.500	1500.	2085.	0.90	0.70	5.	0.10	225.0	Clay underfloor : Clay underfloor layer (inorganic-porous)
2	200.0	1.500	1500.	2085.	0.90	0.70	5.	0.13	300.0	Clay underfloor : Clay underfloor layer (inorganic-porous)
3	200.0	1.500	1500.	2085.	0.90	0.70	5.	0.13	300.0	Clay underfloor : Clay underfloor layer (inorganic-porous)
4	200.0	1.500	1500.	2085.	0.90	0.70	5.	0.13	300.0	Clay underfloor : Clay underfloor layer (inorganic-porous)
5	25.0	0.770	1700.	940.	0.90	0.65	12.	0.03	42.5	Brick slips : Brick slips thin cladding typically 25mm (UK code) (inorganic-porous)
6	150.0	1.350	2000.	1000.	0.90	0.70	13.	0.11	300.0	Cast concrete (UK) : Cast concrete (UK code)
7	100.0	0.026	12.	1030.	0.90	0.70	30.	3.85	1.2	PUR : notional floor UK material
Int	50.0	0.410	1200.	1000.	0.91	0.70	19.	0.12	60.0	Screed (UK code) : Flooring screed typically 50mm thick (UK code)

ISO 6946 U values (horiz/upward/downward heat flow)= 0.209 0.210 0.207 (partition) 0.205
 Weight per m² of this construction 1528.70
 Total area of v3_1_floor_n is 237.50

Appendix B – GHA ESP-r Parameters

Multi-layer constructions referenced in the model.

Wall_EW_2002

Details of opaque construction: Wall_EW_2002 with an overall thickness of 0.359m.

In category walls also shown in menus as: EngWls brick block circa 2002

Wall_EW_2002 is a typical 2002 brick insulated (100mm) cavity block wall with plasterboard on battens.

Layer	Thickness (mm)	Conductivity (W/(mK))	Density (kg/m ³)	Specific heat (J/(kgK))	Emissivity	Absorption	Diffusivity	R (m ² K/W)	kg/m ²	Description
Ext	102.0	0.770	1700.	1000.	0.90	0.70	12.	0.13	173.4	Brick outer leaf : Brick (UK code) (inorganic-porous)
2	22.0	0.000	0.	0.	0.99	0.99	1.	0.17	0.0	air
3	100.0	0.040	25.	1000.	0.90	0.70	30.	2.50	2.5	Mineral wool batt : Insulation (Mineral wool batt k=0.04) (non-hygroscop
4	100.0	1.060	1950.	1000.	0.90	0.40	18.	0.09	195.0	concrete block : concrete block (milton keynes)
5	22.0	0.000	0.	0.	0.99	0.99	1.	0.17	0.0	air
Int	13.0	0.210	900.	1000.	0.91	0.70	11.	0.06	11.7	Plasterboard (UK code) : Plasterboard (UK code)

ISO 6946 U values (horiz/upward/downward heat flow)= 0.303 0.306 0.300 (partition) 0.295
Weight per m² of this construction 382.65

Total area of Wall_EW_2002 is 67.63

int_doors

Details of opaque construction: int_doors with an overall thickness of 0.025m.

In category doors also shown in menus as: internal wood door 25mm

internal solid oak door 25mm.

Layer	Thickness (mm)	Conductivity (W/(mK))	Density (kg/m ³)	Specific heat (J/(kgK))	Emissivity	Absorption	Diffusivity	R (m ² K/W)	kg/m ²	Description
1	25.0	0.190	700.	2390.	0.90	0.65	12.	0.13	17.5	oak : Oak (radial cut)

ISO 6946 U values (horiz/upward/downward heat flow)= 3.316 3.682 2.928 (partition) 2.554
Weight per m² of this construction 17.50

Total area of int_doors is 19.80

dbl_glz

Details of transparent construction dbl_glz with DCF7671_06nb optics and overall thickness of 0.024m.

Layer	Thickness (mm)	Conductivity (W/(mK))	Density (kg/m ³)	Specific heat (J/(kgK))	Emissivity	Absorption	Diffusivity	R (m ² K/W)	kg/m ²	Description
-------	----------------	-----------------------	------------------------------	-------------------------	------------	------------	-------------	------------------------	-------------------	-------------

```

Ext  6.0      0.760      2710.      837.      0.83  0.05  19200.  0.01
16.3 plate glass : Plate glass with placeholder single layer optics
  2 12.0      0.000      0.         0.         0.99  0.99   1.     0.17   0.0
air 0.17 0.17 0.17
Int  6.0      0.760      2710.      837.      0.83  0.05  19200.  0.01
16.3 plate glass : Plate glass with placeholder single layer optics

```

ISO 6946 U values (horiz/upward/downward heat flow)= 2.811 3.069 2.527 (partition) 2.243
 Weight per m² of this construction 32.53

Clear float 76/71, 6mm, no blind: with id of: DCF7671_06nb
 with 3 layers [including air gaps] and visible trn: 0.76

: Direct transmission @deg

```

0  40  55  70  80
-----
0.611 0.583 0.534 0.384 0.170

```

: Absorption @deg

```

Layer 0  40  55  70  80
-----
  1  0.157 0.172 0.185 0.201 0.202
  2  0.001 0.002 0.003 0.004 0.005
  3  0.117 0.124 0.127 0.112 0.077

```

Total area of dbl_glz is 4.83

Doorfrm_ext

Details of opaque construction: Doorfrm_ext with an overall thickness of 0.094m.
 In category frames also shown in menus as: Larch architrave for ext door
 Doorfrm_ext is 94mm thick larch frame for an exterior door.

Layer	Thickness (mm)	Conductivity (W/(mK))	Density (kg/m ³)	Specific heat (J/(kgK))	Emissivity
1	94.0	0.140	590.	1800.	0.90

Absorption	Diffusivity	R (m ² K/W)	kg/m ²	Description
0.67	12.	0.65	0.90	55.5 western larch : Wester Larch from simetric.co.uk and matbase specific ht

ISO 6946 U values (horiz/upward/downward heat flow)= 1.188 1.232 1.135 (partition) 1.074
 Weight per m² of this construction 55.46

Total area of Doorfrm_ext is 1.68

roof

Details of opaque construction: roof with an overall thickness of 0.111m.
 In category roofs also shown in menus as: metal insulated roof pnl U=0.427
 A formed uncoated aluminium roof panel including air gap and 80mm quilt insulation to yield
 U=0.427.

Layer	Thickness (mm)	Conductivity (W/(mK))	Density (kg/m ³)	Specific heat (J/(kgK))	Emissivity
1	94.0	0.140	590.	1800.	0.90

Absorption	Diffusivity	R (m ² K/W)	kg/m ²	Description
0.67	12.	0.65	0.90	55.5 western larch : Wester Larch from simetric.co.uk and matbase specific ht

Ext	3.0	210.000	2700.	880.	0.22	0.20	19200.	0.00
8.1 aluminium : Aluminium								
2	25.0	0.000	0.	0.	0.99	0.99	1.	0.17
air 0.17 0.17 0.17								
3	80.0	0.040	12.	840.	0.90	0.65	30.	2.00
1.0 glass fibre quilt : Glass Fibre Quilt (non-hygroscopic)								
Int	3.0	210.000	2700.	880.	0.22	0.20	19200.	0.00
8.1 aluminium : Aluminium								

ISO 6946 U values (horiz/upward/downward heat flow)= 0.427 0.433 0.420 (partition) 0.412
 Weight per m² of this construction 17.19

Total area of roof is 62.51

ceiling

Details of opaque construction: ceiling linked to ceiling_rev with an overall thickness of 0.110m.
 In category ceil_floor also shown in menus as: suspended acoustic ceiling acous
 A mineral time with 100mm acoustic treatment. For use as a suspended ceiling. To be referenced from room. Reversed version is ceiling_rev

Layer	Thickness (mm)	Conductivity (W/(mK))	Density (kg/m ³)	Specific heat (J/(kgK))	Emissivity	Absorption	Diffusivity	R (m ² K/W)	Description
-------	----------------	-----------------------	------------------------------	-------------------------	------------	------------	-------------	------------------------	-------------

Ext	100.0	0.040	250.	840.	0.90	0.30	4.	2.50	
25.0 glasswool : Glasswool (generic) (non-hygroscopic)									
Int	10.0	0.030	290.	2000.	0.90	0.60	8.	0.33	
2.9 ceiling mineral : Ceiling acoustic tile (mineral fibre based)									

ISO 6946 U values (horiz/upward/downward heat flow)= 0.333 0.336 0.329 (partition) 0.323
 Weight per m² of this construction 27.90

Total area of ceiling is 53.46

ceiling_rev

Details of opaque construction: ceiling_rev linked to ceiling with an overall thickness of 0.110m.
 In category ceil_floor also shown in menus as: rev suspended acoustic ceiling
 A mineral time with 100mm acoustic treatment. For use as a suspended ceiling. To be referenced from ceiling void. Reversed version is ceiling

Layer	Thickness (mm)	Conductivity (W/(mK))	Density (kg/m ³)	Specific heat (J/(kgK))	Emissivity	Absorption	Diffusivity	R (m ² K/W)	Description
-------	----------------	-----------------------	------------------------------	-------------------------	------------	------------	-------------	------------------------	-------------

Ext	10.0	0.030	290.	2000.	0.90	0.60	8.	0.33	
2.9 ceiling mineral : Ceiling acoustic tile (mineral fibre based)									
Int	100.0	0.040	250.	840.	0.90	0.30	4.	2.50	
25.0 glasswool : Glasswool (generic) (non-hygroscopic)									

ISO 6946 U values (horiz/upward/downward heat flow)= 0.333 0.336 0.329 (partition) 0.323
 Weight per m² of this construction 27.90

Total area of ceiling_rev is 53.46

grnd_floor

Details of opaque construction: grnd_floor with an overall thickness of 0.975m.

In category ground also shown in menus as: carpet conc floor hardcore-earth

An uninsulated slab on grade foundation over hardcore and 600mm of earth with a built-up of chipboard and carpet above.

Layer Thickness (mm) Conductivity (W/(mK)) Density (kg/m³) Specific heat (J/(kgK)) Emissivity
Absorption Diffusivity R (m²K/W) kg/m² Description

Layer	Thickness (mm)	Conductivity (W/(mK))	Density (kg/m ³)	Specific heat (J/(kgK))	Emissivity	Absorption	Diffusivity	R (m ² K/W)	kg/m ²	Description
Ext	200.0	1.280	1460.	879.	0.90	0.85	5.	0.16		
292.0	earth std : Common_earth									
2	200.0	1.280	1460.	879.	0.90	0.85	5.	0.16		
292.0	earth std : Common_earth									
3	200.0	1.280	1460.	879.	0.90	0.85	5.	0.16		
292.0	earth std : Common_earth									
4	150.0	0.520	2050.	184.	0.90	0.85	2.	0.29		
307.5	gravel based : Gravel based (non-hygroscopic)									
5	150.0	1.400	2100.	653.	0.90	0.65	19.	0.11		
315.0	heavy mix concrete : Heavy mix concrete									
6	50.0	0.000	0.	0.	0.99	0.99	1.	0.17	0.1	
air	0.17	0.17	0.17							
7	19.0	0.150	800.	2093.	0.91	0.65	96.	0.13		
15.2	chipboard : Chipboard									
Int	6.0	0.060	186.	1360.	0.90	0.60	10.	0.10		
1.1	Wilton : Wilton weave wool carpet (organic-hygroscopic)									

ISO 6946 U values (horiz/upward/downward heat flow)= 0.699 0.714 0.680 (partition) 0.657

Weight per m² of this construction 1514.88

Total area of grnd_floor is 53.46

Appendix C – 4010 ESP-r Parameters

Multi-layer constructions used:

Details of opaque construction: exWall_typic and overall thickness 0.304
In category UK_code also shown in menus as: Uk code typical external wall
code compliant typical external wall SBEM equivalent

Layer	Thick (mm)	Conduc- tivity	Density	Specif heat	IR emis	Solar abs	Diffu resis	R m ² K/W	Kg m ²	Description
Ext	102.0	0.770	1700.	1000.	0.90	0.70	12.	0.13	173.4	Brick outer leaf : Brick (UK code) (inorganic-porous)
2	63.5	0.040	25.	1000.	0.90	0.70	30.	1.59	1.6	Mineral wool batt : Insulation (Mineral wool batt k=0.04) (non-hygroscopic)
3	100.0	1.130	1800.	1008.	0.90	0.70	13.	0.09	180.0	Concrete med density (1800) : Blockwork (UK code)
4	25.0	0.000	0.	0.	0.99	0.99	1.	0.18	0.0	air 0.18 0.18 0.18
Int	13.0	0.210	900.	1000.	0.91	0.70	11.	0.06	11.7	Plasterboard (UK code) : Plasterboard (UK code)

ISO 6946 U values (horiz/upward/downward heat flow)= 0.450 0.457 0.442 (partition) 0.433
Weight per m² of this construction 366.72
Total area of exWall_typic is 132.27

Details of opaque construction: mass_part and overall thickness 0.240
In category partitions also shown in menus as: concrete block partition 240mm
partition - 240mm concrete block partition (white painted).

Layer	Thick (mm)	Conduc- tivity	Density	Specif heat	IR emis	Solar abs	Diffu resis	R m ² K/W	Kg m ²	Description
1	240.0	0.510	1400.	1000.	0.90	0.25	10.	0.47	336.0	block white ptd : block white painted inner (3% mc)

ISO 6946 U values (horiz/upward/downward heat flow)= 1.561 1.638 1.469 (partition) 1.369
Weight per m² of this construction 336.00
Total area of mass_part is 120.31

Details of opaque construction: party_wall_n and overall thickness 0.076
In category UK_code also shown in menus as: UK Nireland code party-wall
partition - UK Northern Ireland code acoustic stud party wall.

Layer	Thick (mm)	Conduc- tivity	Density	Specif heat	IR emis	Solar abs	Diffu resis	R m ² K/W	Kg m ²	Description
Ext	13.0	0.210	900.	1000.	0.91	0.70	11.	0.06	11.7	Plasterboard (UK code) : Plasterboard (UK code)
2	50.0	0.050	12.	1000.	0.90	0.70	30.	1.00	0.6	Min wool quilt betwnstuds : Min wool quilt between studwork
Int	13.0	0.210	900.	1000.	0.91	0.70	11.	0.06	11.7	Plasterboard (UK code) : Plasterboard (UK code)

ISO 6946 U values (horiz/upward/downward heat flow)= 0.773 0.791 0.750 (partition) 0.723
Weight per m² of this construction 24.00
Total area of party_wall_n is 1.97

Details of opaque construction: door and overall thickness 0.025
In category doors also shown in menus as: solid wood door 25mm
solid wood oak door 25mm.

Layer	Thick (mm)	Conduc- tivity	Density	Specif heat	IR emis	Solar abs	Diffu resis	R m ² K/W	Kg m ²	Description
1	25.0	0.170	700.	1700.	0.90	0.70	11.	0.06	11.7	Solid wood door 25mm

1 25.0 0.190 700. 2390. 0.90 0.65 12. 0.13 17.5 oak : Oak (radial cut)
 ISO 6946 U values (horiz/upward/downward heat flow)= 3.316 3.682 2.928 (partition) 2.554
 Weight per m² of this construction 17.50
 Total area of door is 28.21

Details of opaque construction: door_u1.5 and overall thickness 0.061
 In category doors also shown in menus as: insulated (U1.5) wood door 60mm
 insulated (woodwool U1.5) wood door 60mm.

Layer	Thick (mm)	Conduc- tivity	Density	Specif heat	IR emis	IR abs	Solar resis	Diffu	R	Kg	Description
Ext	12.5	0.190	700.	2390.	0.90	0.65	12.	0.07	8.8		oak : Oak (radial cut)
2	36.5	0.100	500.	1000.	0.90	0.50	5.	0.36	18.2		woodwool : Woodwool (organic-hygroscopic)
Int	12.5	0.190	700.	2390.	0.90	0.65	12.	0.07	8.8		oak : Oak (radial cut)

ISO 6946 U values (horiz/upward/downward heat flow)= 1.500 1.571 1.415 (partition) 1.322
 Weight per m² of this construction 35.75
 Total area of door_u1.5 is 4.13

Details of transparent construction: dbl_glz with DCF7671_06nb optics and overall thickness 0.024

Layer	Thick (mm)	Conduc- tivity	Density	Specif heat	IR emis	IR abs	Solar resis	Diffu	R	Kg	Description
Ext	6.0	0.760	2710.	837.	0.83	0.05	19200.	0.01	16.3		plate glass : Plate glass with placeholder single layer optics
2	12.0	0.000	0.	0.	0.99	0.99	1.	0.17	0.0	air	0.17 0.17 0.17
Int	6.0	0.760	2710.	837.	0.83	0.05	19200.	0.01	16.3		plate glass : Plate glass with placeholder single layer optics

ISO 6946 U values (horiz/upward/downward heat flow)= 2.811 3.069 2.527 (partition) 2.243
 Weight per m² of this construction 32.53

Clear float 76/71, 6mm, no blind: with id of: DCF7671_06nb
 with 3 layers [including air gaps] and visible trn: 0.76

Direct transmission @ 0, 40, 55, 70, 80 deg
 0.611 0.583 0.534 0.384 0.170

Layer| absorption @ 0, 40, 55, 70, 80 deg

1	0.157	0.172	0.185	0.201	0.202
2	0.001	0.002	0.003	0.004	0.005
3	0.117	0.124	0.127	0.112	0.077

Total area of dbl_glz is 8.53

Details of transparent construction: fictitious with SC_fictit optics and overall thickness 0.004

Layer	Thick (mm)	Conduc- tivity	Density	Specif heat	IR emis	IR abs	Solar resis	Diffu	R	Kg	Description
1	4.0	20.000	10.	10.	0.99	0.01	19200.	0.00	0.0		fict : fictitious material (almost not there)

with matching single layer optics
 ISO 6946 U values (horiz/upward/downward heat flow)= 5.875 7.133 4.757 (partition) 3.843
 Weight per m² of this construction 0.04

Fictitious 99/99, 4mm, no blind: with id of: SC_fictit
 with 1 layers [including air gaps] and visible trn: 0.99

Direct transmission @ 0, 40, 55, 70, 80 deg
 0.998 0.987 0.986 0.985 0.984

Layer| absorption @ 0, 40, 55, 70, 80 deg

1	0.001	0.001	0.001	0.001	0.001
---	-------	-------	-------	-------	-------

Total area of fictitious is 5.20

Details of opaque construction: `insul_frame` and overall thickness 0.088

In category frames also shown in menus as: aluminium insulated frame
grey aluminium frame with 80mm of fibre insulation to yield U value of ??.

Layer	Thick (mm)	Conduc- tivity	Density	Specif heat	IR emis	IR abs	IR resis	Solar m ² K/W	Diffu	R	Kg	Description
Ext	4.0	210.000	2700.	880.	0.82	0.72	19200.	0.00	10.8	grey cotd alum	10.8	grey coated aluminium
	2	80.0	0.040	12.	840.	0.90	0.65	30.	2.00	1.0	glass fibre quilt	Glass Fibre Quilt (non-hygroscopic)
Int	4.0	210.000	2700.	880.	0.82	0.72	19200.	0.00	10.8	grey cotd alum	10.8	grey coated aluminium

ISO 6946 U values (horiz/upward/downward heat flow)= 0.461 0.467 0.452 (partition) 0.442
Weight per m² of this construction 22.56
Total area of `insul_frame` is 2.91

Details of opaque construction: roof and overall thickness 0.111

In category roofs also shown in menus as: metal insulated roof pnl U=0.427

A formed uncoated aluminium roof panel including air gap and 80mm quilt insulation to yield U=0.427.

Layer	Thick (mm)	Conduc- tivity	Density	Specif heat	IR emis	IR abs	IR resis	Solar m ² K/W	Diffu	R	Kg	Description
Ext	3.0	210.000	2700.	880.	0.22	0.20	19200.	0.00	8.1	aluminium	8.1	aluminium : Aluminium
	2	25.0	0.000	0.	0.99	0.99	1.	0.17	0.0	air	0.17	0.17 0.17
	3	80.0	0.040	12.	840.	0.90	0.65	30.	2.00	1.0	glass fibre quilt	Glass Fibre Quilt (non-hygroscopic)
Int	3.0	210.000	2700.	880.	0.22	0.20	19200.	0.00	8.1	aluminium	8.1	aluminium : Aluminium

ISO 6946 U values (horiz/upward/downward heat flow)= 0.427 0.433 0.420 (partition) 0.412
Weight per m² of this construction 17.19
Total area of roof is 51.06

Details of opaque construction: ceiling linked to `ceiling_rev` & with overall thickness 0.110

In category `ceil_floor` also shown in menus as: suspended acoustic ceiling `acous`

A mineral time with 100mm acoustic treatment. For use as a suspended ceiling. To be referenced from room. Reversed version is `ceiling_rev`

Layer	Thick (mm)	Conduc- tivity	Density	Specif heat	IR emis	IR abs	IR resis	Solar m ² K/W	Diffu	R	Kg	Description
Ext	100.0	0.040	250.	840.	0.90	0.30	4.	2.50	25.0	glasswool	25.0	glasswool : Glasswool (generic) (non-hygroscopic)
Int	10.0	0.030	290.	2000.	0.90	0.60	8.	0.33	2.9	ceiling mineral	2.9	ceiling mineral : Ceiling acoustic tile (mineral fibre based)

ISO 6946 U values (horiz/upward/downward heat flow)= 0.333 0.336 0.329 (partition) 0.323
Weight per m² of this construction 27.90
Total area of ceiling is 42.48

Details of opaque construction: `ceiling_rev` linked to ceiling & with overall thickness 0.110

In category `ceil_floor` also shown in menus as: rev suspended acoustic ceiling

A mineral time with 100mm acoustic treatment. For use as a suspended ceiling. To be referenced from ceiling void. Reversed version is ceiling

Layer	Thick (mm)	Conduc- tivity	Density	Specif heat	IR emis	IR abs	IR resis	Solar m ² K/W	Diffu	R	Kg	Description
Ext	10.0	0.030	290.	2000.	0.90	0.60	8.	0.33	2.9	ceiling mineral	2.9	ceiling mineral : Ceiling acoustic tile (mineral fibre based)
Int	100.0	0.040	250.	840.	0.90	0.30	4.	2.50	25.0	glasswool	25.0	glasswool : Glasswool (generic) (non-hygroscopic)

ISO 6946 U values (horiz/upward/downward heat flow)= 0.333 0.336 0.329 (partition) 0.323

Weight per m² of this construction 27.90
 Total area of ceiling_rev is 42.48

Details of opaque construction: cpt_cel2flr linked to cpt_flr2cel & with overall thickness 0.142
 In category ceil_floor also shown in menus as: mid-floor carpeted wood floor
 A residential carpeted wood floor structure for interior use. To be referenced from the lower room. Reversed version is cpt_flr2cel

Layer	Thick (mm)	Conduc- tivity	Density	Specif heat	IR emis	IR abs	IR resis	IR m ² K/W	R	Kg	Description
Ext	6.0	0.060	186.	1360.	0.90	0.85	10.	0.10	1.1	dk grey Wilton	: Dark grey Wilton carpet (organic-hygroscopic)
	2	6.0	0.100	400.	1360.	0.90	0.65	1000.	0.06	2.4	cellular rub underlay : Cellular rubber carpet underlay (non-hygroscopic)
	3	18.0	0.150	700.	1420.	0.90	0.65	576.	0.12	12.6	plywood 700d : Plywood (700 density)
	4	100.0	0.000	0.	0.	0.99	0.99	1.	0.17	0.1	air 0.17 0.17 0.17
Int	12.5	0.190	950.	840.	0.91	0.22	11.	0.07	11.9	white gypboard	: White painted Gypboard (inorganic-porous)

ISO 6946 U values (horiz/upward/downward heat flow)= 1.458 1.525 1.378 (partition) 1.289
 Weight per m² of this construction 28.11
 Total area of cpt_cel2flr is 46.04

Details of opaque construction: cpt_flr2cel linked to cpt_cel2flr & with overall thickness 0.142
 In category ceil_floor also shown in menus as: rev mid-floor carpeted wood flr
 A residential carpeted wood floor structure for interior use. To be referenced from the upper room. Reversed version is cpt_cel2flr

Layer	Thick (mm)	Conduc- tivity	Density	Specif heat	IR emis	IR abs	IR resis	IR m ² K/W	R	Kg	Description
Ext	12.5	0.190	950.	840.	0.91	0.22	11.	0.07	11.9	white gypboard	: White painted Gypboard (inorganic-porous)
	2	100.0	0.000	0.	0.	0.99	0.99	1.	0.17	0.1	air 0.17 0.17 0.17
	3	18.0	0.150	700.	1420.	0.90	0.65	576.	0.12	12.6	plywood 700d : Plywood (700 density)
	4	6.0	0.100	400.	1360.	0.90	0.65	1000.	0.06	2.4	cellular rub underlay : Cellular rubber carpet underlay (non-hygroscopic)
Int	6.0	0.060	186.	1360.	0.90	0.85	10.	0.10	1.1	dk grey Wilton	: Dark grey Wilton carpet (organic-hygroscopic)

ISO 6946 U values (horiz/upward/downward heat flow)= 1.458 1.525 1.378 (partition) 1.289
 Weight per m² of this construction 28.11
 Total area of cpt_flr2cel is 46.04

Details of opaque construction: grnd_floor and overall thickness 0.975
 In category ground also shown in menus as: carpet conc floor hardcore-earth
 An uninsulated slab on grade foundation over hardcore and 600mm of earth with a built-up of chipboard and carpet above.

Layer	Thick (mm)	Conduc- tivity	Density	Specif heat	IR emis	IR abs	IR resis	IR m ² K/W	R	Kg	Description
Ext	200.0	1.280	1460.	879.	0.90	0.85	5.	0.16	292.0	earth std	: Common_earth
	2	200.0	1.280	1460.	879.	0.90	0.85	5.	0.16	292.0	earth std : Common_earth
	3	200.0	1.280	1460.	879.	0.90	0.85	5.	0.16	292.0	earth std : Common_earth
	4	150.0	0.520	2050.	184.	0.90	0.85	2.	0.29	307.5	gravel based : Gravel based (non-hygroscopic)
	5	150.0	1.400	2100.	653.	0.90	0.65	19.	0.11	315.0	heavy mix concrete : Heavy mix concrete
	6	50.0	0.000	0.	0.	0.99	0.99	1.	0.17	0.1	air 0.17 0.17 0.17
	7	19.0	0.150	800.	2093.	0.91	0.65	96.	0.13	15.2	chipboard : Chipboard
Int	6.0	0.060	186.	1360.	0.90	0.60	10.	0.10	1.1	Wilton	: Wilton weave wool carpet (organic-hygroscopic)

ISO 6946 U values (horiz/upward/downward heat flow)= 0.699 0.714 0.680 (partition) 0.657
Weight per m² of this construction 1514.88
Total area of grnd_floor is 42.48

Appendix D – Python Covariance Matrix Script

Example for 4010 Covariance Matrix:

```
import pandas as pd
import pandas as pd
import scipy as sc
import numpy as np
import matplotlib.pyplot as plt

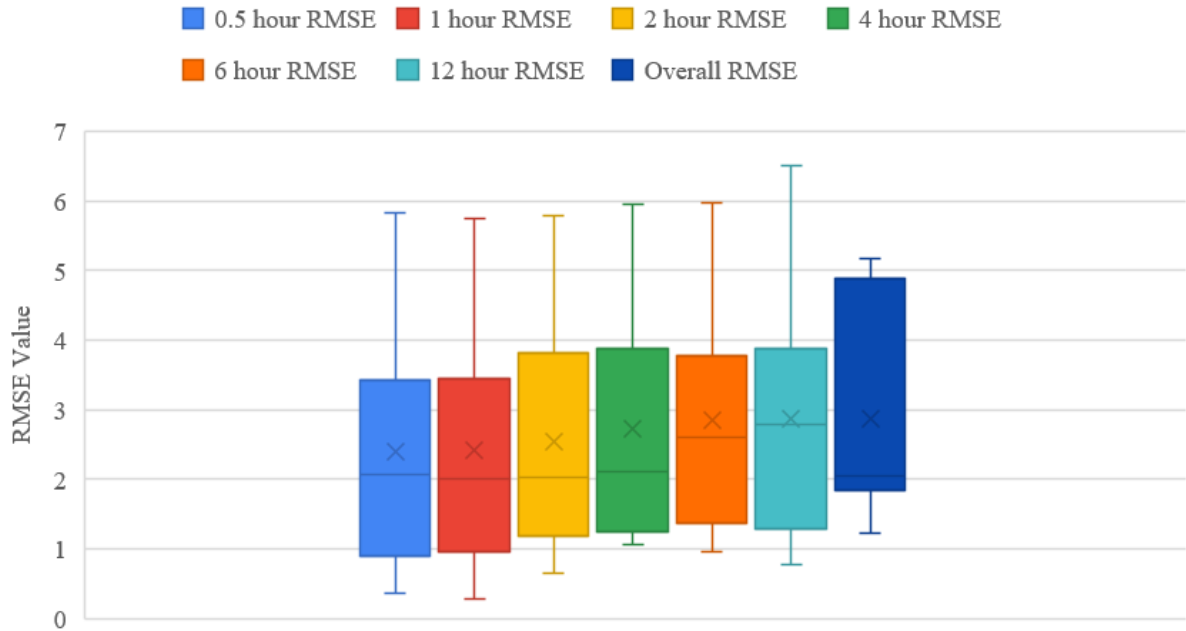
data_1 = pd.read_csv (r' file name)
temp_data = pd.DataFrame (data_1, columns= ['Time' 'Bedroom 1' 'Bedroom 2'
      'Bathroom' 'Hall' 'Living Room' 'Kitchen' 'Roof' 'Average' ])

array = data_1.values
data_1.hist(figsize = (12,10))
plt.show()

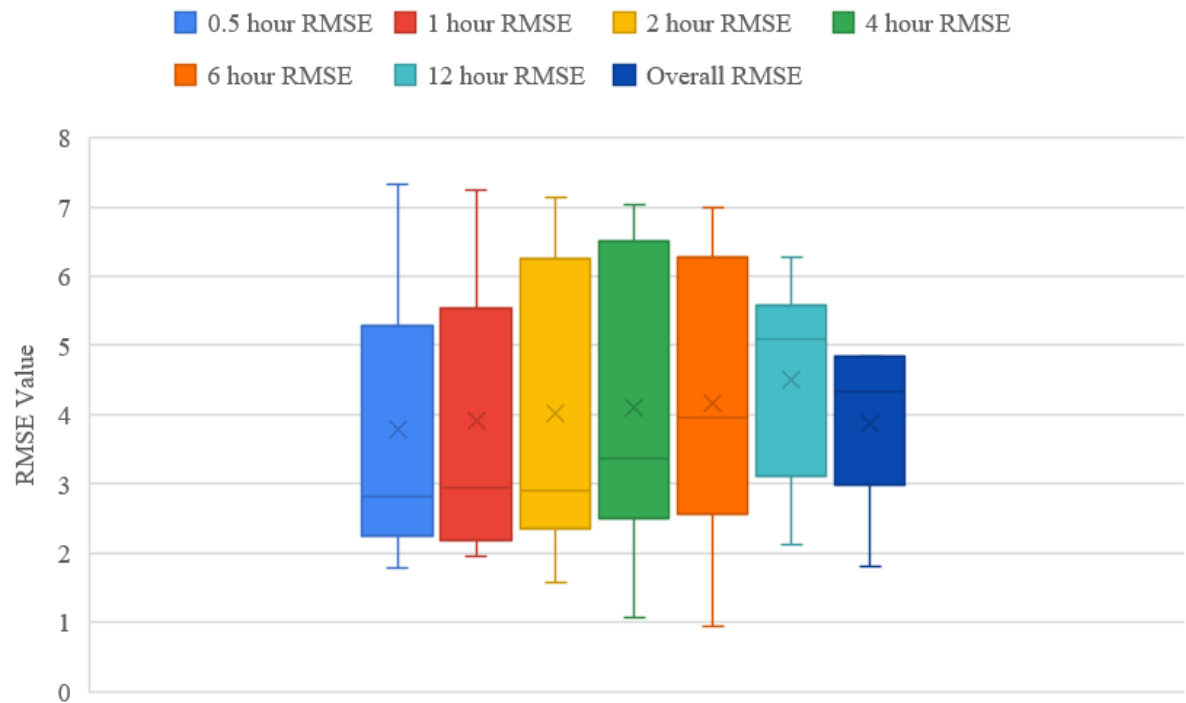
C_mat = data_1.corr()
fig = plt.figure(figsize = (6,6))
sb.heatmap(C_mat, vmax = .8, square = True)
plt.show()
```

Appendix E – HDDT Monthly RMSE Boxplots

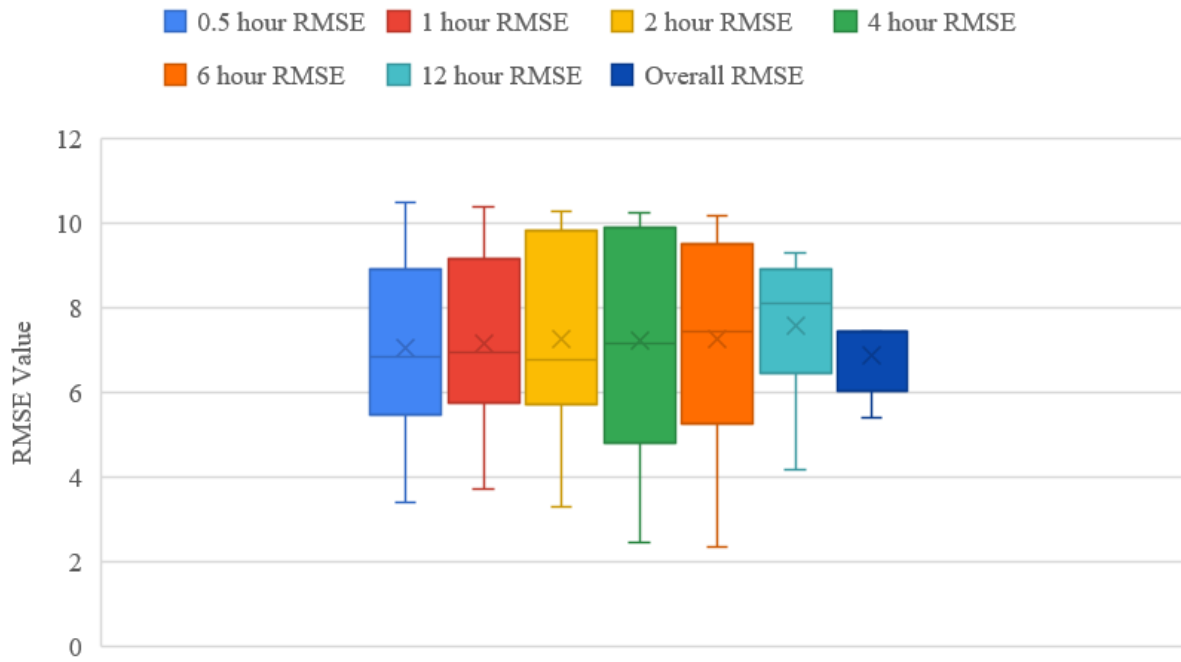
HDDT January RMSE Profile



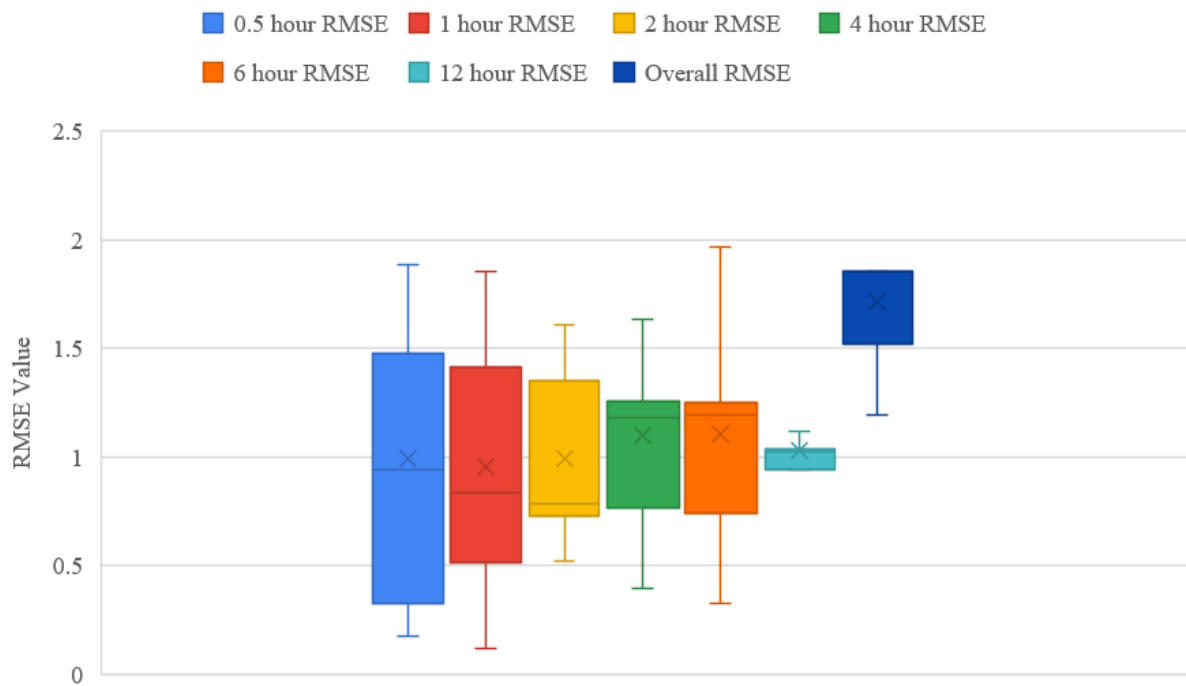
HDDT April RMSE Profile



HDDT July RMSE Profile

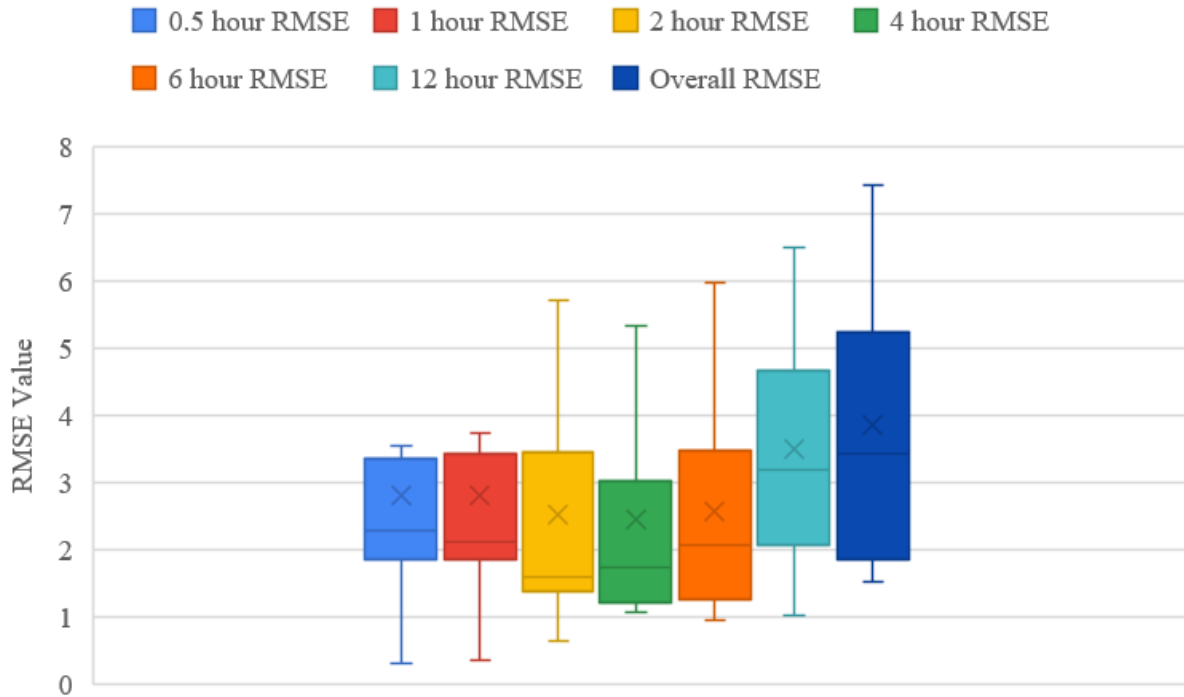


HDDT October RMSE Profile

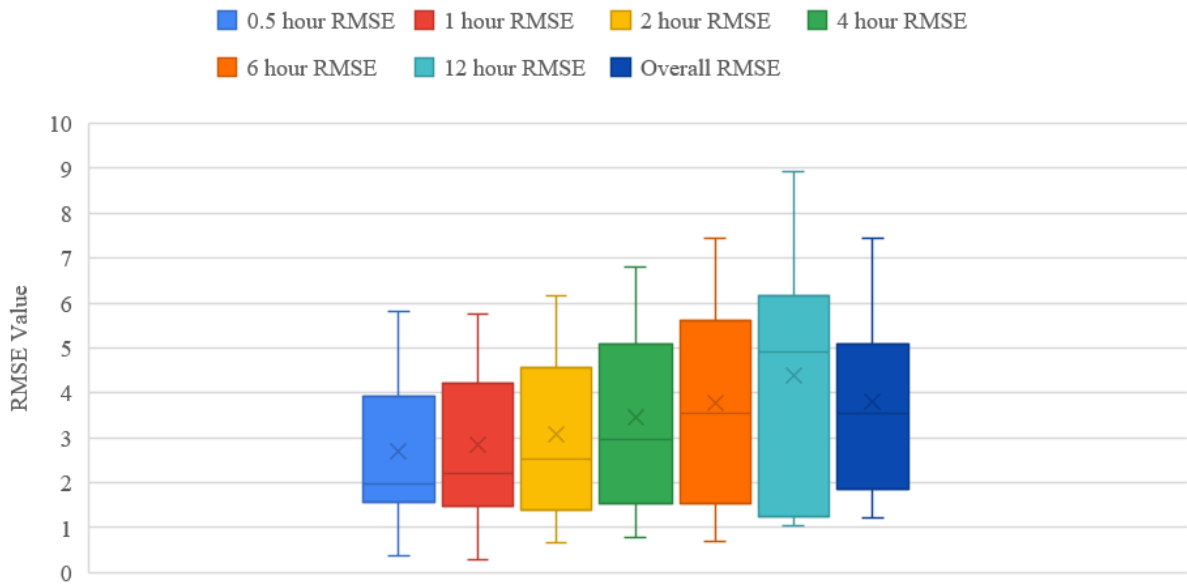


Appendix F – HDDT Switch off RMSE Boxplots

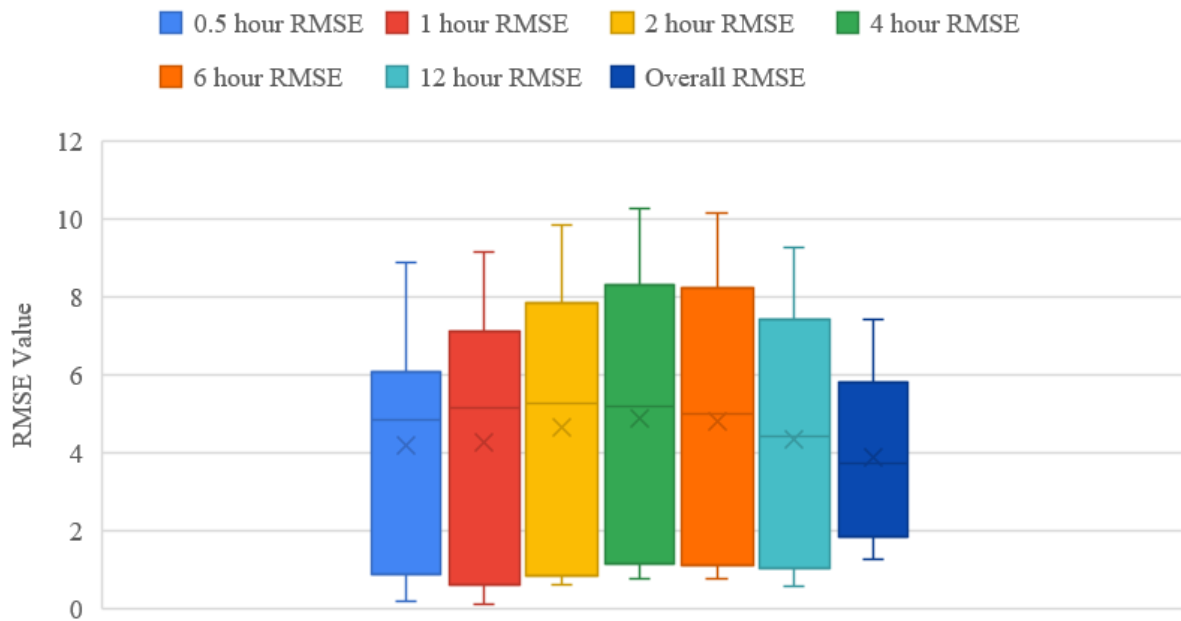
HDDT 0600 switch off RMSE profile



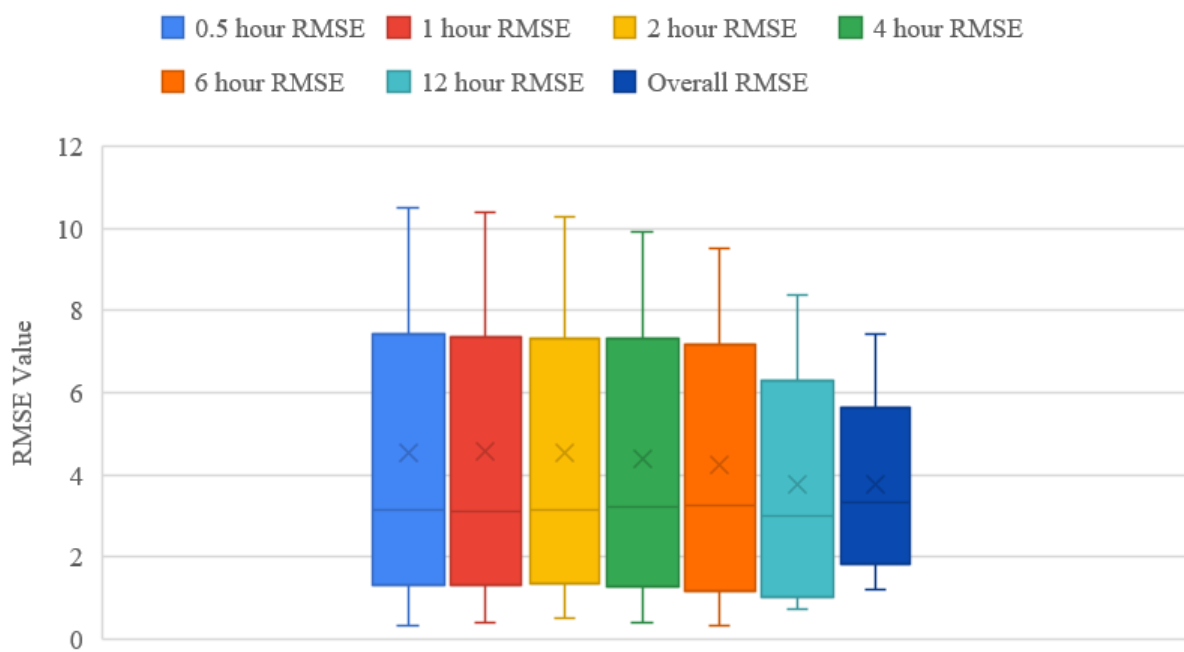
HDDT 1200 switch off RMSE profile



HDDT 1700 switch off RMSE profile

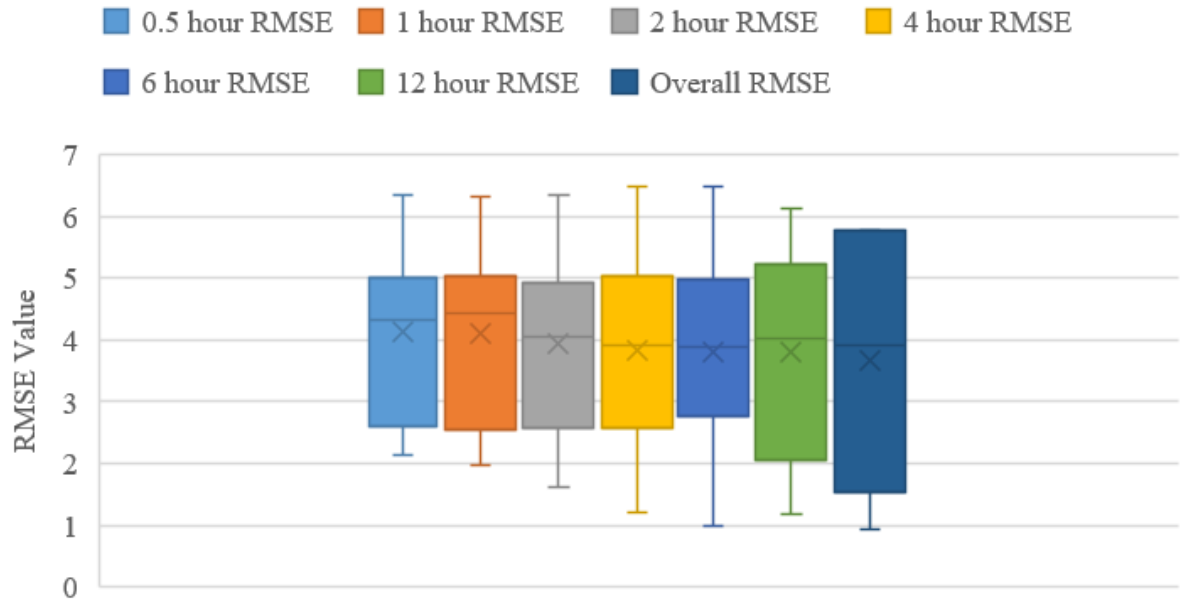


HDDT 2000 switch off RMSE Profile

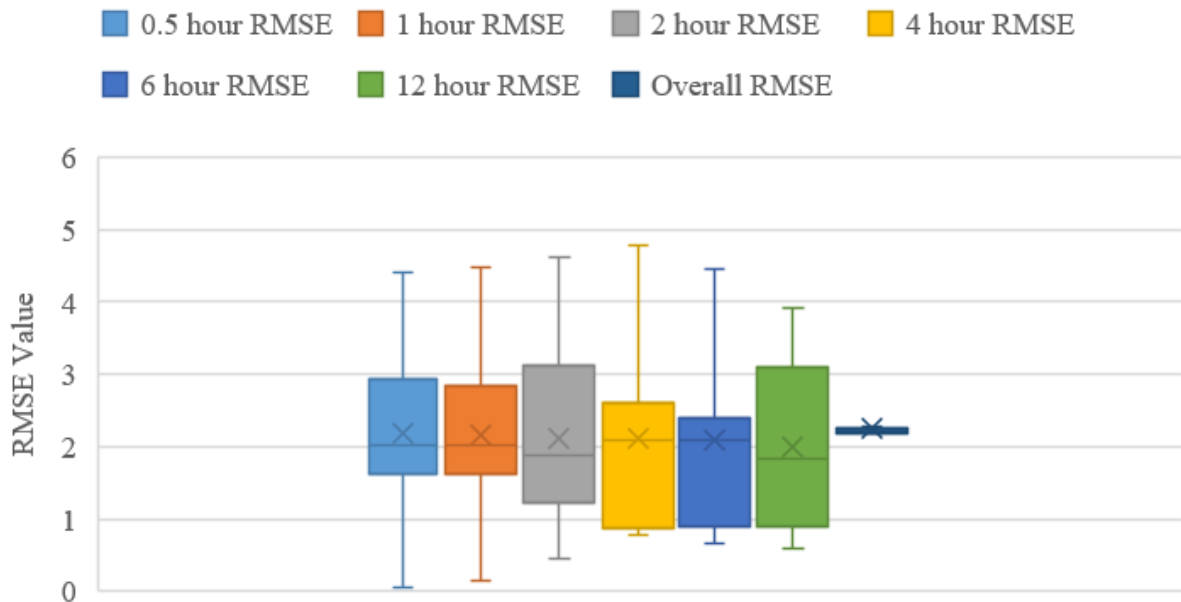


Appendix G – GHA Monthly RMSE Boxplots

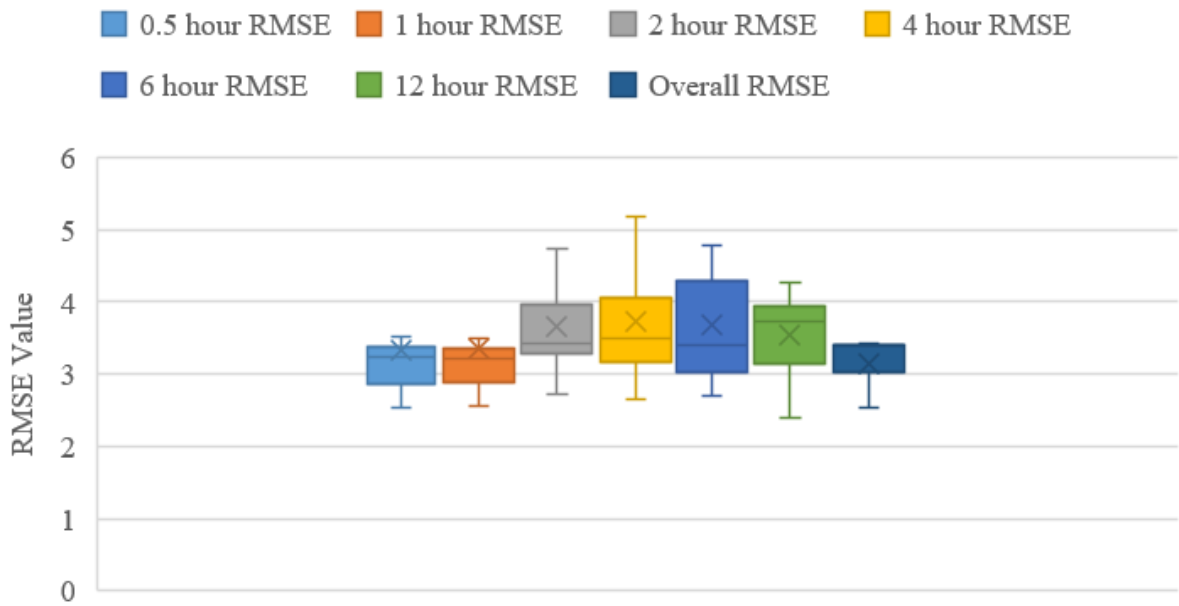
GHA January RMSE Profile



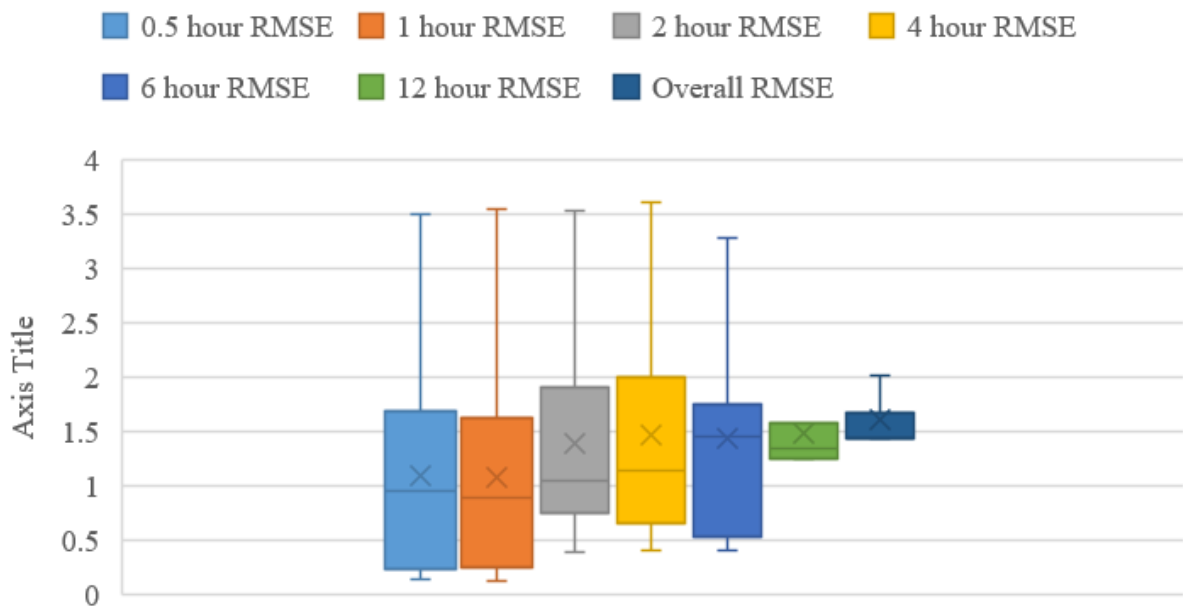
GHA April RMSE Profile



GHA July RMSE Profile

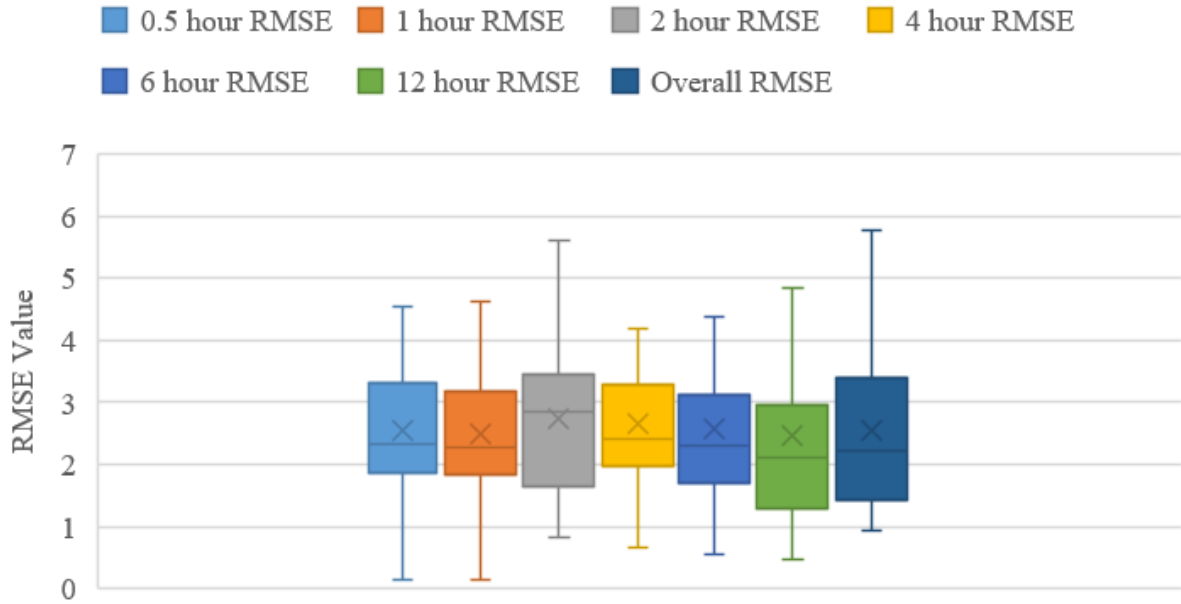


GHA October RMSE Profile

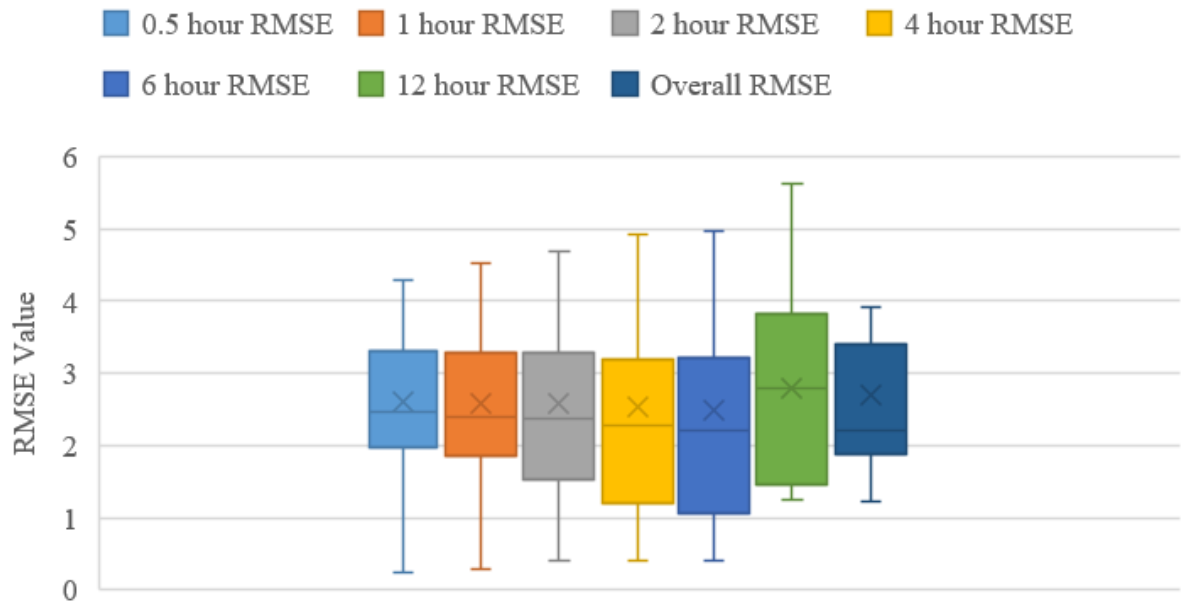


Appendix H – GHA Switch off RMSE Boxplots

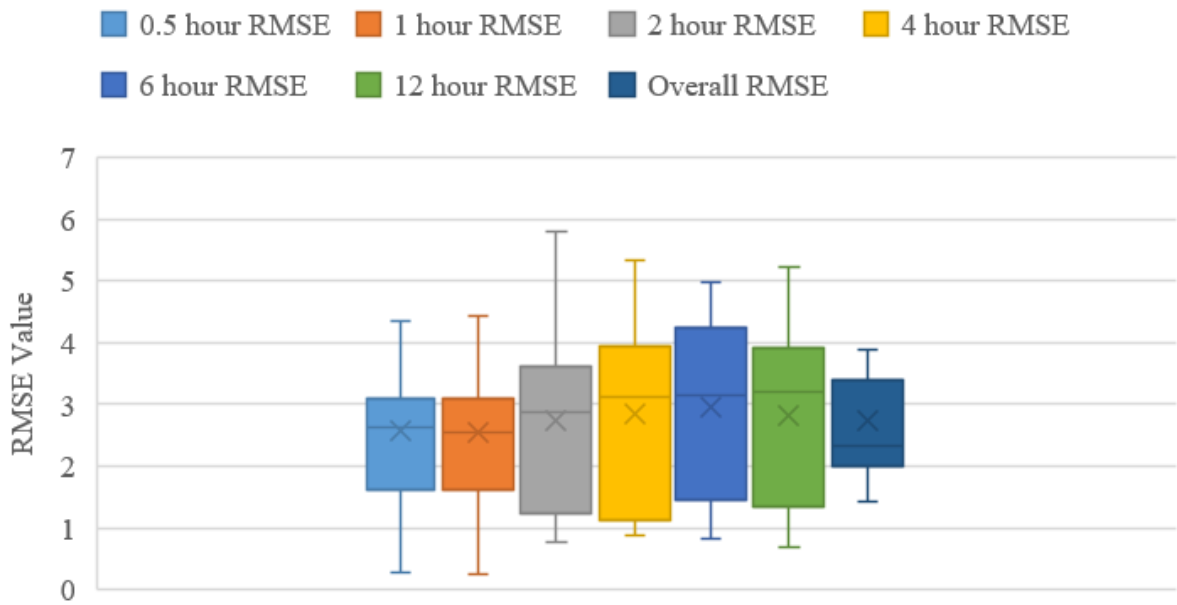
GHA 0600 Switch off RMSE Profile



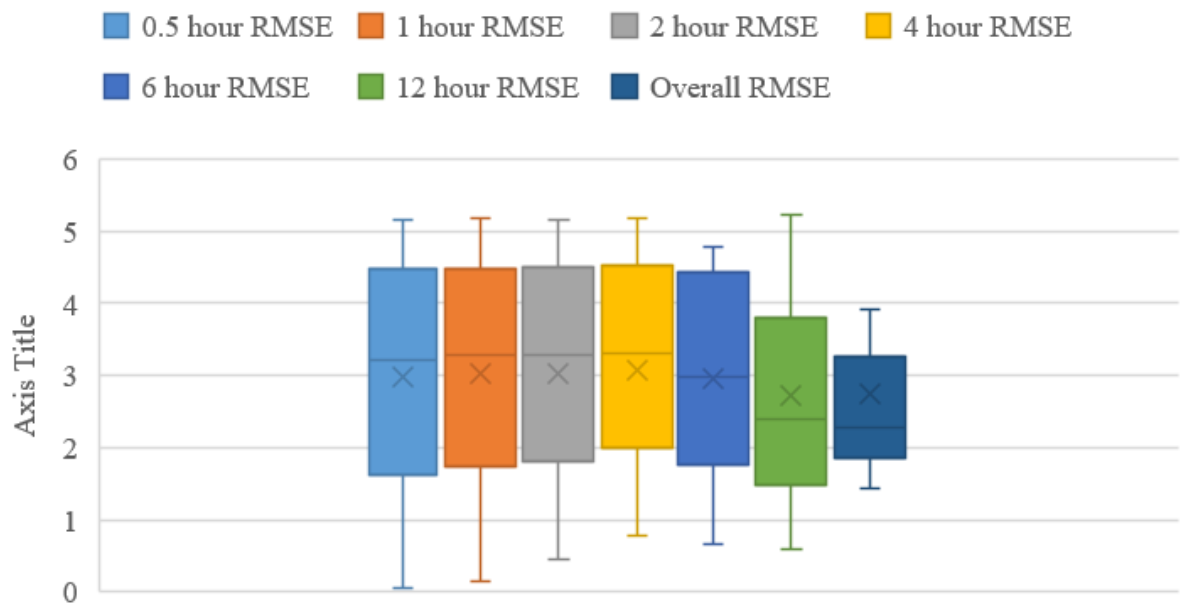
GHA 1200 Switch off RMSE Profile



GHA 1700 Switch off RMSE Profile

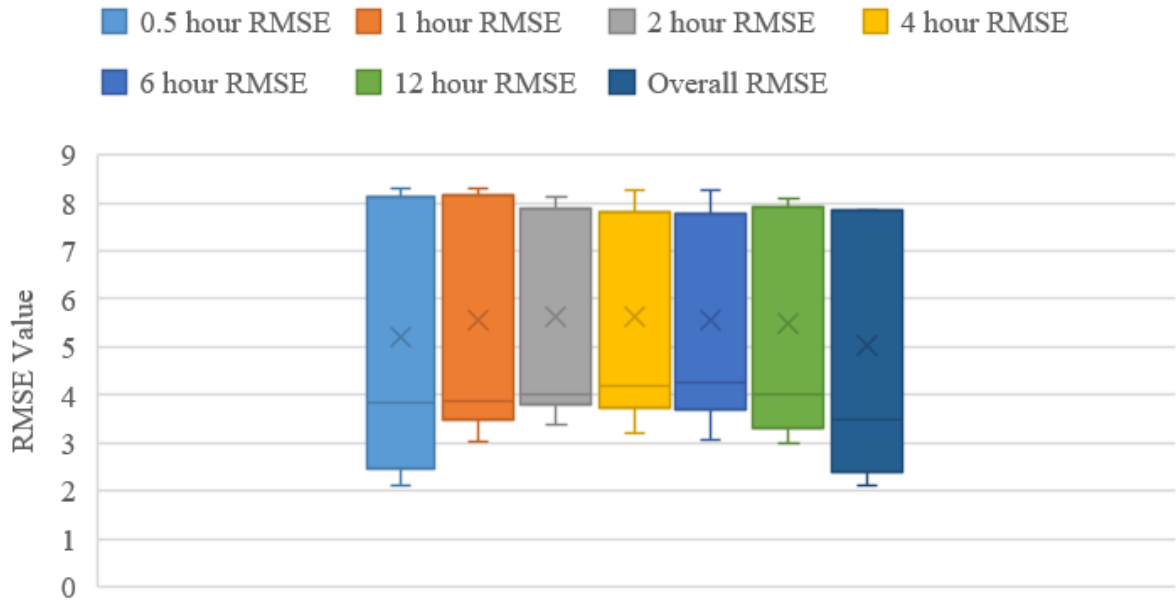


GHA 2000 Switch off RMSE Profile

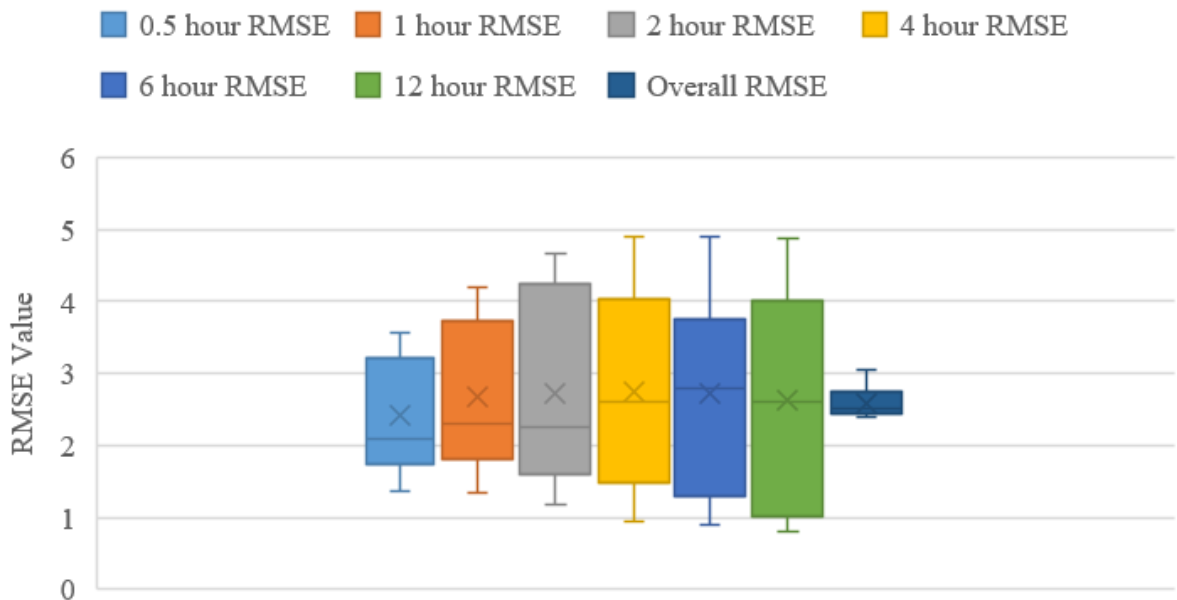


Appendix I – 4010 Monthly RMSE Boxplots

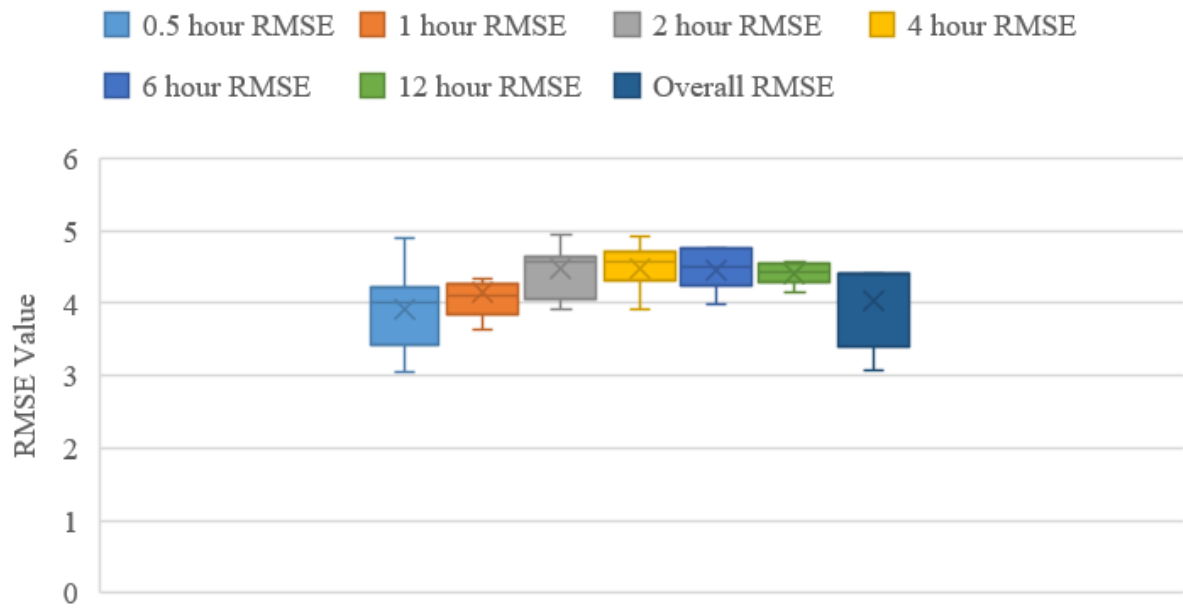
4010 January RMSE Profile



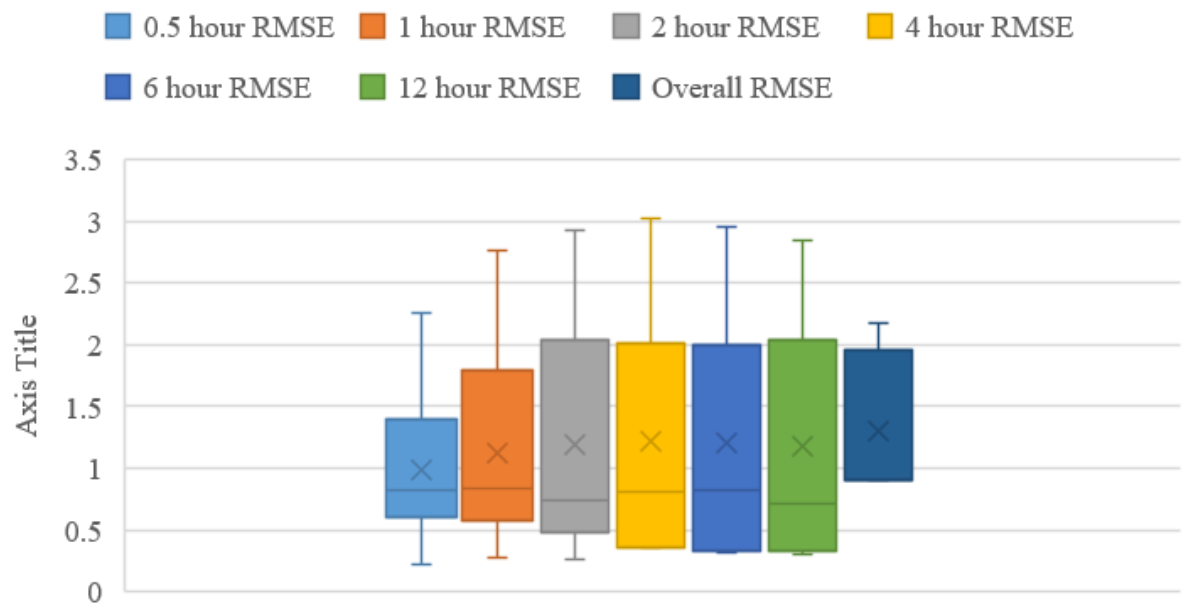
4010 April RMSE Profile



4010 July RMSE Profile

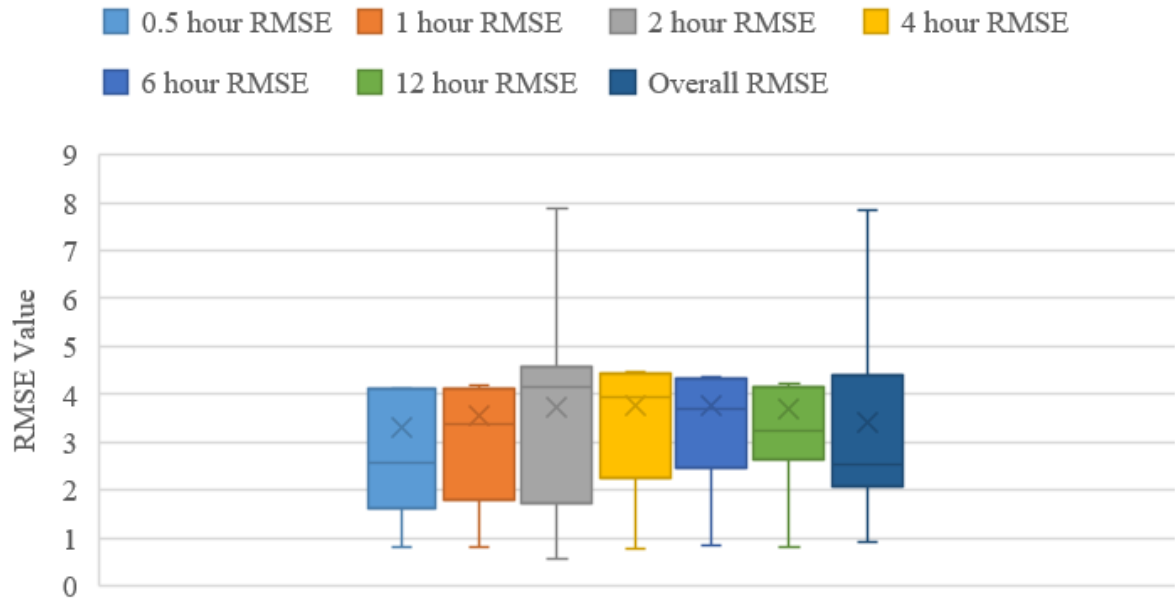


4010 October RMSE Profile

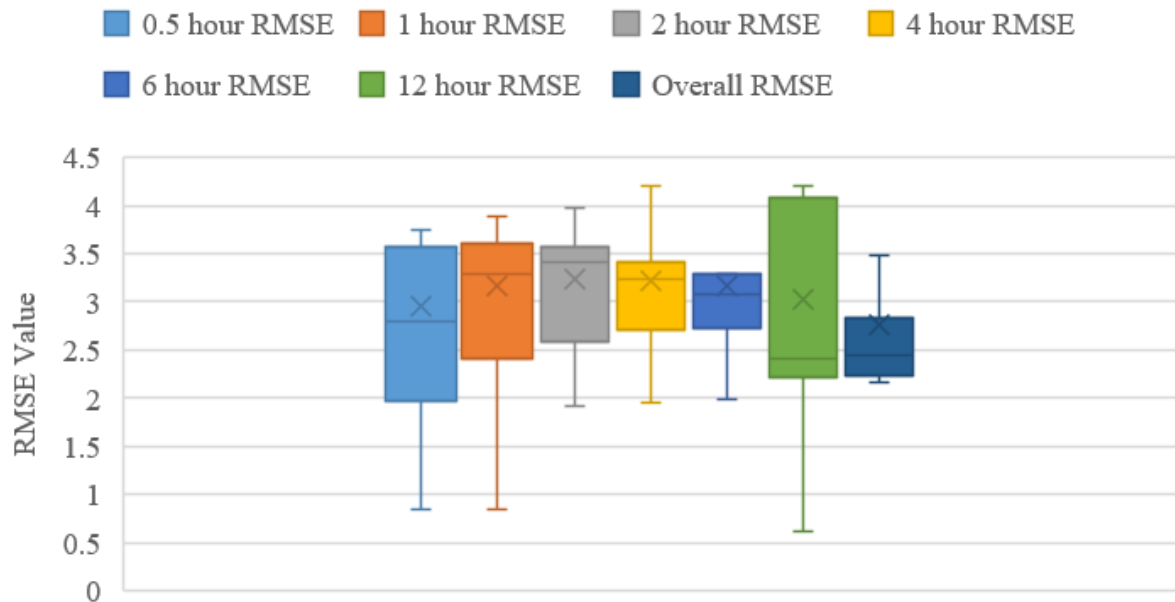


Appendix J – 4010 Switch off RMSE Boxplots

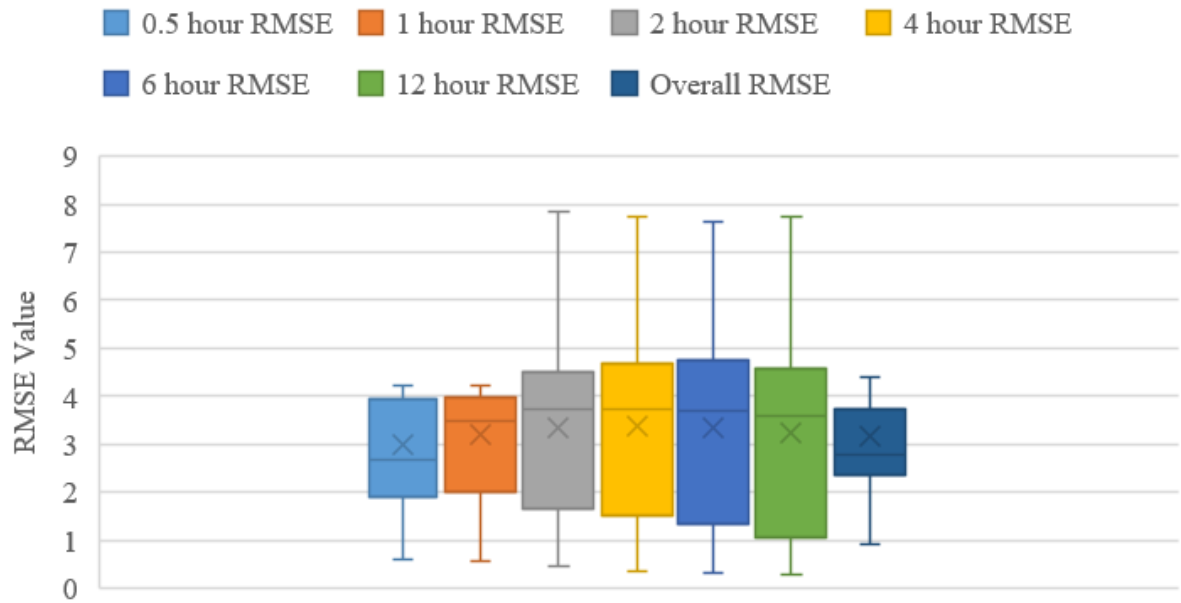
4010 0600 Switch off RMSE Profile



4010 1200 Switch off RMSE Profile



4010 1700 Switch off RMSE Profile



4010 2000 Switch off RMSE Profile

